2020-11

GEOSPATIAL-BASED ENVIRONMENTAL MODELLING FOR COASTAL DUNE ZONE MANAGEMENT

Chen Suo
Technological University Dublin

TECHNOLOGICAL UNIVERSITY DUBLIN

School of Surveying and Construction Management

GEOSPATIAL-BASED ENVIRONMENTAL MODELLING FOR COASTAL DUNE ZONE MANAGEMENT

Chen Suo

A thesis presented to the Technological University Dublin in fulfilment of the requirements for the degree of Doctor of Philosophy

November 2020

Research supervisors: Dr. Eugene McGovern, Dr. Alan Gilmer

School of Surveying and Construction Management

PROJECT COVER

STUDENT NAME	Chen Suo
COURSE & YEAR	PhD Research Programme 2015-2020
PROJECT TITLE	Geospatial-based environmental modelling for coastal dune zone management
MARK ALLOCATION	

FOR OFFICIAL USE

DATE DUE	11/2020
DATE RECEIVED	
SUPERVISORS	Dr. Eugene McGovern Dr. Alan Gilmer
GRADE AWARDED	

Abstract

To maintain biodiversity and ecological function of coastal dune areas, it is important that practical and effective environmental managemental strategies are developed. Advances in geospatial technologies offer a potentially very useful source of data for studies in this environment. This research project aim to develop geospatial data-based environmental modelling for coastal dune complexes to contribute to effective conservation strategies with particular reference to the Buckroney dune complex in Co. Wicklow, Ireland.

The project conducted a general comparison of different geospatial data collection methods for topographic modelling of the Buckroney dune complex. These data collection methods included small-scale survey data from aerial photogrammetry, optical satellite imagery, radar and LiDAR data, and ground-based, large-scale survey data from Total Station (TS), Real Time Kinematic (RTK) Global Positioning System (GPS), terrestrial laser scanners (TLS) and Unmanned Aircraft Systems (UAS). The results identified the advantages and disadvantages of the respective technologies and demonstrated that spatial data from high-end methods based on LiDAR, TLS and UAS technologies enabled high-resolution and high-accuracy 3D dataset to be gathered quickly and relatively easily for the Buckroney dune complex. Analysis of the 3D topographic modelling based on LiDAR, TLS and UAS technologies highlighted the efficacy of UAS technology, in particular, for 3D topographic modelling of the study site.

The project then explored the application of a UAS-mounted multispectral sensor for 3D vegetation mapping of the site. The Sequoia multispectral sensor used in this research has green, red, red-edge and near-infrared (NIR) wavebands, and a normal RGB sensor. The outcomes included an orthomosiac model, a 3D surface model and multispectral imagery of the study site. Nine classification strategies were used to examine the efficacy of UAS-

mounted multispectral data for vegetation mapping. These strategies involved different band combinations based on the three multispectral bands from the RGB sensor, the four multispectral bands from the multispectral sensor and six widely used vegetation indices. There were 235 sample areas (1 m × 1 m) used for an accuracy assessment of the classification of the vegetation mapping. The results showed vegetation type classification accuracies ranging from 52% to 75%. The result demonstrated that the addition of UAS-mounted multispectral data improved the classification accuracy of coastal vegetation mapping of the Buckroney dune complex.

Based on multispectral data, a methodology for environmental modelling for coastal dune complexes was developed. By monitoring the changes of the vegetation and the non-vegetation areas in a growing season, environmental models were generated to simulate the relationships between changes in vegetation and non-vegetation features, and related environmental parameters. In the results, a mathematical model was developed that represented the relationship between vegetation changes with time-series parameters. This mathematical model was also determined that wind, temperature and UV index were the most significant contributors in effecting vegetation changes. In addition, a predicted non-vegetation distribution model was created to represent the probability of non-vegetation occurrence in the site, which are often associated with increased erosion potential. This distribution model demonstrated that elevation and distance from pathlines were the most important factors in effecting non-vegetation occurrence in the site.

In general, this research project identified the efficacy of UAS technology in the collection of high-resolution and high-accuracy spatial data for 3D topographic modelling of a dune complex. This research project also demonstrated that spatial data from UAS-mounted multispectral sensors can improve the accuracy of vegetation mapping of the

study site. Most importantly, environmental models of the study site were successfully developed based on the UAS-mounted multispectral data These environmental models can contribute to better environmental management to help protect the vegetation and monitor and reduce erosion at coastal dune complexes.

Key words: Coastal dune complex; Unmanned Aerial System; multispectral sensor; topographic mapping; environmental modelling; environmental management.

I certify that this thesis entitled *Geospatial-based environmental modelling for coastal dune zone management* which I now submit for examination for the award of degree of Doctor of Philosophy, is entirely my own work and has not been taken from the work of others save, and to the extent that, such work has been cited and acknowledged within the text of my work.

This thesis was prepared according to the regulations for graduate study by research of the Technological University Dublin and has not been submitted in whole or in part for another award in any other third level institution.

The work reported on in this thesis conforms to the principles and requirements of the TU Dublin's guidelines for ethics in research. TU Dublin has permission to keep, lend or copy this thesis in whole or in part, on condition that any such use of the material of the thesis be duly acknowledged.

Signature _____ Chen Suo _____

Date _____10/11/2020_____

ACKNOWLEDGEMENT

I wish to express my sincere gratitude to the following:

- Dr. Eugene McGovern and Dr. Alan Gilmer for their guidance and assistance throughout this project.

- Other members of academic staff, technicians and, in particular, Ronan Hogan of the School of Surveying and Construction Management for their support.

- Technological University Dublin for financial support.

- Ordnance Surveying Ireland for providing data for the research, SLR Environmental for providing equipment for data collection, National Park & Wildlife Service for their assistance and support.

- My family and all my friends, and especially my husband Pengyu, for their continual patience, support and encouragement.

TABLE OF CONTENES

LIST OF FIGURES

CHAPTER 1 **Page**

CHAPTER 2 **Page**

CHAPTER 3 **Page**

CHAPTER 4 **Page**

CHAPTER 5 **Page**

LIST OF TABLES

ABBREVIATIONS, NOTATION AND UNITS

ASMITA	Aggregated Scale Morphological Interaction between Inlets and Adjacent Coast
AVHRR	Advanced Very High Resolution Radiometer
CORS	Continuously Operating Reference Stations
COVE	Coastal One-Line Vector Evolution
CSDMS	Community Surface Dynamics Modelling System
CSHORE	Cross-Shore Model
DMSP/OLS	Defense Meteorological Satellite Program/Operational Linescan System
DTM	Digital Terrain Models
DSM	Digital Surface Model
EDM	Electronic Distance Meter
EHSI	Environmental Health Sciences Institute
EXIF	Exchangeable Image File Format
GCPs	ground control points
GNSS	Global Navigation Satellite System
GPS	Global Positioning System
GSD	Ground sample distance

IG	Irish Grid
ITM	Irish Transverse Mercator
LIDAR	Light Detection and Ranging
MODIS	Moderate-Resolution imaging Spectroradiometer
MP	Megapixels
NDVI	Normalized Differential Vegetation Index
NMA	National Mapping Agencies
NPWS	National Parks and Wildlife Service
NRTK	Network Real Time Kinematic
OSI	Ordnance Survey Ireland
OpenMI	Open Modelling Interface
PPK	Post Processing Kinematic
QR	Quick Response
RAM	Random-access Memory
RGB	Red, green and blue wavebands
RMS	Root-Mean-Square
RPAS	Remotely Piloted Aircraft System
RTK	Real Time Kinematic

SAR	Synthetic Aperture Radar
SFM	Structure from Motion
TLS	Terrestrial Laser Scanning
TM/ETM	Thematic Mapper/Enhanced Thematic Mapper
TS	Total Station
UAS	Unmanned Aerial Systems
UAV	Unmanned Aerial Vehicles
USGS	United States Geological Survey
UV	Ultraviolet
WIRC	Water Innovation Research Centre

Chapter 1

INTRODUCTION

1.1 Motivation

Coastal dune zones are the transition areas between the marine and terrestrial environments, and dune complexes are the main structures at these locations (Lucas et al., 2002). These dune complexes play an essential role in the preservation of ecosystem stability and biological diversity as they provide habitat for special flora and fauna, control soil erosion and flooding, and protect nearby properties from other environmental hazards (Andrews et al., 2002).

The Brittas-Buckroney dune complex (Fig.1.1) is located *c.* 10 km south of Wicklow Town on the east coast of Ireland and comprises two main sand dune systems, *viz.* Brittas Bay and Buckroney Dunes. The study site for this research project is the Buckroney Dunes. The area of the Buckroney dune complex is *c.* 60 ha. At the boundary between the Buckroney dune system and the adjoining golf course, there is a stream flowing through the dune complex. The south part of the dune system is private farmland and along the seaside area is a beach, which is very popular for tourism in summer.

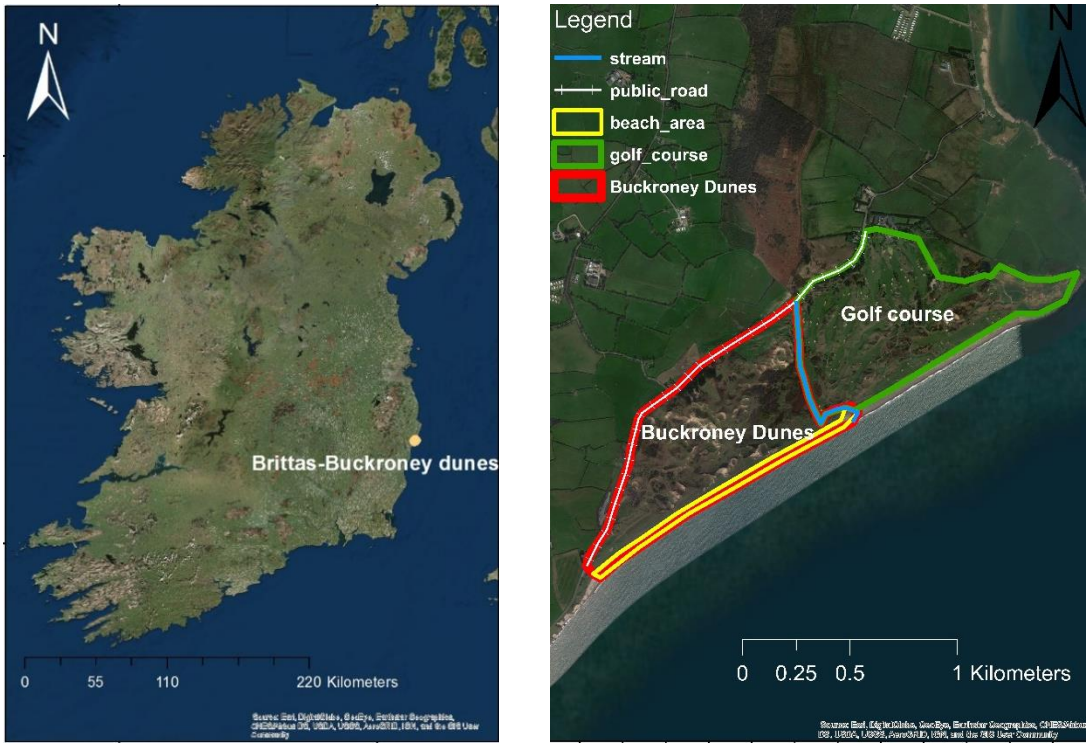

(a) (b)

Fig.1.1 Study site location: (a) General location (b) Study site based on World Imagery (ESA).

Within the Buckroney dune system, ten habitats listed on the EU Habitats Directive are present, including two priority habitats in Ireland, fixed dune and decalcified dune heath. This dune system also contains good examples of different dune types. At the northern end of the Buckroney dune system, there are some representative parabolic dunes. While embryonic dunes mostly occur at the southern part of Buckroney dune system (NPWS, 2016).

Meanwhile, the site has notable meaning for the presence of well-developed plant communities. Despite adjacent farming at the south part of the dune system, there is still a rich and varied flora in Buckroney dune system, especially in the open areas of this site.

The transition area, between the beach area and the dune complex, is dominated by Marram (*Ammophila arenaria*). The height of the well-developed dune complex can reach about 10m at this site, where typical annual strandline vegetation occurs. Marram is less frequent and is replaced by Red Fescue (*Festuca rubra*) at stable fixed dune systems developed at the Buckroney dune complexes. The presence of Sharp Rush (*Juncus acutus*) was observed at wet dune slacks in this site, which was a scarce species in eastern Ireland and an indication plant for saline influence. Another two rare plant species presented in this site are protected under the Flora (Protection) Order of 1999: Wild Asparagus (*Asparagus officinalis subsp. prostratus*) and Meadow Saxifrage (*Saxifraga granulata*) (NPWS, 2016).

With the land acquisition in recent years, beach areas along the sea side were developed as a place of interest for visitors in recent years. The marginal areas of the dune system have been reclaimed as farmland. The increasing anthropogenic activities at the dune system have brought pressure to the dune ecosystem's development, with potential hazards, such as soil erosion, flooding and habitat loss. Thus, proper environmental management needs to be implemented to ensure the continued survival of this mosaic of coastal habitats and to maintain the diversity and stability of the ecosystem on this site.

In recent decades, there have been a number of studies conducted and conservation-related documents published by the Irish National Parks and Wildlife Service (NPWS) that related to Buckroney-Brittas Dunes and Fen. From 1999, a projects was conducted to rank the coastal zones around Ireland based on the conservation value of vegetation and plant species (Moore and Wilson, 1999). In 2004-2006, to comply with obligations under the European Union Habitats Directive, NPWS researched to monitor the conservation status of ten types of habitats in Irish coastlines. These are listed in Annex

I, sand dune habitats, of the resulting report (Ryle et al., 2009). Annex I habitat types were determined as requiring conservation under the designation of Special Areas of Conservation, and priority habitats which are in danger of disappearing within the EU territory, are highlighted in the report (NPWS, 2016). A total of 181 coastal sites around Ireland were investigated. The results indicated that six out of ten had an unfavourable-inadequate habitat conservation status, while the remaining four were rated as unfavourable-bad, including two of the priority dune habitats (Ryle et al., 2009). In general, the conservation status of dune habitats along the Irish coastline is largely unsatisfactory, not achieving the requirement of the EU Habitats Directive. This situation will be difficult to change in a relatively brief period unless structured management plans can be developed and implemented. In 2008, NPWS started a project to continuously monitor and update the conversation assessment of key *Annex I* habitats located throughout Irish coastal zones based on pre-defined polygon maps produced by interpretation of orthorectified Ordnance Survey aerial photographs or high-quality satellite imagery (Perrin et al., 2014). From June 2011 to August 2012, the Sand Dunes Monitoring Project was completed by NPWS, aiming at conservation assessment specific for Annex I sand dune habitat (Delaney et al., 2013). Concerning to Area, Structure and Functions and Future Prospects, the results showed that Annex I sand dune habitat remained in an unfavourable condition, due to anthropogenic activities, such as recreation and land reclamation (Delaney et al., 2013).

Monitoring changes at coastal dune complexes can contribute to the establishment of rigorous and quantitative numerical simulation environmental models, which have significant relevance for the selection of appropriate and effective conservation strategies for such coastal environments. These models can inform targeted land management actions that maintain biodiversity and ecological functions. However, this is a

complicated task as coastal dune complexes are difficult landforms to study due to the multiple interactions between topography, vegetation, wind and sand transfer throughout the whole system.

1.2 Research Aim and Objectives

The overall aim of this research project was to develop geospatial data-based environmental modelling for coastal dune complexes to contribute to the effective conservation strategies with particular reference to the Buckroney dune complex (Fig.1.2) in Co. Wicklow, Ireland.

Fig.1.2 Morphology of the Buckroney dune complex.

The objectives of this research were:

(i) Establish optimal methods for the collection of high-resolution and high-accuracy spatial data of the study area.

(ii) Explore the application of data from a multispectral sensor mounted on a UAS platform to develop high-resolution and high-accuracy functional vegetation abundance maps of the study area including seasonal variability.

(iii) Develop environmental models that relate vegetation and non-vegetation changes with other environmental parameters, such as rainfall, wind, temperature, elevation, and slope.

(iv) Propose efficient and practical management strategies for dune complexes based on the environmental models in (iii) above to protect the habitat and to maintain biodiversity.

1.3 Structure of the project

This project is structured into four separated but interrelated elements.

Element 1 - A critical evaluation of high-end methods for topographic mapping

There are several sources of spatial data available for coastal dunes mapping. National mapping agencies provide a base topographic mapping from aerial photography with, more recently, digital elevation models from airborne laser scanning while satellite imagery provides remotely-sensed panchromatic, spectral and multispectral data. Although valuable, these data may not provide the resolution necessary for accurate numerical modelling of a dune complex. Recent developments in surveying technology have enabled high-resolution and high-accuracy spatial data to be gathered quickly and relatively easily on-site. These technologies include Real Time Kinematic (RTK) Global Positioning System (GPS), robotic total stations (TS), terrestrial laser scanners (TLS) and UAS. This section compares and contrasts these technologies and their deliverables, for

the topographic mapping of coastal dune complexes with particular reference to the Buckroney dune complex in Co. Wicklow.

Element 2 - Development of methodologies for the application of UAS-mounted multispectral sensor data for automatic vegetation classification and abundance mapping of a coastal dune complex

In contrast to Synthetic Aperture Radar (SAR) and Light Detection and Ranging (LiDAR), multispectral data from sensors mounted on a UAS overcomes the limitations of the coverage, cost and revisit times of SAR and LiDAR from third party providers. Such data provides low-cost approaches to meet the requirements of spatial, spectral, and temporal resolutions for dune mapping projects. A high resolution vegetation abundance map was generated using a rotary-based UAS equipped with visible and narrowband multispectral imaging sensors. From flight missions at the study site, surface reflectance imagery was obtained. After radiometric calibration, multispectral data were extracted and used for vegetation mapping at the Buckroney dune complex in Co. Wicklow.

Element 3 - Environmental modelling for vegetation and non-vegetation changes at coastal dune complexes

Environmental modelling, for preservation and effective management of coastal zones, was established to explore and identify important processes at coastal zones, for example, how sand dunes form and change, and how vegetation, aeolian and other environmental variances affect morphology changes at coastal zone. This research involved the process of environmental modelling of coastal dune complexes with particular reference to Buckroney dune complex in Co. Wicklow, Ireland. The study monitored vegetation and non-vegetation features changes at the site in a full growing season using a multispectral sensor mounted on a UAS. Environmental models were established that related vegetation

and non-vegetation changes with selected environmental parameters at the site. Based on those environmental models, efficient and practical management strategies were developed to help maintain and improve the coastal zone environment.

This project resulted in a methodology for the identification of high-risk areas for erosion and a sensitivity analysis of the environmental parameters that impact the site. These outcomes can inform strategies to reduce erosion, to protect the habitat and to maintain biodiversity and have the potential to be widely applied over other coastal areas to reduce negative influences on the environment and economic development. Also, within this project, relevant new generation data collection platforms and sensor technologies were investigated thus increasing understanding of their areas of application and their efficacy.

1.4 Measurable outcomes

Dissemination for the project included:

- Two peer-reviewed journal papers published,
- One paper currently under review for peer-reviewed journal publication,
- National and international conference presentations,
- Contribution to stakeholder workshops (meeting with NPWS)

The outcomes were published and presented in the scientific literature and at conferences for communication with researchers and experts in the field to share knowledge and experiences and, at the same time, to increase public awareness and understanding of the Buckroney Dunes complex and its sustainable use and protection.

At this stage, the peer-reviewed journal paper details resulting from this project are:

Paper 1: Coastal Conservation - Elsevier (Published at 18 July 2020)

Suo, C., McGovern, E., Gilmer, A., Cahalane, C. A comparison of high-end methods for topographic modelling of a coastal dune complex. Journal of Coastal Conservation 2020, 24, 47; https://doi.org/10.1007/s11852-020-00764-6.

Paper 2: Journal of Remote Sensing - MDPI (Published at 2 August 2019)

Suo, C., McGovern, E., Gilmer, A. Coastal Dune Vegetation Mapping Using a Multispectral Sensor Mounted on an UAS. Journal of Remote Sensing. 2019, Volume 11, Issue 15, 1814; doi:10.3390/rs11151814.

Journal 3: Ocean & Coastal Management - Elsevier (Under review).

Suo, C., McGovern, E., Gilmer, A. Development of environmental models for a coastal dune complex using drone-mounted multispectral sensor data.

For particular element of the dissertation, the outcome details are presented below.

Element 1:

- Developed spatial data collection and processing methodologies appropriate to the sand dune complex environment.
- Compared and contrasted spatial data collection processes and data deliverables appropriate to the sand dune complex environment.
- Developed 3D modelling workflows appropriate to the sand dune complex environment.

The above details are included in Paper 1 (*Suo, C., McGovern, E., Gilmer, A., Cahalane C. A comparison of high-end methods for topographic modelling of a coastal dune complex. Journal of Coastal Conservation 2020, 24, 47; https://doi.org/10.1007/s11852-020-00764-6*).

Element 2:

- Developed procedures for the operation of drone-mounted multispectral sensors appropriate to the sand dune complex environment.
- Developed procedures for the processing of drone-mounted multispectral sensor data appropriate to the sand dune complex environment.
- Developed procedures for vegetation abundance mapping by digital image classification of drone-based sensor data.
- Developed a procedure, utilising drone-based data for monitoring seasonal vegetation changes at the dune complex.

The above details are included in Paper 2 (*Suo, C., McGovern, E., Gilmer, A. Coastal Dune Vegetation Mapping Using a Multispectral Sensor Mounted on an UAS. Journal of Remote Sensing 2019, Volume 11, Issue 15, 1814; doi:10.3390/rs11151814*).

Element 3:

- Created a new vegetation index, named BKI index, to distinguish vegetation and non-vegetation features at the site, and also to indicate the vegetation health and density.

- Developed a mathematical model to reflect the relationships between vegetation changes in a growing season and time-series environmental parameters.

- Developed a non-vegetation distribution model that was related to position-related environmental parameters.

- Proposed efficient and practical management strategies for erosion mitigation at dune complexes.

The above details are included in Paper 3 (*Suo, C., McGovern, E., Gilmer, A. Development of environmental models for a coastal dune complex using drone-mounted multispectral sensor data. Under reviewing of Journal of Ocean & Coastal Management*).

1.5 Research Value

This study compared different high-end methods based on LiDAR, TLS and UAS technologies, for the topographic modelling of coastal dune complexes with particular reference to the Brittas-Buckroney dune complex in the South East of Ireland. The results identified the advantages and disadvantages of the respective technologies and highlighted the efficacy of UAS for topographic modelling of coastal dune complexes.

This study also developed a methodology for 3D vegetation mapping of a coastal dune complex using a multispectral sensor mounted on a UAS. The outcomes from captured imagery included an orthomosiac model, a 3D surface model and multispectral images of the study site, in the Irish Transverse Mercator coordinate system. Vegetation mapping was created based on these outcome data and on imagery classification. The accuracies of vegetation mapping ranged from 52% to75%. The study illustrated the efficiency of a

multispectral sensor mounted on UAS for high-accuracy and high-resolution vegetation mapping.

Based on the vegetation mapping solution as presented, environmental modelling of a coastal dune complex that related vegetation changes with other environmental factors such as precipitation, wind and elevation, was created. Environmental modelling, the core objective of this research, is essential for the development of coastal zone management actions to reduce the influence of environmental and anthropogenic actions. This research presented a methodology for the development of a mathematical model for vegetation features changes related to primary environmental variables at the Buckroney coastal dune complex over twelve months. The resulting mathematical model had an accuracy of 92%, predicting the vegetation growing status (represented by a vegetation index value) according to the available values of time-series environmental parameters. From the modelling, 'Temp', 'Wind', and 'UV_index' were shown to be the most important environmental variables for vegetation features changes at the site. A predicted non-vegetation distribution geographical model was also created in this research to show those areas with a higher probability of non-vegetation occurrence. The model shows that 'elevation' and 'distance from pathlines' were the most important parameters in effecting non-vegetation presence in the site. This research provides reference information for similar research for environmental modelling for the coastal zone.

This project addresses an important area of coastal environmental management that has been highlighted in numerous reports, publications and EU directives. The research can inform a better understanding with respect to coastal dune zone erosion and stability in the context of observation and monitoring of land features and environmental parameters using the latest high-end spatial data collection and modelling methodologies.

1.6 Reference

Andrews, B., Gares, P.A., Colby, J.D., 2002. Techniques for GIS modelling of coastal dunes. Geomorphology, 48(1–3), 289–308.

Delaney, A., Devaney, F.M, Martin, J.M., Barron, S.J., 2013. Monitoring survey of Annex I sand dune habitats in Ireland. Irish Wildlife Manuals, No. 75. National Parks and Wildlife Service, Department of Arts, Heritage and the Gaeltacht, Dublin, Ireland.

Lucas, N.S., Shanmugam, S., Barnsley, M., 2002. Sub-pixel habitat mapping of a coastal dune ecosystem. Applied Geography, 22(3), 253–270.

Moore, D., Wilson F., 1999. National Shingle Beach Survey of Ireland 1999: Synoptic Report. National Parks & Wildlife Service Publication.

National Parks & Wildlife Service (NPWS), 2016. Site Synopsis: Buckroney-Brittas Dunes and Fen SAC. NPWS site documents, 000729_Rev13.Doc. https://www.npws.ie/protected-sites/sac/000729.

Perrin, P.M., Barron, S.J., Roche, J.R., O'Hanrahan, B., 2014. Guidelines for a national survey and conservation assessment of upland vegetation and habitats in Ireland. Version 2.0. Irish Wildlife Manuals, No. 79. National Parks and Wildlife Service, Department of Arts, Heritage and the Gaeltacht, Dublin, Ireland.

Ryle, T., Murray, A., Connolly, K., Swann, M., 2009. Coastal Monitoring Project 2004-2006. Irish Wildlife Manuals, National Parks and Wildlife Service, Department of Arts, Heritage and the Gaeltacht, Dublin, Ireland.

Chapter 2

LITERATURE REVIEW

2.1 Coastal dune complex

2.1.1 General introduction

Coastal zones comprise 2% of the earth's land area (Acosta et al., 2005). They are the transition areas between the marine and terrestrial environments, and dune complexes are the main structures at these coastal zones (Lucas et al., 2002). Coastal dune zones are dynamic environments, and their characteristics are determined by the action of waves, tides on the available sediment and many other environmental processes (Kumar et al., 2010; Amaro et al., 2015). Within this dynamic setting, there is an important exchange of sand, biological matter and other constituents between the dunes and intertidal zones and surf zones. These coastal zones play an essential role in the preservation of ecosystem stability and biological diversity as they provide drinking water, mineral resources and habitat for special flora and fauna (Clark, 1977; Andrews et al., 2002). Activities at coastal zones can contribute to local and national economic development in areas like aquaculture, fisheries and tourism. Coastal zones also have important functions to control erosion and flooding thus protecting and maintaining environmental functions (Fenu et al., 2012).

Vegetation at coastal zones is also a critical environmental component of the coastal ecosystem for food production, resource conservation, nutrient cycling, and carbon sequestration (Woo et al., 1997; Kuplich, 2006). Vegetation at coastal dune complexes has a strong impact on dune morphology and dynamics as it can influence sand transport and be effective in dissipating the energy of storm surges (Sabatier et al., 2009). Vegetation can contribute to effective protection to the coastal zones against sea-level rise, tsunami and other natural calamities (Kuplich, 2006).

Populations in coastal zones have significantly increased in recent decades. Nicholls et al. (2007) estimated that 23% of the world's population lives within 100 km of the coast and less than 100 m above sea level. More recently, in 2010 the United Nations Atlas of the Oceans (www.oceansatlas.org) indicated that about 44% of the world's population lives within 150 km of the coast as an inevitable consequence of economic progress (Amaro et al., 2015). Also, urbanization and the rapid growth of coastal cities have been dominant population trends over the last few decades, leading to the development of numerous megacities in coastal regions around the world. At least 200 million people were estimated to live in coastal floodplains in 1990 and it is likely that this number will increase to 600 million by the year 2100 (Mimura and Nicholls, 1998).

2.1.2 Pressures

Coastal zones are experiencing intense and sustained pressures from a wide range of factors. Global climate change is having a strong impact on sea-level rise and may lead to an extreme wave climate (*e.g.* Komar and Allan, 2008; Dodet et al., 2010; Young et al., 2011; IPCC, 2013; Serafim et al., 2019). Over the last 100 years, global sea level rose by 1.0–2.5 mm/y. Estimates of future sea-level rise induced by climate change range from 20 to 86 cm for the year 2100, with the best estimate of 49 cm (IPCC, 2001).

Increasing anthropogenic activities can produce significant hazards to dune complexes. For example, seaside infrastructure frequently installed without proper knowledge of coastal processes may obstruct natural sand transport, affect the sediment budget and this can cause severe erosion and serious socioeconomic damage (Amaro et al., 2015). Such activities have classically had a long-term trend of negative impact on the coastal dune systems, an adverse effect that can also be detected in the short-term analysis. Moreover, human activities, together with a range of consequent environmental changes, can alter

the natural ecosystem processes and cause changes in coastal zones (Gonçalves and Henriques, 2015). In some respects, these changes may also affect the social and economic development in coastal areas.

In addition, increasing human activities and global climate changes have threatened the balance of the ecosystem at coastal zones, resulting in environmental issues including soil erosion, flooding and habitat loss (Phillips and Jones, 2006; Martinez et al., 2016). These coastal environmental issues have a potential, economic, ecological and social influence which is a concern for government, the public and academic research (Kumar et al., 2010; L´opez Royo et al., 2016). In light of these risks, effective coastal zone management has become important and necessary in many coastal countries. Preservation and effective management of coastal zones require a good understanding of the key processes that control the dynamical morphology of coastal zones (Mitasova et al., 2005; Payo et al., 2017). However, the processes at coastal zones are difficult to study because of the complex relationships linking topography, hydrology, aeolian processes and sand movement throughout the system (Andrews et al., 2002; Payo et al., 2017).

2.1.3 Current Irish situation

Ireland has a coastline of approximately 7,400 km (+/-5%) (Devoy, 2008). Topography, together with linked geological controls, has resulted in extensive (about 3,000 km) rock-dominated coasts, which particularly occur in the southwestern, western and northern regions of Ireland. In contrast, the eastern and south-eastern regions are composed of unconsolidated Quaternary glaciogenic sediments and fewer rock exposures. Glacial and fluvial actions have also created major sedimentary areas on the western coasts in the form of large bays and estuaries. Within the different coastal settings, significant coastal systems include cliffs, beaches, and barriers (sand and gravel types); lagoons; dunes and

machair (sand ‘‘plains’’); salt marshes, mudflats and other wetlands (Devoy, 2008). Most of the Irish Sea coast is experiencing a long-term recession, wherein beaches and dunes are retreating. The rate of recession is highly variable in time and space (Salman et al., 2004).

The vulnerability of Ireland to sea level rise is relatively low (Devoy, 2008). Coastal defences and other infrastructure are often old, and less than 4% of the coastline is protected by shoreline defences (Devoy, 2008). In many rural areas, structures now serving as defences were originally built as property or agricultural boundaries. Existing structures frequently have their origin in the 19th century and have been modified subsequently on a piecemeal, needs-must basis. Until the 1990s, the extent of coastal defence works only conducted for about the 3.8% length of the Irish coastline (Cooper and Boyd, 2011).

Sediment deficit is noticeable on Irish coasts (Devoy, 2008). The transfer of ‘‘new’’ sediments to most coasts from offshore sources has almost ceased (Devoy, 2008). In the last century, coastal barriers became stranded against the uplands and landwards-rising hard-rock surfaces. Consequently, beach-barrier sediments are being lost through reworking alongshore and diffused into other coastal environments. This leaves a regionally to locally varied and often limited capacity for further onshore movement and adjustment of soft-sedimentary coasts to sea level rise impacts (Salman et al., 2004).

Coastal erosion rates upon ‘‘soft’’ (sediment-dominated) coasts, *e.g.*, sandy systems and glacial sediments, have reached average values of 0.2–0.5 m/y, commonly rising to 1–2 m/y on southern and eastern coasts while retreat rates for rocky shorelines are not well known (Devoy, 2008). Devoy (2008) further states that current total rates of land loss for

Ireland from erosion and flooding are estimated to be approximately 1.6 km^2/y, concentrated in about 300 sites.

Along the Irish coastline, the conservation status of dune habitats is largely unsatisfactory, not achieving the requirement of the EU Habitats Directive 1992 (Moore and Wilson, 1999; Ryle et al., 2009; Delaney et al., 2013). This situation is difficult to change in a relatively brief period unless structured management plans can be developed and implemented. In 2008, the Irish National Parks and Wildlife Service (NPWS) began a scoping study and pilot survey to continuously monitor and update the conservation assessment of key habitats located nationally based on pre-defined polygon maps derived from the interpretation of orthorectified Ordnance Survey aerial photographs or high-quality satellite imagery (Perrin et al., 2014). The 2014 result showed that these key sand dune habitats remained in an unfavourable condition, due to increasing anthropogenic activities, such as recreation and land reclamation.

2.1.4 Coastal management

Neither Ireland nor Northern Ireland has yet adopted a strategic approach to coastal management. Responsibility for coastal erosion management remains fragmented. The emphasis still appears to remain on protection schemes but with an anticipated increased reliance on beach nourishment in Ireland (Cooper and Boyd, 2011). At present, there are no specific national (or islandwide) policies in place to manage the effects of sea-level rise under global warming (Devoy, 2008).

Awareness of climate-warming issues and flood risk has led many local authorities, and the Environmental Protection Agency in the Republic of Ireland responsible for implementing Environmental Impact Assessments (EIAs), to prohibit developments in

coastal zones and close to vulnerable dunes and eroding coastal areas. EIAs for large-scale coastal developments are now required. However, politics and economy, and planning guidelines are increasingly becoming infringed in the absence of clear Integrated Coastal Zone Management (ICZM) policy and linked legislation (Devoy, 2008). In essence, Ireland's coastal vulnerability lies more with the attitudes of the people towards ICZM than in any physical susceptibility of the coast for the response to climate changes.

Concern for the increasing threat to coastal dune ecosystems has generated a greater interest in coastal dune conservation and management (MacLeod et al., 2002; Olbert et al., 2017). Accurate 'baseline' topographic maps, with detailed information concerning the earth's surface, are considered critical to the development of effective coastal environmental modelling (Acosta et al., 2005). High-resolution vegetation mapping of coastal dune complexes, with accurate distribution and population estimates for different functional plant species, can be used to analyse vegetation dynamics, quantify spatial patterns of vegetation evolution, analyse the effects of environmental changes on vegetation, and predict spatial patterns of species diversity (Vaca et al., 2011). Such information can contribute to the development of targeted land management actions that maintain biodiversity and ecological functions. Accurate coastal environmental modelling can also assist managers in developing an in-depth understanding of coastal dynamics and evolution for preservation and effective management (Mitasova et al., 2005). The primary driving component of sand dune systems is the localised wind regime acting on its surface. However, numerous other environmental parameters also affect the movement patterns of the coastal dune system. These factors include sediment supply, vegetation, moisture and antecedent conditions or form (Jackson et al., 2013). Environmental modelling can simulate the response of coastal dune systems by localising forcing variables through field observation and measurements, combined with monitoring

topographic data to infer longer-term environmental processes and changes at the dune systems (McKenna et al., 2005). For a better understanding of coastal zones, environmental modelling was established to explore and identify the important processed at coastal zones, for example, how sand dune form and change, how vegetation, aeolian and other environmental variances affect morphology changes at coastal zones (Alhajraf, 2004; Zhang et al., 2010; Xia and Dong, 2016).

2.2 Technologies for topographic modelling

A foundation factor for establishing a spatially-related environmental model is high-resolution and high-accuracy spatial data of the target site. A suitable scale of the spatial data needs to be seriously considered to balance the contradiction between modelling detail requirement and labour for data collection (Hugenholtz et al., 2012). Some National Mapping Agencies (NMA) can provide small-scale spatial data, which is easy to access. However, such data may not be sufficiently detailed with regard to representation of certain specific land features, which may cause difficulty in monitoring changes of coastal zones (Kempeneers et al., 20019). On-site ground surveying technology has contributed to large-scale spatial data collection in coastal process research and management (D'iorio et al., 2007). But for large study sites, such as coastal dune complexes, multiple data acquisition missions may be required for a complete and accuracy modelling project. To set a proper scale of spatial data for coastal modelling, it is necessary to have knowledge about different data collection technologies, including operational procedures, data capture quality, time and financial investment. The following sections present the spatial data collection technologies considered relevant to studies of coastal dune complexes.

2.2.1 Satellite data

Optical satellite imagery was first used for topographic modelling in the 1970s (Brabec et al., 2002). Such imagery is based on reflected solar radiation from different land cover features, such as forest, water, grass, bare soil, paved roads and buildings (Bartsch et al., 2016). At present, there are different sources of optical satellite imagery, including Landsat TM/ETM (Thematic Mapper/Enhanced Thematic Mapper), MODIS (Moderate-Resolution Imaging Spectroradiometer), Hyperion, AVHRR (Advanced Very High-Resolution Radiometer) and DMSP/OLS (Defense Meteorological Satellite Program/Operational Linescan System) (Shao et al., 2016).

The United States Geological Survey (USGS), NMA of the United States, provides remotely sensed panchromatic, spectral and multispectral data around the world. Their official website, USGS Earth Explorer, is free to access and download available datasets. In general, the resolution of the freely available optical satellite dataset on USGS Earth Explorer is 15 m~30 m. Higher-resolution aerial spatial data can be purchased from NMAs or other commercial mapping companies. However, conditions that affect solar illumination, such as cloudy weather, can have a great influence on the availability of remotely-sensed data used for topographic modelling (McGovern et al., 2002).

2.2.2 Synthetic Aperture Radar data

Synthetic Aperture Radar (SAR) is a form of radar data used to create two- or three-dimensional images of objects, collected from a moving platform, such as an aircraft or spacecraft (Satyanarayana et al., 2011). These platforms travel over a target area and record the radar pulses returning to the antenna of the unit. The returning radar pulses are used to create the large "synthetic" antenna aperture representing the target feature. Shao et al. (2016) illustrated the practical application of SAR data for generating an accurate urban impervious surface map of a study site (Shao et al., 2016).

SAR is considered an alternative for generating high-resolution remote sensing imagery without the limitation of weather conditions. In Ireland, the most commonly used resource of SAR data is from the Sentinel Science Data Hub. The Sentinel Scientific Data Hub (changed to The Copernicus Open Access Hub since 2016) provides free and open access to SAR dataset products (ESA, 2016).

Data from the sentinel-1 SAR satellite is a suitable resource for coastal zones modelling as its images cover all global landmasses, coastal zones, shipping routes in European waters and the global oceans in high spatial resolution (achieving 5 m) and at regular intervals (Campos-Taberner et al., 2017). Besides the geographical coverage, Sentinel-1 data also features high reliability, good revisit times and rapid dissemination, which are suitable properties for coastal topographic modelling. The Sentinel-1 SAR sensor acquires data in four exclusive modes: Stripmap (SM), Interferometric Wide swath (IW), Extra Wide swath (EW) and Wave (WV) (ESA, 2016). These four modes lead to different resolutions of the captured imagery as shown in Table 2.1. In this table, the range resolution stands for the ability of the radar system to distinguish between two or more targets on the same bearing but at different ranges. The degree of range resolution depends on the width of the transmitted pulse, the types and sizes of targets, and the efficiency of the receiver and indicator. The azimuth resolution refer to the width of the ground area illuminated by each pulse of electromagnetic radiation. The azimuth increases with increasing distance from the radar. The azimuth resolution and the slant-range resolution govern the resolution of a radar.

Table 2.1 Four modes acquisition resolution of Sentinel-1 Synthetic Aperture Radar (SAR) (rg×az: Range×Azimuth) (ESA, 2016)

Mode	**SM**	**IW**	**EW**	**WV**
Resolution (rg × az: Range×Azimuth)	1.7×4.3m-3.6×4.9m	2.7×22m-3.5×22m	7.9×43m-15×43m	2.0×4.8m-3.1×4.8m

However, depending on the mission area and the acquisition time of the imagery, the full operational dataset may not be available to download. For higher resolution SAR data in a particular area, a proposal can be sent to the European Space Agency (ESA) for free Third Party Mission data via the ESA website. The commercial Terra-SARX is an alternative providing SAR data with the resolution in 1m cell size.

2.2.3 Light Detection and Ranging data

Light Detection and Ranging (LiDAR) data from a laser profiling scanner on an airborne system, can be used to generate dense 3D point clouds, which can be transformed to 3D models (Peneva et al., 2008; Grebby et al., 2014). Bolivar et al. (1995) used LiDAR data to generate a high-resolution topographic mapping of 250 km of Florida coastline in 2 hours and obtained approximately 27 million georeferenced data points for modelling the coastal dune complexes in a storm damage research (Bolivar et al., 1995). Along the coast of northern France, a study used airborne LiDAR topographic data to create a contour Digital Terrain Model (DTM) of a coastal dune zone. Filtering of raw data was used to remove vegetation, buildings and other objects, aiding to the study of the potential impacts of sea-level rise (Crapoulet et al., 2016). For a study at a coastal dune zone in North Carolina, 1–2 m resolution LiDAR data provided with a reliable representation of

the dune complexes and accurate volumetric change measurements were possible (Woolard and Colby, 2002).

Ordnance Survey Ireland (OSi), the NMA of the Republic of Ireland, supplies a variety of products for representing height and ground relief which are available as high accuracy datasets. The OSi products include contour tiles, Digital Terrain Models (DTM) and also LiDAR data (OSi, 2017). LiDAR data is supplied in the Irish Grid (IG) and the Irish Transverse Mercator (ITM) projections, with a positioning accuracy of ±2 m and a minimum vertical accuracy of ±25 cm. The final outputs from LiDAR are a point cloud, a Digital Surface Model (DSM) and DTM.

However, because of incomplete coverage, LiDAR data is not available for all areas of Ireland. Since 2015, OSi has supplied data products captured by the Bluesky Company, including LiDAR, thermal airborne acquisition and panchromatic imagery at selected areas in counties Wicklow, Waterford, Carlow, Tipperary and Kilkenny. LiDAR data from Bluesky has ±25 cm horizontal resolution and ±12.5 cm horizontal resolution for particular urban areas. The price of LiDAR data from OSi is currently €250 per square kilometre (OSi, 2017).

2.2.4 Total Station and Robotic Total Station

Total Station (TS) surveying, as a commonly used ground surveying method, is considered as one of the most accurate surveying methods (Projovi, 2017). Positioning information collected by TS technology, formatted as x, y, z or Northing, Easting, Elevation, is one option for topographic modelling. In general, the distance measurement accuracy of a total station is 2 mm + 2 ppm over a distance of about 1 km (Lee et al., 2013).

Integrated with an electronic theodolite and an electronic distance meter (EDM), the total station instrument is comprised of three parts; mainframe, prism and field controller (Artese and Perrelli, 2018). To conduct a surveying project with a TS, usually, two persons are required, one to operate the mainframe set up at a known position point while the other person holds the prism at the points of interest. The instrument determines the coordinate position of the prism stand-point and stores the result in the field controller (Tsaia et al., 2012). For further data processing, the stored data (x, y, z or Easting, Northing, Elevation) in the field controller are typically downloaded to a computer. However, the operation and performance of TS in a field surveying project is limited by access and poor visibility circumstances, such as rain, snow, night-time thickets or physical obstructions, such as sand dunes (Afeni and Cawood, 2013).

The Robotic Total Station (RTS) (Fig.2.1) is an upgraded version of the TS with a development at the mainframe to adjust the orientation and find the prism automatically. In this case, one person can conduct the field surveying project and, consequently, the work efficiency is improved.

Fig.2.1 Robotic Total Station working on-site.

2.2.5 Network Real Time Kinematic Technology

Network Real Time Kinematic (NRTK) Technology, such as the Trimble R10 (Fig.2.2), can be used to collect accurate position information (formatted as x, y, z or Easting, Northing, Elevation). NRTK is based on a network of Continuously Operating Reference Stations (CORS) as a base stations network, to against a false initialization by a single base station and increase the accuracy of positioning. Real Time Kinematic (RTK) positioning is a technique used to enhance the precision of position data derived from the Global Navigation Satellite System (GNSS) (Mieczysław, 2013). According to a single reference station or interpolated virtual station to make real-time corrections, the obtained data resulting in centimetre-level accuracy. With lighter equipment and easier operation, this technique can save significant labour and time in collecting the same amount of mapping data as TS and RTS technologies (Glabsch et al., 2009).

Fig.2.2 Network RTK working on-site.

2.2.6 Terrestrial Laser Scanning

In recent decades, due to non-contact, rapidity and high accuracy, Terrestrial Laser Scanning (TLS) (Fig.2.3) has been widely used to build three-dimensional models

(Parrish et al., 2016). TLS allows the easy and fast acquisition of complex geometric data for 3D models of the objects. This technique utilizes Light Detection and Ranging methods by transmitting a pulse of laser light, recording and analysing return pulses of the light to capture the point cloud of the target (Wang, 2018). The recording information includes the target position, intensity and colour information. As a result of the scanning process, a three-dimensional scan view of the target area appears on the screen comprised of dense points. The positioning accuracy of TLS is up to the nearest millimetre (Staiger, 2003; Ersilia et al., 2012). The operation of the laser scanner is almost fully automatic, which reduce the possibility of error as human influence plays a less important role in the surveying project.

Fig.2.3 Terrestrial Laser Scanner working on-site.

During field-work, control points are set around the target area to provide the integral 3D view of the area (Kasperski et al., 2010). With the position information of theses control points measured typically by the NRTK GPS, the point cloud containing 3D position

information is generated after the scanning process. These point clouds captured at each control point, lead to different scanner views of the area, which are registered together to create an integrated 3D dataset.

2.2.7 Unmanned Aerial Systems

Most recently, Unmanned Aerial Systems (UAS) (Fig.2.4), variously referred as Remotely Piloted Aircraft System (RPAS), Unmanned Aerial Vehicles (UAV's), "Aerial Robots" or simply "drones" (Turner et al., 2016), have enabled high quality, ground-based data to be gathered quickly and easily on-site. The application of UAS represents a new opportunity to survey relatively large areas in significantly less time compared to other on-site surveying methods (Zelizn, 2016). UAS, integrated with modern digital camera technology, breaks the time and space constraint, allowing a study site to be remotely surveyed in a significantly reduced time with the result of a large number of high-resolution and high-accuracy images.

Fig.2.4 Fixed wing UAS (e-Bee) on-site.

In the camera model, it represents a 3D real world as a 2D image. Structure from Motion (SfM) is a technique that emerged in the last decade to construct a photogrammetry-based 3D model, creating 3D surface models, from a large number of overlapping photographs (Colomina and Molina, 2014). From each two overlapping pictures, specialized software using SfM can determine the unique coordinate position (x, y, z or Easting, Northing, Elevation) of a set of particular points presented in both images. To maintain the accuracy of the map, the overlapping area for each two images should be at least 60%, making sure enough shared points can be recognised by the software for the map construction (Hodgson et al., 2013). In this way, 3D models can be generated by numerous overlapping images without user intervention.

2.2.8 Summary

Generally, according to the relevant research in recent decades, there are a number of data collection methods appropriate for topographic mapping, including aerial photogrammetry, optical satellite imagery, SAR data, LiDAR data, TS, RTS, NRTK, TLS and UAS. For topographic mapping of a particular coastal dune complex, national aerial photogrammetry, optical satellite imagery and SAR data from the NMA are often unsuitable for their regional national scale, limited coverage and often unsuitable acquisition dates. Surveying with TS, RTS and NRTK technology allows for the on-site recording of topographic features in the study site. However, the time and labour investment for topographic modelling of a coastal dune area is considerable and can limit the number of points surveyed. Thus, considering data resolution, availability and labour investment, LiDAR, TLS and UAS are considered more suitable for topographic modelling of coastal dune complexes. The first objective of this research was to establish optimal methods based on these three choices to create high-resolution and high-accuracy

topographic modelling of the study area. This topographic modelling will contribute to the development of a landscape model relating sand transfer and vegetation functional abundance. This model contributes to the efficient management of the dune complex in the context of reducing erosion, targeting intervention and preservation actions to protect the habitat and to maintain biodiversity.

2.3 Vegetation mapping of coastal dune complexes

Vegetation at coastal dune complexes has a significant impact on dune morphology and dynamics as it can influence sand transport (Sabatier et al., 2009). Vegetation is also a critical environmental component of a coastal ecosystem, for food production, resource conservation, nutrient cycling, and carbon sequestration (Woo et al., 1997; Kuplich, 2006). A high-resolution vegetation map across a coastal dune complex, with accurate distribution and population estimates of different functional plant species, can be used to analyse vegetation dynamics, quantify spatial patterns of vegetation evolution, analyse the effect of environmental changes on vegetation, and predict spatial patterns of species diversity (Vaca et al., 2011). These parameters can contribute to the development of targeted land management actions that maintain biodiversity and ecological functions.

2.3.1 Remote sensing methods for vegetation mapping

Traditionally, field survey methods (like TS or RTK) have been the most commonly used methods for vegetation mapping (Song et al., 2007). However, field survey methods are time-consuming, expensive, and limited in spatial coverage (Song et al., 2007). Remote sensing, in contrast, offers a more efficient means of obtaining such data. Each vegetation community exhibits different plant species composition and structure, which consequently has a unique spectral response in satellite images (Verbesselt et al., 2010;

Qi et al., 2013). Satellite-based hyperspectral data can be a useful tool for vegetation mapping on a regional scale. However, in the context of species-level classification, it is limited to homogeneous species because of limited spatial resolution (*e.g.*, 30 m of EO1 Hyperion images) and low signal to noise ratio (Kozhoridze et al., 2016).

Airborne remote sensing provides higher spatial resolution data of coastal dune complexes which is suitable for coastal dune mapping and monitoring (Launeau et al., 2018). LiDAR is a remote-sensing technique measuring the return time of a laser pulse backscattered by a target as an echo signal whose intensity is proportional to the reflectance properties of the target (Baltsavias, 1999). Classical LiDAR survey records discrete echoes in real-time but may not be able to distinguish targets that are too close to each other. The minimum target separation is typically 0.4 m in airborne LiDAR (Launeau et al., 2018). LiDAR data is often available from national mapping agencies (NMAs), such as Ordnance Survey Ireland (OSi). However, LiDAR data from NMAs is restricted for vegetation mapping of coastal dune complex because of the limited spatial resolution (2 m from OSi) and historic acquisition date.

2.3.2 UAS technology used for vegetation mapping

In recent years there has been a significant advance in exploring the capabilities of small Unmanned Aerial Systems (UAS) as part of vegetation mapping research (Anderson and Gaston, 2013; Kaneko and Nohara, 2014; Pajares, 2015; Weil et al., 2017). In a comparison of other remote sensing platforms, UAS typically has a lower operating height which enables the collection of higher spatial resolution in a small area (Venturi et al., 2016). UAS also has flexible revisit times whereas the availability of other remote sensing data is limited in acquisition date and coverage depending on the national

committees. UAS also provides the possibility for data acquisition at inaccessible areas or hazardous environments.

Importantly, Structure from Motion (SfM), for UAS-collected data processing, is a technique that emerged in the last decade to construct photogrammetry-based 3D models (Tonkin and Midgley, 2016). The critical element for the implementation of photogrammetry to 3D mapping using SfM is the collection of numerous overlapping images of the study area (Uysal et al., 2015). From each pair of overlapping pictures, SfM can calculate the unique coordinate position (x, y, z or Easting, Northing, Elevation) of a set of particular points presented in both images. To maintain the accuracy of the mapping, the overlapping area for each two images should be at least 60%, ensuring sufficient shared points can be recognised by software for the map construction. To generate a 3D model, many thousands of matching object and textural features are automatically detected in multiple overlapping images of the ground surface, from which a high-density point cloud with 3D coordinate positions is derived.

2.3.3 Multispectral sensor mounted on UAS for vegetation mapping

A multispectral camera mounted on a UAS allows both visible and multispectral imagery to be captured that can be used for characterizing land feature, vegetation health and function. The Sequoia multispectral sensor has green (530-570 nm), red (640-680 nm), red edge (730-740 nm) and near-infrared (NIR) (770-810 nm) wavebands and a RGB sensor (400 nm to 700 nm) (Ren et al., 2017). Colour, structure and surface texture of different land features can influence the reflectance pattern of the wavebands (Fernández-Guisuraga et al., 2018). By analysing these different spectral reflectance patterns, different earth surface features can be identified. Multispectral sensors are also capable of discriminating vegetation in coastal dune complexes by calculating different visible

spectral indices. For example, Normalized differential vegetation index (NDVI), relates the reflectance of the land feature at NIR and red waveband, is widely used to differential green vegetation area from other land feature, such as water and soil (Gini et al., 2012). The index range is from -1 to 1, where 0-1 basically representing vegetation, negative values are mainly formed from clouds, water and snow, and values close to zero 0 representing the approximate value of no vegetation (Silleos et al., 2006). There are other spectral indices (Table 2.2) that can be calculated from multispectral bands for vegetation mapping (Weil et al., 2017).

Table 2.2 List of spectral indices calculated from multispectral bands for vegetation mapping

Vegetation index	**Formula**	**Explanation**
Relative Green	Green / (Red + Green + Blue)	The relative component of green, red and blue bands over the total sum of all camera bands. Less affected from scene illumination conditions than the original band value.
Relative Red	Red / (Red + Green + Blue)	
Relative Blue	Blue / (Red + Green + Blue)	
NDVI	(NIR - Red) / (NIR + Red)	Relationship between the NIR and red bands indicates vegetation condition due to chlorophyII absorption within the red spectral range and high

		reflectance within the NIR range.
gNDVI	(NIR - Green) / (NIR + Green)	Improvement of NDVI in assessing chlorophyll content.
GRVI	(Green –Red) / (Green + Red)	Relationship between the green and red bands in an effective index for detecting phenophases.

2.3.4 Classification accuracy of vegetation mapping

To create reliable vegetation mapping, accuracy classification of land-cover features at coastal zones is essential. Classification accuracy needs to be considered where O'Donoghue and Regan (2007) quote an overall classification accuracy of 65% as the minimum acceptable for reliable vegetation mapping. Supervised classification is a widely used method for vegetation mapping and is based on analysing the spectral pattern of the training types in different wavebands.

Mixed pixels, which are combinations of material, can be challenging to the classification process for vegetation mapping. The spectral library, as an option for vegetation mapping, is a collection of captured imagery of pure material based on field measurements. As each location has different characteristic materials, it is not always easy to find the corresponding materials in the spectral library with the materials in the target site. But relying on the spectral pattern of similar or closely related materials, a spectral library can still provide useful information for vegetation mapping. There is free and available spectral information for different land cover materials in the spectral library of the U.S.

Geological Survey (USGS) and the Ecostress spectral library of the California Institute Technology.

2.3.5 Influence of shadow areas on vegetation mapping

Weak reflectance from shaded areas complicates the classification of vegetation mapping. Various image of pre-processing methods have been applied to minimize the effects of shadows on image classification. These methods include band ratios (*e.g.* Helmer et al., 2000; Huang and Cai, 2009), additional topographic data (*e.g.* Liu et al., 2002), and topographic correction (*e.g.*, Tokola et al., 2001; Cuo et al., 2010). Band ratios can minimize changes in solar illumination caused by variations in the slope and aspect (Elvidge and Lyon, 1985). Song and Woodcock (2003) demonstrated that simulated NDVI is resistant to topographic effects at all illumination angles.

2.3.6 Summary

Surveying technologies, such as satellite-based hyperspectral data, airborne remote sensing data (LiDAR data) and UAS, are used to provide spatially-related land-cover data for vegetation mapping. Considering the limitation of coverage, acquisition date and spatial resolution of remote sensing data (including satellite data and LiDAR data), UAS offers a more flexible, high-resolution and more efficient method for data collection. The spectral library provides a collection of spectral patterns of land cover features, which can contribute to a better understanding of spectral patterns of different species in the site and help to improve the classification accuracy of vegetation mapping. A multispectral sensor mounted on a UAS enables a wider range of wavebands than only RGB sensor integrated with UAS. These additional wavebands from the multispectral sensor can be used to calculate vegetation indices values which represent the different growing status of

vegetation. But the influence of these additional wavebands from the multispectral sensor on the classification accuracy of vegetation mapping is significant and this has not been discussed yet in previous studies.

2.4 Environmental modelling for coastal dune complexes

2.4.1 The aim of environmental modelling at coastal dune complexes

Increasing human activities and global climate changes have threatened ecosystem maintenance at coastal zones, resulting in issues including soil erosion, flooding and habitat loss (Phillips and Jones, 2006; Martinez et al., 2016). Preservation and effective management of coastal zones require a full understanding of the key processes that control the dynamical morphology of coastal zones (Mitasova et al., 2005; Payo et al., 2017). However, coastal zones are difficult to study because of the complex relationships linking topography, hydrology, aeolian processes and sand movement throughout the system (Andrews et al., 2002; Payo et al., 2017). For a better understanding of coastal zones, environmental models were developed to explore and identify important processes at coastal zones, for example, how sand dunes form and change, and how vegetation, aeolian and other environmental variances effect morphology changes at coastal zones (Alhajraf, 2004; Zhang et al., 2010; Xia and Dong, 2016).

According to the relevant research in recent decades, environmental modelling is essential for the development of coastal zone management actions to reduce the influence of the environmental issues (Alhajraf, 2004; Martinez et al., 2016; Payo et al., 2017). Such modelling aims to represent the various environmental processes at coastal dune complexes.

2.4.2 Approaches to environmental modelling

There are five approaches to environmental model that are most commonly applied at coastal zones to better understand the environmental processes occurring at such areas and, hence, to contribute to improve environmental management. These five types of environmental modelling approaches are physical modelling, mathematic modelling, vegetation distribution modelling, 3D modelling and coastal vulnerability assessment modelling, and they will be considered in the following sections.

2.4.2.1 Physical modelling

A physical coastal zone model represents complex, real-world, three-dimensional coastal geomorphology by using simple geometries (Payo et al., 2017). Such a physical, or hardware, model uses materials of the natural system which are geometrically and dynamically similar to the real world (Mendoza et al., 2017). This type of modelling is often used to simulate the interactions between waves and coastal dune erosion. It has also been used to evaluate the performance of mathematical models by laboratory experiments (Kobayashi et al., 2009; Mendoza et al., 2017; Payo et al., 2017). Figure 1 represents the process of generating a physical model.

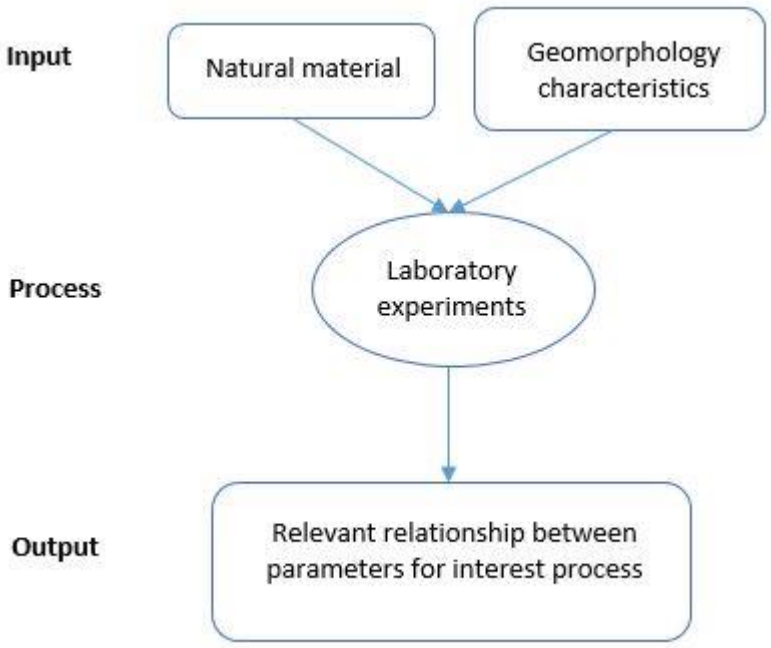

Fig.2.5 Flowchart of physical modelling procedures.

Physical models often deal with processes that occur along coastlines. These include the effects of water levels, tides, waves, currents, and winds on beaches, islands, harbours, and coastal structures (Hughes, 1993; Briggs, 2013). As an example of the procedures outlined in Figure 2.5, to create a physical model of vegetation influence at coastal zones, Mendoza et al (2017) sought to model the reality by constructing a scale-down replica using the natural material in a same geomorphological surface as the research site. In this research, another 24 experiments, with different vegetation coverages, were conducted to conclude that vegetation increases the resistance and the resilience of the beach profile; as it was observed in the experiments that the vegetation supports the dune providing sediment to the beach in the reflective profile and strengthens the dune in the dissipative profile.

2.4.2.2 Mathematic modelling

In modelling environmental systems, one of the more widely used options is a mathematical simulation model (Hardisty et al., 1993). There are three most-used mathematical model types for coastal zones modelling, *viz.* profile models, coastline models and volumetric models (DeVriend et al., 1993; Hanson et al., 2003).

Coastal profile models simplify coastal zones to a two-dimensional system assuming uniformity in the direction. Such 2D models simulate vertical changes and along-shoreline changes at the coastal zones (Zheng and Dean, 1997; Kobayashi, 2016). The Cross-Shore Model (CSHORE) is an example of a coastal profile model which is capable of predicting nearshore morphological changes on the time scale of storms and seasons (Kobayashi, 2016; Mendoza et al., 2017). The CSHORE model is used to predict profile changes which can be compared with observed profile changes for accuracy assessment. The CSHORE model can quite accurately (errors smaller than 10%) represent the cross-shore significant wave height distribution in the surf zone which may have influence on shoreline retreat (van Rijn et al., 2003).

In coastline models (also referred as one-line models), sand beach morphology is represented by a single contour line, ignoring the elevation and width of the beach surface (Hanson and Kraus, 2011). The Coastal One-line Vector Evolution (COVE) model is one such model that is specialized for complex coastal geometries with high planform curvature shorelines (Larson and Hanson, 1997). COVE models are coastal evolution models in which the coast is represented by a single line. They are built around a central assumption that the cross-shore beach profile maintains some average morphology, which is only temporarily perturbed by storm events (Masselink et al., 2015), and therefore, a single shoreline contour is sufficient to describe the planform morphology of the coast. The later innovation of COVE is a two-line model because a second line represents the

coastal cliffs top, which interacts with the shoreline, eroding to provide beach sediment which then offers protection to the cliff against further erosion. COVE models of shoreline evolution can reproduce embayed beach morphology in the lee of a headland or promontory (Rea and Komar, 1975; Hanson, 1989; Weesakul et al., 2010). Rea and Komar (1975) used simple rules to describe the adjustment in wave height and direction due to diffraction in the shadow of a promontory and demonstrated that the resulting bay forms were similar in form to a logarithmic spiral. Weesakul et al. (2010) presented a similar model that found good agreement when compared to experimental data and the empirical parabolic model for bay morphology. Both of these studies examined the formation of bays under the influence of a single dominant wave direction, with the morphology of the highly curved portion of the bay controlled by diffraction of waves into the shadowed region.

Volumetric models represent characterises and changes of sediment in coastal zones by a single variable volume (Stive et al., 1997; Woolard and Colby, 2002; Eamer and Walker, 2013). The Aggregated Scale Morphological Interaction between Inlets and Adjacent Coast (ASMITA) model is a behaviour-orientated model for predicting the large-scale evolution of estuaries over decades to centuries (Stive et al., 1997). Within ASMITA the estuary must be schematised into morphological elements, such as channels, tidal flats and ebb-tidal deltas. For each element a morphological equilibrium is defined relating the morphology to the hydrodynamic forcing (usually tidal prism). The volumes of the schematised elements are predicted through time, based on sediment exchange between elements which is driven by difference between current volume and equilibrium volume. The notion of an ASMITA was early proposed by Stive et al. (1998) for the study of estuaries and inlet response to sea level rise. This ASMITA model has recently been used to investigate the morphological evolution of tidal basins on different time scales and the

results demonstrated that this model can be used successfully to study complicated morphological situations especially for tidal inlet systems (Hibma et al., 2003; Elias, 2006). The ASMITA was helpful for improving understanding of the processes governing tidal inlet evolution as it requires detailed information of the hydrodynamics and sedimentary processes for long-term time scales. As detailed information on the long-term evolution of a tidal inlet system is far more difficult to obtain from a field survey or a scale model experiment, the ASMITA model can be utilized as a "numerical laboratory" to better understand the dynamics of a tidal inlet system. It also enables forecasting the effects of a modification of a tidal inlet system due to changing hydrodynamic conditions, for example as a result of extreme events (Eamer and Walker, 2013).

Previous research also illustrates some valid examples of mathematical modelling to represent different specialized processes at coastal zones. The open source model, Xbeach, is widely used for beach environmental modelling. It is specifically design for small-scale (project-scale) coastal applications, but can also be used for the morphology model system (Roelvink et al., 2009). The model solves coupled 2D horizontal equations for wave propagation, flow, sediment transport and bottom changes, for varying (spectral) wave and flow boundary conditions. Thus, XBeach model was used as a modelling tool for beach and dune erosion, for example at Sateague Island in Maryland (Roelvink et al., 2009) and Santa Rosa Island in Florida (McCall et al., 2010). More recently, the tool has been applied for the modelling of post-storm beach accretion and recovery (Pender and Karunarthna, 2013) and gravel beach variability (McCall et al., 2015). Although XBeach has been extensively examined and validated for beach erosion and accretion, it cannot predict post-storm coastal sand dune erosion accurately (Roelvink et al., 2009).

As coastal zones include multiple landforms, the modelling should consider the interactions between the component landforms, for example beaches and dune complexes (Payo et al., 2017). This is difficult as the interactions are complicated and not fully understood. At this stage, researchers have found solutions by using model-to-model interfaces, integrating several software suites to develop component models in the same platform. Significant development has been achieved in this field in the last decade, especially by the Open Modelling Interface (OpenMI) and Community Surface Dynamics Modelling System (CSDMS) (Gregerse et al., 2005; Hutton et al., 2014). They both aim to provide access by linking various different models together to explore broader system processes and interactions. OpenMI enables the exchange of data between process simulation models and also between models and other modelling tools such as databases and analytical and visualization applications. The results can contribute to an understanding of how processes interact and to predict the likely outcomes of those interactions under given conditions. CSDMS provides new ways of developing and employing software to understand earth system dynamics. CSDMS supports the development, dissemination, and archiving of community open-source software, that reflects and predicts earth-surface processes over a range of temporal and spatial scales. For example, Computational Dynamics Software (OpenFOAM) is specialised for modelling the near surface wind flow throughout the coastal zones (Jackson et al., 2013). OpenFOAM was applied to model water turbulence by simulating flow over complex foredune and topography (Parsons et al., 2004; Smyth et al., 2012). However, there are still some challenges for linking the component models in this way, including difficulties to unify the assumption for the integrated model based on the various assumptions for component models (Payo et al., 2017). Moreover, different spatial structures of

component models, for example geometries, volumes and locations of sediment, may have some unknown influence on the last frameworks of modelling.

2.4.2.3 Vegetation distribution modelling

Vegetation modelling, capturing land-cover and land-use information which represent ecological aspects of nature in detail, is essential for mapping and monitoring changes in nature (Bryn and Hemsing 2012; Ullerud et al., 2016).

Vegetation at coastal zones has a strong impact on morphology and dynamics as it can protect the surface sand layer and can influence sand transport (Sabatier et al., 2009). Vegetation is also a critical environmental component of the coastal ecosystem for food production, resource conservation, nutrient cycling, and carbon sequestration (Woo et al., 1997; Kuplich, 2006). Vegetation modelling of coastal zones, with accurate distribution and population estimates for different functional plant species, can be used to analyse vegetation dynamics, quantify spatial patterns of vegetation evolution, analyse the effects of environmental changes on vegetation, and predict spatial patterns of species diversity (Vaca et al., 2011). Such information can contribute to the development of targeted land management actions that maintain biodiversity and ecological functions.

Vegetation distribution modelling is increasingly used for predictions of potential occurrences of species within applied ecology (Guisan and Zimmermann, 2000; Drew et al., 2011; Yackulic et al., 2013). Most vegetation distribution models have an emphasis at the species level, but the method has been used also in studies that focus on the vegetation- or habitat-type level (Miller et al., 2007; Weber, 2011; Hemsing and Bryn, 2012), as well as higher levels such as floristic or landscape regions (Zhang et al., 2012; Moriondo et al., 2013).

There are principally two types of approaches for vegetation distribution modelling (Austin, 2007; Halvorsen, 2013). Firstly, spatial approaches aim at modelling the potential present distribution of a target category into the space around present points using explanatory variables (*e.g.* Guisan and Zimmermann, 2000; Ashcroft et al., 2012). Secondly, there are temporal approaches aimed at modelling the potential future, or reconstructing the past distribution, of a target category into a new space given temporal changes in explanatory variables (*e.g.* Wiens et al., 2009; Legault et al., 2013).

Vegetation types are discrete ecological entities with differences in species composition and physiognomy. Thus, the ability of the modelling will vary depending on how well their distributions are explained by explanatory variables (Franklin, 2009), and also on how strictly the vegetation types have been defined in environmental and species specific terms. Abundant vegetation types might be affected by a large range of environmental parameters, which may make it difficult to find specific criteria for their distribution. Rare vegetation types, however, are often strongly correlated with more narrow ranges along several gradients (Halvorsen, 2012) and this could make them easier to model. Following the same logic, vegetation types appearing in different ecosystems, such as in wetlands and mountains, could be regulated by, and related to, different sets of environmental variables, resulting in varying modelling performance among ecosystems.

2.4.2.4 3D modelling

To monitor the geographical features at coastal zones, 3D models can be developed to simulate the morphology of the areas. Technological advancements in remote sensing, laser altimetry, spatial surveys using a Global Positioning System (GPS), particularly in kinematic mode, have been used to accurately map morphological features and indicators of coastal zones. Multisensor, multiscale, and multitemporal remote images have

contributed greatly to coastal geomorphological studies and have been used to measure both short and long-term erosion/accretion processes (Moore, 2000; Kumar and Jayappa, 2009; Deepika et al., 2013). Multisource database integration through Geographic Information Systems (GIS) promotes the understanding and quantification of the erosion/accretion rate from year to year and from decade to decade (*e.g.*, Crowell et al., 1993; Boak and Turner, 2005; Klemas, 2011).

3D models allow for the simulation of coastal processes in a more precise way than in possible using the two-dimensional models, especially when the processes to be simulated are characterized by a strong three-dimensionality in terms of geometry (Krueger et al., 2011). For example, a detailed 3D model can represent the geo-structural characterization of a rock cliff surface and also support the deterministic analyses aimed at assessing the stability of the cliff.

With the rapid development in technologies, some researchers have focused on the different aspects of Virtual Reality (VR)-based 3D coastal environment visualisation in recent years (Żywicki et al., 2017). Currently, standard VR systems use headsets and multi-projected environments to generate realistic images, sounds and other sensations that simulate a user's physical presence in a virtual environment (Burdea and Coiffet, 2015; Wang, 2018). A person using virtual reality equipment is able to look around the artificial world, move around in it, and interact with virtual features or items. VR technology integrates computer graphics, image processing, multimedia, sensors, networks and other multidisciplinary achievements (Zhou et al., 2011). In the 3D digital coastal environment, real-time rendering of large-scale scenes is one of the important issues to be solved, because the number of models in the digital scene can be very large.

2.4.2.5 Coastal vulnerability assessment model

Coastal vulnerability assessment modelling provides vulnerability analysis of coastal zones, with respect to disciplines such as geography, physical, urban, and territorial planning, economics, and environmental management. Coastal vulnerability is the identification of resources at risk from coastal hazards, while a coastal hazard may be defined as the occurrence of a phenomenon, which has the potential for causing damage to natural ecosystems, buildings, and infrastructure (Serafim et al., 2019). The main coastal hazards are tropical storms and hurricanes, storm surges, tsunamis, flooding, landslides, volcanic eruptions, earthquakes and sea-level rise. More recently, as a result of population growth, urbanisation and a movement towards the coast, the vulnerability of coastal areas has greatly increased (ISDR, 2004).

Coastal vulnerability assessment modelling is important as the assessment models can provide required data for the adequate identification of danger or hazard zones. Computer science tools such as Geographic Information Systems (GIS) have facilitated this type of identification and analysis (Kumar et al., 2010). Such risk analysis has increasingly been used to contribute data on threats, or risk, to physical and territorial planning specialists, which is helpful in the decision making process (Bankoff et al., 2003).

One of the most widespread methods to assess coastal vulnerability is the application of multi-criteria indices to support preventive management measures (Adger, 2006; Kantamaneni, 2016; Nguyen et al., 2016; Kantamaneni et al., 2018). The Coastal Vulnerability Index (CVI), described by Gornitz and Kanciruk (1989) and Gornitz (1991), has been widely applied, with adjustments to the local variables and available data, for example geomorphology, cliff type, coastline orientation, regional coastal slope, tidal range, significant wave height, relative sea-level rise, and long-term shoreline erosion and accretion rates. Geoprocessing and numerical techniques are commonly employed in coastal vulnerability assessment modelling, for example, GIS, remote

sensing and numerical modelling (Bonetti et al., 2013). Coastal vulnerability assessment modelling allows for the translation of information from experts into simple models, and data into comparable quantitative data and to aggregate the data into a single multi-criteria framework (Le Cozannet et al., 2013).

Gornitz (1990) assessed the vulnerability of the east coast of the United States with emphasis on future sea-level rise. Thieler and Hammer-Klose (1999) used the coastal slope, geomorphology, relative sea-level rise rate, shoreline change rate, mean tidal range and mean wave height for assessment of coastal vulnerability of the same coast. The results demonstrated that 28% of the U.S. Atlantic coast is of low vulnerability, 24% of the coast is of moderate vulnerability, 22% is of high vulnerability, and 26% is of very high vulnerability. Belperio et al. (2001) considered elevation, exposure, aspect, and slope as the physical parameters for assessing coastal vulnerability to sea-level rise and concluded that coastal vulnerability was strongly correlated with elevation and exposure, and that regional scale and distributed coastal process modelling might be suitable as a ‘‘first cut’’ in assessing coastal vulnerability to sea-level rise in tide-dominated, sedimentary coastal regions.

Pendleton et al. (2005) assessed the coastal vulnerability of sea level rise by calculating a CVI using both geologic (shoreline-change rate, coastal geomorphology, coastal slope) and physical process variables (sea-level change rate, mean significant wave height, mean tidal range). The CVI allows the six variables to be related in a quantifiable manner that expresses the relative vulnerability of the coast to physical changes due to future sea-level rise. Kumar (2006) used CVI with the sea-level rise scenario for calculating the potential vulnerability for coastal zones of Cochin, southwest coast of India, and concluded that climate induced sea-level rise will bring profound effects on coastal zones. Rajawat et al. (2006) delineated the hazard line along the Indian coast with CVI using data on coastline

displacement, tide, waves, and elevation. Hegde and Reju (2007) developed a coastal vulnerability index for the Mangalore coast using geomorphology, regional coastal slope, shoreline change rates, and population. However, they opined that additional physical parameters like wave height, tidal range, probability of the storm, can enhance the quality of the CVI.

The Analytical Hierarchical Process (AHP) method is suitable for complex decisions which involve the comparison of decision elements that are difficult to quantify. AHP has great value in the case of coastal vulnerability assessment as the data are highly heterogeneous in terms of its scale and temporal resolution and there is a lack of a purely deterministic method owing to the huge data involved from different sources (Le Cozannet et al., 2013; Mani Murali et al., 2013). AHP involves building a hierarchy of decision elements and then making comparisons between each possible pair in each cluster (as a matrix). This gives a weighting for each element within a cluster (or level of the hierarchy) and also a consistency ratio (useful for checking the consistency of the data). There are few examples of the use of AHP integrated to coastal vulnerabilities assessments. Chang et al. (2012) applied the method to rank different coastal protection in Miaoli coast, Taiwan. Yin et al. (2012) have made an assessment of the coastal vulnerability to sea level rise for the Chinese coast. Le Cozannet et al. (2013) extensively discussed the advantages, disadvantages and uncertainties of the incorporation of AHP into coastal vulnerability assessments. Mani Murali et al. (2013) combined socioeconomic and physical variables with AHP derived weights to calculate the coastal vulnerability index for the Puducherry coast, India.

However, a lack of consensus about the terminology is observed in vulnerability studies as a function of the variety of research objectives and phenomena studied (Adger, 2006; Bonetti and Woodroffe, 2017). Since there is a wide range of areas in which vulnerability

can be applied, a clear explanation of the adopted terminology is needed to support ongoing research.

2.4.3. Modelling methodologies

To start a modelling project, the first thing is to consider whether a model is necessary and if so, to decide what type is the most appropriate (Hardisty et al., 1993). The choice of model type depends on the aims of the project, the nature of the target system and the level of understanding of the processes operating in the system. Thornes (1989) said 'The credibility of models hinges upon the credibility of their science base'.

The next step is to identify an appropriate model structure by estimating the environmental parameters which may have influence on the interest process (Roelvink et al., 2009). These parameters will characterise the model and finally will be used to validate the model. Estimation of parameters for a mathematical model is based on field observation. The values of parameters should be adjusted during calibration to minimize the difference between the model output and observation. For a complex modelling project, this adjustment may need running the model many times to set parameters values correspondingly according to each comparison of the output with observation (Kankara et al., 2013). A more practical solution is to conduct a sensitivity analysis, by deliberately changing parameter values to assess their effects on model outputs. Usually only a relatively small number of parameters can be identified as sensitive parameters, which has greater influence on modelling structure and are considered as the emphasis in the modelling project (Williams et al., 2014).

The final step for modelling is a validation test, conducted by a comparison between the model and the real world system. In principle, a validation test requires a completely different set of data from that used to construct the model in the first place (Gupta et al.,

2003). If the modelling output of the test dataset is similar to the observation, the model is considered valid. However, there will always exist some degree of uncertainty in modelling output because models are only absolutely valid under the assumptions of their original context.

2.4.4. Spatial datasets for environmental modelling

One of the constraints of spatially-related environmental modelling is the appropriate observation georeferenced datasets, *viz.* physical modelling, mathematical modelling, vegetation distribution modelling, 3D modelling and coastal vulnerability modelling projects. High-resolution and high-accuracy spatial datasets can contribute to the development of accurate coastal dune complex models (Acosta et al., 2005). However, accurate spatial data collection for a coastal dune complex is a challenging task as it requires a considerable investment in time and resources (McKenna et al., 2005).

Generally, according to the relevant research in recent decades, there are a number of spatial data collection methods appropriate for modelling, including aerial photogrammetry, optical satellite imagery, Synthetic Aperture Radar (SAR) data, Light Detection and Ranging (LiDAR) data, Total Station (TS), Robotic Total Station (RTS), Network Real Time Kinematic (NRTK), Terrestrial Laser Scanning (TLS) and Unmanned Aircraft System (UAS). Aerial photogrammetry and optical satellite imagery have been used for modelling for monitoring coastal line changes in the long term (Curr et al., 2000). However, a single dune complex is typically represented as a long and narrow strip because such mapping is generally produced at national and regional scales (Acosta et al., 2005). There are, notwithstanding, a number of data processing approaches for generating finer-scale mapping from the more traditional sources (Stuart et al., 2002; Timm and McGarigal, 2012; Rapinel et al., 2014). However, it is still quite difficult to

produce, from these sources, modelling with accurate and detailed land cover information for small coastal dune complexes. A considerable limitation of optical satellite imagery, in particular, is the influence of weather, especially cloud-cover which can interfere with the view of the earth's surface (McGovern et al., 2002).

Satellite-based SAR is a valid option for generating (two-dimensional) mapping or (three-dimensional) modelling, eliminating the influence of weather conditions (Shao et al., 2016). Orthorectified SAR images were used to map the complete coastline of Antarctica with a spatial resolution of 25 m. The absolute accuracy of planimetric positioning of the resultant coastline was estimated at 130 m and was considered adequate for supporting cartographic and scientific applications at 1:50,000 scale (Liu and Jezek, 2004). TerraSAR-X, SAR imagery with much higher resolution (3 × 3 m), was used to monitor and assess larger-scale coastal dynamics (Vandebroek et al., 2017). SAR, a greyscale dataset, is capable of distinguishing building, roads and water areas for urban mapping but it has limitations regarding the separation of species of vegetation, which influence land feature classification for mapping of coastal dune complexes.

Aircraft-based LiDAR is an alternative resource for 3D models even for a smaller target area eg. 50-100 ha (Bolivar et al., 1995; Grebby et al., 2014). It is often available from national mapping agencies (NMA's), such as OSi. OSi quote spatial resolutions and vertical accuracies in rural areas of 0.5 m and 0.5 m respectively (OSi 2017) and charge *c.* €250 per square kilometre for the data. LiDAR data can be used to generate both Digital Terrain Models (DTM) and Digital Surface Models (DSM) (Crapoulet et al., 2016). For a study at a coastal dune complex in North Carolina, a LiDAR dataset was used to represent coastal dunes for volumetric change analysis (Woolard and Colby, 2002).

Ground surveying methods, including TS and Global Navigation Satellite System (GNSS), are suitable for modelling of smaller target areas (D'iorio et al., 2007; Lee et al., 2013). These on-site data collection methods provided more ground truth, and up-to-date and accurate information than many alternatives (D'iorio et al., 2007). The distance measurement accuracy of TS is 2 mm+2 ppm over a distance of about 1 km (Lee et al., 2013). However, the operation and performance of TS in field surveying projects is limited by poor visibility circumstances, such as darkness, rain, snow, thickets or physical occlusions (Schneider et al., 2008). There are three techniques based on GNSS to enhance the precision of satellite position data. These are Post Processing Kinematic (PPK), Real Time Kinematic (RTK) and NRTK (Li et al., 2015). The accuracy of GNSS is 10-20 mm (Dow et al., 2009). With lighter equipment and easier operation, these GNSS techniques can save labour and time in collecting the same amount of modelling data as TS (Mieczysław, 2013).

In recent decades, TLS, considered as a ground-based version of the airborne LIDAR, has been frequently used for high-resolution terrain vegetation, and other landscape features mapping over limited distances in the range of 50–300 m (Parrish et al., 2016). TLS is able to record a highly detailed 3D point cloud that can be transformed into digital 3D landscape models and GIS DEMs. TLS can also acquire digital photos of the same areas being laser-scanned, and RGB colour values can be extracted from the photos. These RGB values can be used to create a highly photorealistic 3D landscape model. For beach mapping, the resulting digital models are highly accurate renditions of in-situ conditions at the time the scanning is done, and they can be used for both visualization purposes (as photorealistic models) as well as morphometric measurements (as DEMs) (Ersilia et al., 2012). The spatial resolution of the resulting models is orders of millimetres, which is

much higher than data derived from satellite data or other airborne remote sensing techniques (Staiger, 2003).

Most recently, UAS platforms are typically grouped into two main categories: rotary-wing UAS and fixed-wing UAS (Gomez and Green, 2017). Rotary-wing UAS has more complex mechanics, which result in lower speeds and shorter flight ranges. While fixed-wing UAS have a relatively simple structure making stable platforms for planning autonomous flights. Fixed-wing UAS enables longer flight duration and higher speeds, which is more suitable for aerial survey over large areas.

UAS, integrated with modern digital camera technology, breaks the time and space constraint allowing a study site to be remotely surveyed in a significantly reduced time with the result of a large number of high resolution and high accuracy images (Smith et al., 2009; Colomina and Molina, 2014). UAS imagery, using Structure from Motion (SfM) processing techniques, has created a new opportunity for photogrammetry to create 3D surface models from a large number of overlapping photographs (Hodgson et al., 2013). To maintain the spatial accuracy of the data, the overlapping area for each two images should be at least 60%, making sure enough shared points can be recognised by the software for map construction (Zelizn, 2016). UAS is also a user-friendly and scalable methodology albeit with the requirement of specialized software and with restrictive image collection conditions such as wind speed and light intensity (Bemis et al., 2014). For the management of UAS, different countries have different mandatory requirements established by their national aviation authorities and particular operating licenses and insurances should be in place before operating a UAS (Tomasello et al., 2016).

2.4.5. Summary

Environmental modelling is considered an efficient means to explore, study and identify key processes at coastal zones and has been used for research about complex relationships linking topography, hydrology, aeolian processes and sand movement throughout the system. Results from such modelling can contribute to coastal environmental management by finding solutions for environmental issues at coastal zones, for example sand erosion, storm influence, flooding and habitat loss.

Five environmental modelling types have been widely applied at coastal zones, which are physical modelling, mathematic modelling, vegetation distribution modelling, 3D modelling and coastal vulnerability assessment modelling. Each of these modelling types has its specific applied condition and emphasis at its output. For example, vegetation distribution modelling concentrates on vegetation changes and other position-related environmental factors (*e.g.* slope, elevation, aspect), whilst 3D modelling including height information which is more suitable for cliffs or dune system analysis. Results from coastal vulnerability assessment models have an emphasis on finding vulnerability priority areas, which is important for efficient implementation of environment management for coastal protection. Physical modelling is often used in laboratory experiments to simulate the processes at coastal zones or evaluate the performance of other models. Mathematical models are most widely used in coastal environmental modelling and have become well-developed in recent years. There are some available model patterns, for example CSHORE coastal profile model, COVE coastline model, ASMITA coastal volumetric model, beach modelling Xbeach, OpenMI and CSDMS for the coastal zone with component landforms, and OpenFOAM for near surface wind flow throughout the coastal zones.

In general, it is essential to have a good knowledge of these modelling types before starting a project for which modelling might be appropriate. With the exception of

physical modelling which only needs simple geomorphology information, the other four modelling types need accurate and precise geomorphology information of the target area. Thus, spatial dataset collection is a necessary part for coastal environmental modelling.

2.5 References

Acosta, A., Carranza, M.L., Izzi, C.F., 2005. Combining land cover mapping of coastal dunes with vegetation analysis. Applied Vegetation Science 8, 133-138.

Adger, W.N., 2006. Vulnerability. Global Environmental Change 16, 268–281.

Afeni, T.B., Cawood, F.T., 2013. Slope Monitoring using Total Station: What are the Challenges and How Should These be Mitigated? South African Journal of Botany, 2, 41–53.

Alhajraf, S., 2004. Computational fluid dynamic modeling of drifting particles at porous fences. Environmental Modelling & Software 19, 163–170.

Amaro, V.E., Gomes, L.R.S., De Lima, F.G.F., Scudelari, A.C., Neves, C.F., Busman, D.V., Santos, A.S., 2015. Multitemporal Analysis of Coastal Erosion Based on Multisource Satellite Images, Ponta Negra Beach, Natal City, Northeastern Brazil. Marine Geodesy 38, 1–25.

Anderson, T.R., Ryabchenko, V.A., Fasham, M.J.R., Gorchakov, V.A., 2007. Denitrification in the Arabian Sea: a 3D ecosystem modelling study. Deep-Sea Research I 54, 2082–2119.

Andrews, B., Gares, P.A., Colby, J.D., 2002. Techniques for GIS modeling of coastal dunes. Geomorphology 48, 1–3, 289–308.

Artese, S., Perrelli, M., 2018. Monitoring a Landslide with High Accuracy by Total Station: A DTM-Based Model to Correct for the Atmospheric Effects. Geosciences 2076-3263, 8, 2, 1-23.

Ashcroft, M.B., French, K.O., Chisholm, L.A., 2012. A simple post-hoc method to add spatial context to predictive species distribution models. Ecological Modelling 228, 17–26.

Austin, M., 2007. Species distribution models and ecological theory: a critical assessment and some possible new approaches. Ecological Modelling 200, 1–19.

Baltsavias, E.P., 1999. Airborne laser scanning: Existing systems and firms and other resources. ISPRS Journal of Photogrammetry and Remote Sensing 54, 164–198.

Bankoff, G., Frerks, G., Hilhorst, D., 2003. Mapping Vulnerability: Disasters, Development and People, chapter 3. London, Earthscan Publishers.

Bartsch, A., Höfler, A., Kroisleitner, C., Trofaier, A.M., 2016. Land Cover Mapping in Northern High Latitude Permafrost Regions with Satellite Data: Achievements and Remaining Challenges. Remote Sensing 8, 9791–28.

Belperio, T., Bourman, B., Bryan, B., Harvey, N., 2001. Distributed process modeling for regional assessment of coastal vulnerability to sea-level rise. Environmental Modeling and Assessment 6, 1, 57–65.

Bemis, S.P., Micklethwaite, S., Turner, D., James, M.R., Akciz, S., Thiele, S.T., Bangash, H.A., 2014. Ground-based and UAV-Based photogrammetry: A multi-scale, high-resolution mapping tool for structural geology and paleoseismology. Journal of Structural Geology 69, 163-178.

Boak, E.H., Turner, I.L., 2005. Shoreline definition and detection: A review. Journal of Coastal Research 21, 4, 688–703.

Bolivar, L., Carter, W., Shrestha, R., 1995. Airborne laser swath mapping aids in assessing storm damage. Florida Engineering, 26–27.

Bonetti, J., Klein, A.H.F., Muler, M., de Luca, C.B., Silva, G.V., Toldo, J.R., E. E, González, M., 2013. Spatial and numerical methodologies on coastal erosion and flooding risk assessment. Coastal Hazards, Research Library Series, Springer, Dordrecht, 423–442.

Bonetti, J., Woodroffe, C.D., 2017. Spatial analysis on GIS for coastal vulnerability assessment. Geoinformatics for Marine and Coastal Management. CRC Press, Boca Raton, 367–396.

Briggs, M., 2013. Basics of Physical Modeling in Coastal and Hydraulic Engineering. US Army Engineer Research and Development Center, Coastal & Hydraulics Laboratory, ERDC/CHL-XIII-3.

Bryn, A., Hemsing, L.Ø., 2012. Impacts of land use on the vegetation in three rural landscapes of Norway. International Journal of Biodiversity Science, Ecosystem Services & Management 8, 360–371.

Burdea, G., Coiffet, P., 2015. Virtual Reality Technology. Digital Technology and Application 95, 6, 663-664.

Campos-Taberner M, García-Haro F, Boschetti M., 2017. Exploitation of SAR and Optical Sentinel Data to Detect Rice Crop and Estimate Seasonal Dynamics of Leaf Area Index. Remote Sensing 9, 3, 1-17.

Chang, H.K., Liou, J.C., Chen, W.W., 2012. Protection priority in the coastal environment using a hybrid ahp-topsis method on the Miaoli coast, Taiwan. Journal of Coast Research 28, 369–374.

Clark, J.R., 1977. Coastal environment management. John Wiley & Sons, New Jersey, U.S., ISBN 0471158542.

Colomina, I., Molina, P., 2014. Unmanned aerial systems for photogrammetry and remote sensing : A review. ISPRS Journal of Photogrammetry and Remote Sensing 92, 79–97.

Cooper, J.A.G., Boyd S.W., 2011. Climate change and coastal tourism in Ireland. In: Jones and Phillips, Disappearing destinations, 125-143.

Crapoulet, A., Héquette, A., Levoy, F., Bretel, P., 2016. Using LiDAR Topographic Data for Identifying Coastal Areas of Northern France Vulnerable to Sea-Level Rise. Journal of Coastal Research, 75, 1067-1071.

Crowell, M., Leatherman, S.P., Buckley, M.K., 1993. Shoreline change rate analysis: Long-term versus short-term data. Shore and Beach 61, 2, 13–20.

Cuo L., Vogler J.B., Fox J.M., 2010. Topographic normalization for improving vegetation classification in a mountainous watershed in Northern Thailand. International Journal of Remote Sensing 31, 3037–3050.

Deepika, B., Avinash, K., Jayappa, K.S., 2013. Shoreline change rate estimation and its forecast: remote sensing, geographical information system and statistics-based approach. International Journal of Environmental Science and Technology 11, 2, 395–416.

Delaney, A., Devaney, F.M, Martin, J.M., Barron, S.J., 2013. Monitoring survey of Annex I sand dune habitats in Ireland. Irish Wildlife Manuals, No. 75. National Parks and Wildlife Service, Department of Arts, Heritage and the Gaeltacht, Dublin, Ireland.

Devoy, R.J.N., 2008. Coastal Vulnerability and the Implications of Sea-Level Rise for Ireland. Journal of Coastal Research 24, 325-341.

DeVriend, H.J., Zyserman, J., Nicholson, J., Roelvink, J.A., et al., 1993. Medium-term 2-DH coastal area modelling. Coastal Engneering 21, 193–224.

D'iorio, M., Jupiter, S.D., Cochran, S.A., Potts, D.C., 2007. Optimizing remote sensing and GIS tools for mapping and managing the distribution of an invasive mangrove (Rhizophora mangle) on South Molokai, Hawaii. Marine Geodesy 30, 1–2, 125–144.

Dodet, G., Dertin, X., Taborda, R., 2010. Wave climate variability in the north-east Atlantic Ocean over the last six decades. Ocean Model. 31, 120–131.

Dow, J.M., Neilan, R.E., Rizos, C., 2009. The international GNSS service in a changing landscape of global navigation satellite systems. Journal of Geodesy 83, 191–198.

Drew, C.A., Wiersma, Y.F., Huettmann, F., 2011. Predictive species and habitat modelling in landscape ecology: concepts and applications. Springer, Berlin, DE.

Eamer, J.B.R., Walker, I.J., 2013. Quantifying spatial and temporal trends in beach–dune volumetric changes using spatial statistics. Geomorphology 191, 94–108

Elias, E., 2006. "Morphodynamics of Texel Inlet," PhD thesis, Delft University of Technology, IOS Press, The Netherlands, 261.

Elvidge, C., Lyon, R., 1985. Influence of rock–soil spectral variation on the assessment of green biomass. Remote Sensing of Environment 17, 265–279.

Ersilia, O., Constantin, C., Marius, S., 2012. Terrestrial Laser Scanner Surveying Versus Total Station Surveying for 3D Building Model Generation. Mathematical Modelling in Civil Engineering 4, 168–178.

ESA (European Space Agency), 2000-2018. User guides introduction. ESA sentinel online, https://sentinels.copernicus.eu/web/sentinel/about-sentinel-online.

Fenu, G., Cogoni, D., Ferrara, C., Pinna, M.S., Bacchetta, G., 2012. Relationships between coastal sand dune properties and plant community distribution: The case of Is Arenas (Sardinia). Plant Biosystems 146, 3, 586–602.

Fernández-Guisuraga, J.M., Sanz-Ablanedo, E., Suárez-Seoane, S., Calvo, L., 2018. Using Unmanned Aerial Vehicles in Postfire Vegetation Survey Campaigns through Large and Heterogeneous Areas: Opportunities and Challenges. Sensors 18, 2, 1-17.

Franklin, J., 2009. Mapping species distributions: spatial inference and prediction. Cambridge University Press, Cambridge, UK.

Gini, R., Passoni, D., Pinto, L., Sona, G., 2012. Aerial images from an UAV system: 3d modeling and tree species classification in a park area. Int. Arch. Photogram. Remote Sensing Spatial Information Science 39, B1, 361–6.

Glabsch, J., Heunecke, O., Schuhbäck, S., 2009. Monitoring the Hornbergl landslide using a recently developed lowcost GNSS sensor network. Journal of Applied Geodesy 3, 179–192.

Gomez, C., Green, D.R., 2017. Small unmanned airborne systems to support oil and gas pipeline monitoring and mapping. Arabian Journal of Geosciences 10, 202.

Gonçalves, J.A., Henriques, R., 2015. UAV photogrammetry for topographic monitoring of coastal areas. ISPRS Journal of Photogrammetry and Remote Sensing 104, 101–111.

Gornitz, V., 1990. Vulnerability of the east coast, U.S.A. to future sea level rise. Journal of Coastal Research 9, 201–237.

Gornitz, V., 1991. Global coastal hazards from future sea level rise. Palaeogeogr. Palaeoclimatol. Palaeoecol. 89, 379–398.

Gornitz, V., Kanciruk, P., 1989. Assessment of global coastal hazards from sea-level rise. In: Symposium on Coastal and Ocean Management 6, Proceedings Charleston.

Gregerse, J.B., Gijsbers, P.J.A., Westen, S.J.P., Blind, M., 2005. OpenMI: the essential concepts and their implications for legacy software. Advances in Geosciences 4, 37–44.

Grebby, S., Cunningham, D., Tansey, K., Naden, J., 2014. The impact of vegetation on lithological mapping using Airborne Multispectral Data: A case study for the North Troodos Region, Cyprus. Remote Sensing 6, 10860–10887.

Guisan, A., Zimmermann, N.E., 2000. Predictive habitat distribution models in ecology. Ecological Modelling 135, 147–186.

Gupta, I., Dbage, S., Chandorkar, A.A., Srivastav, A., 2003. Numerical modelling for Thane creek. Environmental Modelling and Software 19, 6, 571-579

Hanson, H., 1989. Genesis-A generalized shoreline change numerical model, Journal of Coastal Research 5, 1–27.

Hanson, H., Aarninkhof, S., Capobianco, M., Jimenez, J., et al., 2003. Modelling of coastal evolution on yearly to decadal time scales. Journal of Coastal Research 19, 790–811.

Halvorsen, R., 2012. A gradient analytic perspective on distribution modelling. Sommerfeltia 35, 1–165.

Halvorsen, R., 2013. A maximumlikelihood explanation of Max-Ent, and some implications for distribution modelling. Sommerfeltia 36, 1–132.

Hanson, H., Kraus, N.C., 2011. Long-term evolution of a long-term evolution model. Journal of Coastal Research 59, 118–129.

Hardisty, J., Taylor, D.M., Metcalfe, S.E., 1993. Computerised Environmetal Modelling: A Practical Introduction Using Excel. John Wiley & Sons, New Jersey, US.

Hegde, A.V., Reju, V.R., 2007. Development of coastal vulnerability index for Mangalore coast, India. Journal of Coastal Research 23, 1106–1111.

Helmer, E.H., Brown, S., Cohen, W.B., 2000. Mapping montane tropical forest successional stage and land use with multi-date Landsat imagery. International Journal of Remote Sensing 21, 2163–2183.

Hemsing, L.Ø., Bryn, A., 2012. Three methods for modelling potential natural vegetation (PNV) compared: a methodological case study from south-central Norway. Norsk geografisk tidsskrift – Norwegian Journal of Geography 66, 11–29.

Hibma, A., De Vriend, H.J., Stive., M.J.F., 2003. “Numerical modelling of shoal pattern formation in well-mixed elongated estuaries,” Estuarine Coastal and Shelf Science 57, 5-6, 981-991.

Hodgson, A., Kelly, N., Peel, D., 2013. Unmanned Aerial Vehicles (UAVs) for Surveying Marine Fauna : A Dugong Case Study. PLOS ONE 8, 11, e79556.

Huang, Q.H., Cai, Y.L., 2009. Mapping karst rock in Southwest China. Mountain Research and Development 29, 14–20.

Hugenholtz, C.H., Levin, N., Barchyn, T.E., Baddock, M.C., 2012. Remote sensing and spatial analysis of aeolian sand dunes: A review and outlook. Earth-Science Reviews 111, 3–4, 319–334.

Hughes, S.A., 1993. Physical models and laboratory techniques in coastal engineering. Advanced Series on Ocean Engineering. Volume 7.

Hutton, E.W., Piper, M.D., Peckham, S.D., Overeem, I., et al., 2014. Building sustainable software-the CSDMS approach. arXiv Preprint, 4106.

IPCC (Intergovernmental Panel on Climate Change). 2001. IPCC Report, Working Group-I, Climate Change–2001: The Scientific Basis. Cambridge, UK: Cambridge University Press. http://www. ipcc.ch/ipccreports/tar/wg1/408.htm (accessed April 10, 2007).

IPCC (Intergovernmental Panel on Climate Change), 2013. Climate Change 2013: the Physical Science Basis. Cambridge University Press, Cambridge, pp. 1535.

ISDR (International Strategy for Disaster Reduction), 2004. Living with Risk: a Global Review of Disaster Reduction Initiatives. World Meteorological Organization and the Asian Disaster Reduction Center, Geneva, pp. 429.

Jackson, D.W.T., Cruz-Avero, N., Smyth, T.A.G., Hernández-Calvento, L., 2013. 3D airflow modelling and dune migration patterns in a mobile coastal dune field Journal of Coastal Research 65, 1301-1306, ISSN 0749-0208.

Kaneko, K., Nohara, S., 2014. Review of effective vegetation mapping using the UAV (Unmanned Aerial Vehicle) method. International Journal of Geographical Information Science 6, 733.

Kankara, R.S., Mohan, R., Venkatachalapathy, R., 2013. Hydrodynamic modelling of Chennai coast from a coastal zones management perspective. Journal of Coastal Research 29, 2, 347-357, ISSN 0749-0208.

Kantamaneni, K., 2016. Coastal infrastructure vulnerability: an integrated assessment model. Natural Hazards 84, 139–154.

Kantamaneni, K., Phillips, M., Thomas, T., Jenkins, R., 2018. Assessing coastal vulnerability: development of a combined physical and economic index. Ocean Coastal Management 158, 164–175.

Kasperski, J., Delacourt, C., Allemand, P., Potherat, P., Jaud, M., Varrel, E., 2010. Application of a Terrestrial Laser Scanner (TLS) to the Study of the Séchilienne Landslide (Isère, France). Remote Sensing 2, 2785–2802.

Kempeneers, P., Deronde, B., Provoost, S., Houthuys, R., 2009. Synergy of Airborne Digital Camera and Lidar Data to Map Coastal Dune Vegetation. Journal of Coastal Research, 10053, 73–82.

Klemas, V., 2011. Remote sensing techniques for studying coastal ecosystems: An overview. Journal of Coastal Research 27, 1, 2–17.

Kobayashi, N., Buck, M., Payo, A., Johnson, B.D., 2009. Berm and dune erosion during a storm. Journal of Waterway, Port, Coastal, and Ocean Engineering 135, 1, 1-10.

Kobayashi, N., 2016. Coastal sediment transport modeling for engineering applications. Journal of Waterway Port Coastal and Ocean Engineering-ASCE 142, 03116001.

Komar, P.D., Allan, J.C., 2008. Increasing hurricane-generated wave heights along the U. S. coast and their climate controls. Journal of Coastal Research 24, 479–488.

Kozhoridze, G., Orlovsky, N., Orlovsky, L., Blumberg, D.G., Golan-Goldhirsh, A., 2016. Remote sensing models of structure-related biochemicals and pigments for classification of trees. Remote Sensing of Environment 186, 184–195.

Krueger, C.P., Soares, C.R., Huinca, S.C.M., Leandro, D., Goncalves. R.M., 2011. Satellite positioning on the coast of the Paran´a, Brazil. Journal of Coastal Research 64, 1352–1356.

Kumar, D., 2006. Potential vulnerability implications of sea level rise for the coastal zoness of Cochin, southwest coast of India.Environmental Monitoring and Assessment 123, 333–344.

Kumar, A., Jayappa, K. S., 2009. Long and short-term shoreline changes along Mangalore Coast, India. International Journal of Environment Research 3, 2, 177–188.

Kumar, T.S., Mahendra, R.S., Nayak, S., Radhakrishnan, K., Sahu, K.C., 2010. Coastal vulnerability assessment for Orissa State, east coast of India. Journal of Coastal Research 26, 3, 523–534. West Palm Beach (Florida), ISSN 0749-0208.

Kuplich, T.M., 2006. Classifying regenerating forest stages in Amazonia using remotely sensed images and a neural network. Forest Ecology and Management 234, 1–9.

Larson, M., Hanson, H., 1997. Analytical solutions of one-line model for shoreline change near coastal structures. Journal of Waterway, Port, Coastal & Ocean Engineering 123, 4, 180. ISSN: 0733950X.

Launeau, P., Giraud, M., Ba, A., Moussaoui, S., Robin, M., 2018. Full-Waveform LiDAR Pixel Analysis for Low-Growing Vegetation Mapping of Coastal Foredunes in Western France. Remote Sensing 10, 669.

Le Cozannet, G., Garcin, M., Bulteau, T., Mirgon, C., Yates, M.L., M'endez, M., Baills, A., Idier, D., Oliveros, C., 2013. An AHP-derived method for mapping the physical vulnerability of coastal areas at regional scales. Nat. Hazards. Earth System Science 13, 5, 1209–1227.

Legault, A., Theuerkauf, J., Chartendrault, V., Rouys, S., Saoumoe, M., Verfaille, L., Desmoulins, F., Barre, N., Gula, R., 2013. Using ecological niche models to infer distribution and population size of parakeets in New Caledonia. Biological Conservation 167, 149–160.

Lee, J., Park, J., Choi, J., 2013. Evaluation of Sub-aerial Topographic Surveying Techniques Using Total Station and RTK-GPS for Applications in Macrotidal Sand Beach Environment. Journal of Coastal Research, Special Issue No. 65, 535–541.

Li, X., Zhang, X., Ren. X., Fritsche, M., Wickert, J., Schuh, H., 2015. Precise positioning with current multi-constellation global navigation satellite systems: GPS, GLONASS. Galileo and BeiDou Scientific Reports 5, 8328.

Liu, H., Jezek, K.C., 2004. A Complete High-Resolution Coastline of Antarctica Extracted from Orthorectified Radarsat SAR Imagery. Photogrammetric Engineering & Remote Sensing 5, 605-616.

Liu, Q.J., Takamura, T., Takeuchi, N., Shao, G., 2002. Mapping of boreal vegetation of a temperate mountain in China by multitemporal LANDSAT imagery. International Journal of Remote Sensing 23, 3385–3405.

L´opez Royo, M., Ranasinghe, R., Jim´enez, J.A., 2016. A rapid, low-cost approach to coastal vulnerability assessment at a national level. Journal of Coastal Research 32, 4, 932–945. Coconut Creek (Florida), ISSN 0749-0208.

Lucas, N.S., Shanmugam, S., Barnsley, M., 2002. Sub-pixel habitat mapping of a costal dune ecosystem. Applied Geography 22, 3, 253–270.

MacLeod, M., Pereira da Silva, C., Cooper, J.A.G. 2002. A Comparative Study of the Perception and Value of Beaches in Rural Ireland and Portugal: Implications for Coastal Zone Management. Journal of Coastal Research 18, 1, 14-24.

Mani Murali, R., Ankita, M., Amrita, S., Vethamony, P., 2013. Coastal vulnerability assessment of Puducherry coast, India, using the analytical hierarchical process. Nat. Hazards. Earth System Science 13, 12, 3291–3311.

Martinez, M.L., Silva, R., Mendoza, E., Odériz, I., 2016. Coastal Dunes and Plants: An Ecosystem-Based Alternative to Reduce Dune Face Erosion. Journal of Coastal Research 75, 303-307.

Masselink, G., Scott, T., Poate, T., Russell, P., Davidson, M., Conley, D., 2015. The extreme 2013/14 winter storms: Hydrodynamic forcing and coastal response along the southwest coast of England, Earth Surface Processes Landforms, doi:10.1002/esp.3836.

McCall, R., Thiel, Van, de Vries, J.S.M., Plant, N., Van Dongeren, A.R., Roelvink, J.A., Thompson, D., Reniers, A., 2010. Two-dimensional time dependent hurricane overwash and erosion modeling at Santa Rosa Island. Coastal Engineering 57, 668–683.

McCall, R.T., Masselink, G., Poate, T.G., Roelvink, J.A., Almeida, L.P., 2015. Modelling the morphodynamics of gravel beaches during storms with XBeach-G. Coastal Engineering 103, 52–66.

McGovern, E.A., Holden, N.M., Ward, S.M., Collins, J.F., 2002. The radiometric normalization of multi-temporal Thematic Mapper imagery of the midlands of Ireland- a case study. International Journal of Remote Sensing 23, 4, 751-766.

McKenna, J., MacLeod, M., Cooper, A., O'Hagan, A.M., Power, J., 2005. Land tenure type as an underrated legal constraint on the conservation management of coastal dunes: examples from Ireland. Area 37, 3, 312–323.

Mendoza, E., Odériz, I., Martínez, M.L., Silva, R., 2017. Measurements and modelling of small scale processes of vegetation preventing dune erosion. Journal of Coastal Research 77, 19-27. Coconut Creek (Florida), ISSN 0749-0208.

Mieczysław, B., 2013. Study of Reliable Rapid and Ultrarapid Static GNSS Surveying for Determination of the Coordinates of Control Points in Obstructed Conditions. Journal of Surveying Engineering ASCE, 188–194.

Mimura, N., Nicholls, R.J., 1998. Regional issues raised by sea level rise and their policy implications. Journal of Climate Research, 11, 5–18.

Miller, J., Franklin, J., Aspinall, R., 2007. Incorporating spatial dependence in predictive vegetationmodels. Ecological Modelling 202, 225–242.

Mitasova, H., Overton, M., Harmon, R.S., 2005. Geospatial analysis of a coastal sand dune field evolution: Jockey's Ridge, North Carolina. Geomorphology 72, 204-221.

Moriondo, M., Jones, G.V., Bois, B., Dibari, C., Ferrise, R., Trombi, G., Bindi, M., 2013. Projected shifts of wine regions in response to climate change. Climatic Change 119, 825–839.

Moore, L.J., 2000. Shoreline mapping techniques. Journal of Coastal Research 16, 1, 111–124.

Moore, D., Wilson F., 1999. National Shingle Beach Survey of Ireland 1999: Synoptic Report. National Parks & Wildlife Service Publication.

Nicholls, R.J., Wong, P.P., Burkett, V.R., Codignotto, J.O., Hay, J.E., McLean, R.F., Ragoonaden, S., Woodroffe, C.D., 2007. Coastal Systems and Low-Lying Areas. Climate Change 2007: Impacts, Adaptation and Vulnerability. Contribution of Working Group II to the Fourth Assessment Report of the Intergovernmental Panel on Climate Change, Cambridge, U.K.: Cambridge University Press, 315–356.

Nguyen, T.T.X., Bonetti, J., Rogers, K., Woodroffe, C.D., 2016. Indicator-based assessment of climate-change impacts on coasts: a review of concepts, approaches and vulnerability indices. Ocean Coastal Management 123, 18–43.

O'Donoghue B., Regan L., 2007. Accuracy Assessment: Cowpens National Battlefield Vegetation Map. NatureServe: Durham, North Carolina.

Olbert, A.I., Comer, J., Nash S., Hartnett, N. 2017. High-resolution multi-scale modelling of coastal flooding due to tides, storm surges and rivers inflows. A Cork City example. Coastal Engineering 121, 278–296.

OSI (Ordnance Survey Ireland), viewed at Feb 2017. Highly Accurate Digital Terrain Models (DTM) or Digital Surface Models (DSM). OSI online document.https://www.osi.ie/wp-content/uploads/2015/05/Lidar_prod_overview.pdf

Parsons, D.R., Wiggs, G.F.S., Walker, I.J., Ferguson, R.I., et al., 2004. Numerical modelling of airflow over an idealised transverse dune. Environmental Modelling and Software 19, 153–162.

Payo, A., Favis-Mortlock, D., Dickson, M., Hall, J.W., et al., 2017. Coastal Modelling Environment version 1.0: a framework for integrating landform-specific component

models in order to simulate decadal to centennial morphological changes on complex coasts. Geoscientific Model Development 10, 2715–2740.

Pajares, G., 2015. Overview and current status of remote sensing applications based on unmanned aerial vehicles (UAVs). Photogrammetric Engineering and Remote Sensing 81, 281–329.

Parrish, C.E., Dijkstra, J.A., Jarlath, P.M.O.N., Mckenna, L., 2016. Post-Sandy Benthic Habitat Mapping Using New Topobathymetric Lidar Technology and Object-Based Image Classification. Journal of Coastal Research, IS 76,200–209.

Pender, D., Karunarathna, H., 2013. A statistical-process based approach for modelling beach profile variability. Coastal Engineering 81, 19-29. https://doi.org/10.1016/j.coastaleng.2013.06.006

Pendleton, E.A., Thieler, E.R., Jeffress, S.W., 2005. Coastal Vulnerability Assessment of Golden Gate National Recreation Area to Sea-Level Rise. USGS Open-File Report 2005-1058.

Peneva, E., Griffith, J.A., Carter, G.A., 2008. Seagrass mapping in the northern Gulf of Mexico using airborne hyperspectral imagery: A comparison of classification methods. Journal of Coastal Research 24, 4, 850–856.

Perrin, P.M., Barron, S.J., Roche, J.R., O'Hanrahan, B., 2014. Guidelines for a national survey and conservation assessment of upland vegetation and habitats in Ireland. Version 2.0. Irish Wildlife Manuals, No. 79. National Parks and Wildlife Service, Department of Arts, Heritage and the Gaeltacht, Dublin, Ireland.

Phillips M.R., Jones A.L., 2006. Erosion and tourism infrastructure in the coastal zone: Problems, consequences and management. Tourism Management 27, 3, 517-524.

Projovi, D.M., 2017. Application of Relative Positioning in Topographic Survey Preparations on a Full Basis in Artillery. Military Technical Courier 65, 1, 25–140.

Qi, X.K., Wang, K.L., Zhang, C.H., 2013. Effectiveness of ecological restoration projects in a karst region of southwest China assessed using vegetation succession mapping. Ecological Engineering 54, 245–253.

Rajawat, A.S., Bhattacharya, S., Jain, S., Gupta, M., Jayaprasad, P., Tamilarasan, V., Ajai, S., 2006. Coastal Vulnerability Mapping for the Indian Coast. Second International Symposium on ‘‘Geoinformation for Disaster Management’’, Dona Paula, Goa, India, International Society for Photogrammetry and Remote Sensing.

Rapinel, S., Clement, B., Magnanon, S., Sellin, V., Laurence, H., 2014. Identification and mapping of natural vegetation on a coastal site using a Worldview-2 satellite image, Journal of Environmental Management 144, 236–246.

Rea, P.D., Komar, C.C., 1975. Computer simulation models of a hooked beach shoreline configuration, Journal of Sediment Research 45, 4, 866–872.

Roelvink, D., Reniers, A., van Dongeren, A., van Thiel de Vries, J., McCall, R., Lescinski, J., 2009. Modelling storm impacts on beaches, dunes and barrier islands. Coastal Engineering 56, 11–12, 1133–1152.

Ryle, T., Murray A., Connolly K., Swann M., 2009. Coastal Monitoring Project 2004-2006. Irish Wildlife Manuals, National Parks and Wildlife Service, Department of Arts, Heritage and the Gaeltacht, Dublin, Ireland.

Sabatier, F., Anthony, E.J., Hquette, A., Suanez, S., Musereau, J., Ruz, M.H., Regnauld, H., 2009. Morphodynamics of beach/dune systems: Examples from the coast of France. Géomorphologie 15, 3–22.

Salman, A., Lombardo, S., Doody, P., 2004. Living with coastal erosion in Europe: sediment and space for sustainability. Part I - Major findings and policy recommendations of the EUROSION project. Service contract B4-3301/2001/329175/MAR/B3.

Satyanarayana, B., Mohamad, K.A., Idris, I.F., Husain, M.L., Dahdouh-Guebas, F., 2011. Assessment of mangrove vegetation based on remote sensing and ground-truth measurements at Tumpat, Kelantan Delta, East Coast of Peninsular Malaysia. International Journal of Remote Sensing 32, 6, 1635–1650.

Schneider, T.D., Panich, L.M., 2008. Total Station Mapping: Practical Examples from Alta and Baja California. Journal of California and Great Basin Anthropology 28, 2, 2327-9400.

Serafim, M.B., Siegle, E., Corsi, A.C., Bonetti, J. 2019. Coastal vulnerability to wave impacts using a multi-criteria index: Santa Catarina (Brazil). Journal of Environmental Management 230, 21–32.

Silleos, N.G., Alexandridis, T.K., Gitas, I.Z., Perakis, K., 2006. Vegetation indices: advances made in biomass estimation and vegetation monitoring in the last 30 years. Geocarto International 21, 4, 21–8.

Smyth, T.A.G., Jackson, D.W.T., Cooper, J.A.G., 2012. High resolution measured and modelled three-dimensional airflow over a coastal bowl blowout. Geomorphology 177-178, 62-73.

Shao, Z., Fu, H., Fu, P., Yin, L., 2016. Mapping Urban Impervious Surface by Fusing Optical and SAR Data at the Decision Level. Remote Sensing 8, 945, 1–22.

Smith, M.J., Chandler, J., Rose, J., 2009. High spatial resolution data acquisition for the geosciences: kite aerial photography. Earth Surface Process, Landforms 34, 155-161.

Song, C.H., Schroeder, T.A., Cohen, W.B., 2007. Predicting temperate conifer forest successional stage distributions with multitemporal Landsat Thematic Mapper imagery. Remote Sensing of Environment, 106, 228–237.

Song, C.H., Woodcock, C.E., 2003. Monitoring forest succession with multitemporal Landsat images: factors of uncertainty. IEEE Transactions on Geoscience and Remote Sensing 41, 2557–2567.

Staiger, R., 2003. Terrestrial Laser Scanning Technology, Systems and Applications. 2nd FIG Regional Conference in Marrakech, Morocco December 2-5, 2003.

Stive, M.J.F., Capobianco, M., Wang, Z.B., Ruol, P., Buijsman, M.C., 1998. "Morphodynamics of a tidal lagoon and adjacent coast," Proc. 8th International Biennial Conference on Physics of Estuaries and Coastal Seas, The Hague, 397-407.

Stive, M.J.F., Ruol, P., Capobianco, M., Buijsman, M., 1997. Behaviour oriented model for the evaluation of long-term lagooncoastal dynamic interaction along the Po River Delta. Coastal Dynamics – Proceedings of the International Conference, American Society Civil Engineers, Plymouth, UK, June 1997, 903–912.

Strand, G.H., 2013. The Norwegian area frame survey of land cover and outfield land resources. Norsk geografisk tidsskrift – Norwegian Journal of Geography 67, 24–35.

Stuart, N., Shanmugam, S., Barnsley, M., 2002. Sub-pixel habitat mapping of a coastal dune ecosystem. Applied Geography, 22, 253–270.

Thieler, E.R., Hammar-Klose, E.S., 1999. National Assessment of Coastal Vulnerability to Sea-Level Rise, U.S. Atlantic Coast: U.S. Geological Survey Open-File Report 99-593.

Thornes, J., 1989. Geomorphology and grass roots models. Remodelling Geography. Blackwell, Oxford, 3-21.

Timm, B.C., McGarigal, K., 2012. Fine-scale remotely-sensed cover mapping of coastal dune and salt marsh ecosystems at Cape Cod National Seashore using Random Forests. Remote Sensing of Environment 127, 106–117.

Tokola T., Sarkeala J., Linden M.V.D., 2001. Use of topographic correction in Landsat TM-based forest interpretation in Nepal. International Journal of Remote Sensing 22, 4, 551–563.

Tomasello, F., Ducci, M., Bell, J., 2016. Safe integration of drones into airspace. European Parliament's Committee on Transport and Tourism (TRAN), IP/B/TRAN/IC/2016-104.

Tonkin, T.N., Midgley, N.G. 2016. Ground-control networks for image based surface reconstruction: an investigation of optimum survey designs using UAV derived imagery and structure-from-motion photogrammetry, Remote Sensing 8, 9, 786.

Tsaia, Z., Youa, G.J.Y., Leea, H.Y., Chiub, Y.J., 2012. Use of a total station to monitor post-failure sediment yields in landslide sites of the Shihmen reservoir watershed. Geomorphology 139, 140, 438–451.

Turner, I.L., Harley, M.D., Drummond, C.D., 2016. UAVs for coastal surveying. Coastal Engineering 114, 19–24.

Ullerud, H. A., Bryn, A., Klanderud, K., 2016. Distribution modelling of vegetation types in the boreal–alpine ecotone. Applied Vegetation Science 19, 528–540.

Uysal, M., Toprak, A.S., Polat, N., 2015. DEM generation with UAV Photogrammetry and accuracy analysis in Sahitler hill, Measurement 73, 539–543.

Vaca, R.A., Golicher, D.J., Cayuela, L., 2011. Using climatically based random forests to downscale coarse-grained potential natural vegetation maps in tropical Mexico. Applied Vegetation Science 14, 388-401.

Vandebroek, E., Lindenbergh, R., Leijen, F.V., Schipper, M.D., Vries, S.D., Hanssen, R., 2017. Semi-Automated Monitoring of a Mega-Scale Beach Nourishment Using High-Resolution TerraSAR-X Satellite Data. Remote Sensing 9, 653, 1–19.

van Rijn, L.C., Walstra, D.J.R., Grasmeijer, B., Sutherland, J., Pan, S., Sierra, J.P., 2003.The predictability of cross-shore bed evolution of sandy beaches at the time scale of storms and seasons using process-based Profile models. Coastal Engineering 47, 295–327.

Venturi, S., Di Francesco, S., Materazzi, F., Manciola, P., 2016. Unmanned aerial vehicles and Geographical Information System integrated analysis of vegetation in Trasimeno Lake, Italy. Lakes and Reservoirs: Research and Management 21, 5–19.

Verbesselt, J., Hyndman, R., Newnham, G., Culvenor, D., 2010. Detecting trend and seasonal changes in satellite image time series. Remote Sensing of Environment 114, 106–115.

Wang, X., 2018. Virtual reality of 3D digital factory based on coastal environment. Journal of Coastal Research, Special Issue No. 83, pp. 507–512. Coconut Creek (Florida), ISSN 0749-0208.

Weber, T.C., 2011.Maximum entropy modeling of mature hardwood forest distribution in four U.S. states. Forest Ecology and Management 261, 779–788.

Weesakul, S., Rasmeemasmuang T., Tasaduak S., Thaicharoen C., 2010. Numerical modeling of crenulate bay shapes, Coastal Engineering 57, 2, 184–193.

Weil, G., Lensky, I., Resheff, Y., Levin, N., 2017. Optimizing the Timing of Unmanned Aerial Vehicle Image Acquisition for Applied Mapping of Woody Vegetation Species Using Feature Selection. Remote Sensing 9, 11, 1-25.

Wiens, J.A., Stralberg, D., Jongsomjit, D., Howell, C.A., Snyder, M.A., 2009. Niches, models, and climate change: assessing the assumptions and uncertainties. Proceedings of the National Academy of Sciences of the United States of America 106, 19729– 19736.

Williams, J.J., Esteves, L.S., Conduche, T., Barber, P., 2014. Using combined modelling approaches to improve coastal defence design: a case study at Hopton, UK. Journal of Coastal Research 70, 018-022, ISSN 0749-0208.

Woo, M.K., Fang, G.X., DiCenzo, P.D., 1997. The role of vegetation in the retardation of soil erosion. Catema 29, 2, 145–159.

Woolard, J.W., Colby, J.D., 2002. Spatial characterization, resolution, and volumetric change of coastal dunes using airborne LIDAR: Cape Hatteras, North Carolina. Geomorphology 48, 269–287.

Xia, J., Dong, P., 2016. A GIS add-in for automated measurement of sand dune migration using LiDAR-derived multitemporal and high-resolution digital elevation models. Geosphere 12, 4, 1316–1322.

Yackulic, C.B., Chandler, R., Zipkin, E.F., Royle, J.A., Nichols, J.D., Grant, E.H.C., Veran, S., 2013. Presence only modelling using MAXENT: when can we trust the inferences? Methods in Ecology and Evolution 4, 236–243.

Yin, J., Yin, Z., Wang, J., Xu, S., 2012. National assessment of coastal vulnerability to sealevel rise for the Chinese coast. Journal of Coastal Conservation 16, 123–133.

Young, I.R., Ziegler, S., Babanin, A.V., 2011. Global trends in the wind speed and wave height. Science 332, 451–455.

Zhang, D., Narteau, C., Rozier, O., 2010. Morphodynamics of barchan and transverse dunes using a cellular automaton model. Journal of Geophysical Research 115, F03041.

Zhang, M.G., Zhou, Z.K., Chen, W.Y., Slik, J.W.F., Cannon, C.H., Raes, C.H., 2012. Using species distribution modelling to improve conservation and land use planning of Yunnan, China. Biological Conservation 153, 257–264.

Zheng, J., Dean, R., 1997. Numerical models and intercomparisons of beach profile evolution. Coastal Engineering 30, 169-201.

Zhou, Z., Feng, Y., Wu, Y., 2011. Virtual reality based process simulation system in refinery. Computer Engineering and Applications 47, 204-208.

Zelizn, V., 2016. Use of low-cost UAV photogrammetry to analyze the accuracy of a digital elevation model in a case study. Measurement 91, 276–287.

Żywicki, K., Zawadzki, P., Górski, F., 2017. Virtual reality production training system in the scope of intelligent factory. International Conference on Intelligent Systems in Production Engineering and Maintenance, 450-458.

Chapter 3

A CRITICAL EVALUTION OF THE LATEST SURVEYING METHODS FOR TOPOGRAPHIC MAPPING

3.1 Prologue

The overall aim of this project was to develop geospatial data-based environmental modelling for coastal dune complexes to contribute to the effective conservation strategies with particular reference to the Brittas-Buckroney dune complex in Co. Wicklow, Ireland. High-end surveying methods to produce topographic mapping were compared and optimized surveying methods, combined with other environmental factors, were used to generate appropriate environmental models for the development of effective coastal management strategies.

To achieve the overall aim of the research, three major elements were designed as follow:

Element 1 - An evaluation of the high-end methods for topographic mapping of a coastal dune complex

Element 2 - Automatic vegetation classification and abundance mapping of a coastal dune complex using UAS-mounted multispectral sensor data.

Element 3 - Environmental modelling for vegetation and non-vegetation changes at coastal dune complexes for coastal environmental management.

This chapter focuses on Element 1, exploring the latest surveying methods for topographic mapping for coastal dune zones. Initial outcomes from this element of the research were orally presented at The 3rd International Symposium on Environment and Health & The 10th International Symposium on Environmental Geochemistry at the National University of Ireland Galway, 14-20th August 2016, and the final results were published in the Coastal Conservation Journal (2020), Volume 24, in a paper entitled "A comparison of high-end methods for topographic modelling of a coastal dune complex". This paper, as published, is reproduced in Chapter 3.

3.2 General information

Abstract: In recent years, increasing tourism and development in the coastal dune area of the South East of Ireland have resulted in greater pressure on the environment, resulting in issues including soil erosion, flooding and habitat loss. Topographic mapping across a dune field is important for the development of targeted land management actions that maintain biodiversity and ecological functions. Developments in surveying technology, including LiDAR, terrestrial laser scanners (TLS) and aerial surveying from Unmanned Aircraft Systems (UAS), have enabled high-resolution and high-accuracy spatial data to be gathered quickly and relatively easily for 3D topographic modelling of a coastal dune complex. To-date, however, the relative efficacies of these three modelling methods, in the context of coastal dune modelling, has not been explored. This paper compares high-end methods based on LiDAR, TLS and UAS technologies, for the topographic modelling of coastal dune complexes with particular reference to the Brittas-Buckroney dune complex in the South East of Ireland. The results identify the advantages and disadvantages of the respective technologies and highlight the efficacy of UAS, in particular, for topographic modelling of coastal dune complexes. These results can provide reference information for others when selecting suitable methods for topographic modelling of similar environments.

Key words: Coastal dune complexes; Topographic modelling; LiDAR; Terrestrial laser scanners; Unmanned aircraft systems.

3.3 Introduction

Coastal zones comprise 2% of the earth's land area and are the transition areas between the marine and terrestrial environments (Acosta et al., 2005). Dune complexes are the main structures at these coastal zones (Lucas et al., 2002). They play an essential role in

the preservation of ecosystem stability and biological diversity as they provide habitat for special flora and fauna, control soil erosion and flooding, and provide protection for nearby properties from other environmental hazards (Clark, 1977; Andrews et al., 2002). Human pressure on coastal zones around the world has increased dramatically in the last 50 years (Curr et al., 2000; Westley and McNeary, 2014).

Concern for the increasing threat to coastal dune ecosystems has generated a greater interest in coastal dune conservation and management (MacLeod et al., 2002; Olbert et al., 2017). Accurate 'baseline' topographic mapping, with detailed information concerning the earth's surface, are considered critical to the development of an effective coastal environmental management plan (Acosta et al., 2005). However, high-resolution and high-accuracy topographic modelling is a challenging task which requires a considerable investment in time and resources (McKenna et al., 2005).

Aerial photogrammetry and optical satellite imagery have been used for topographic mapping for various landscapes including coastal ecosystems (Curr et al., 2000). However, a single dune complex is typically represented as a long and narrow strip because such mapping is generally produced at national and regional scales (Acosta et al., 2005). There are, notwithstanding, a number of data processing approaches for generating finer-scale mapping from the more traditional sources (Lucas et al., 2002; Timm and McGarigal, 2012; Rapinel et al., 2014). Nevertheless, it remains quite difficult to produce, from these sources, topographic mapping with accurate and detailed land cover information for small coastal dune complexes. A considerable limitation of optical satellite imagery, in particular, is the influence of weather, especially cloud-cover which can interfere with the view of the earth's surface (McGovern et al., 2002).

Aircraft-based Light Detection and Ranging (LiDAR) is an alternative resource for 3D topographic models even for a smaller target area *e.g.* 50–100 ha (Bolivar et al., 1995; Grebby et al., 2014). It is often available from national mapping agencies (NMA's), such as Ordnance Survey Ireland (OSi). OSi quotes spatial resolutions and vertical accuracies in rural areas of 0.5 m and 0.5 m respectively (OSi, 2017) and charges c. €250 per square kilometre for the data. LiDAR data can be used to generate both Digital Terrain Models (DTM) and Digital Surface Models (DSM) (Crapoulet et al., 2016). For a study at a coastal dune complex in North Carolina, a LiDAR dataset were used to represent coastal dunes for volumetric change analysis (Woolard and Colby, 2002).

Ground surveying methods, including Total Station (TS) and Global Navigation Satellite System (GNSS), are suitable for topographic modelling of smaller target areas (D'iorio et al., 2007; Lee et al., 2013). These on-site, data collection methods provide more ground truth, and up-to-date and accurate information than many alternatives (D'iorio et al., 2007). The distance measurement accuracy of TS is 2 mm+ 2 ppm over a distance of about 1 km (Lee et al., 2013). However, the operation and performance of TS in field surveying projects is limited by poor visibility circumstances, such as darkness, rain, snow, thickets or physical occlusions (Schneider and Panich, 2008). There are three techniques based on GNSS to enhance the precision of satellite position data. These are Post Processing Kinematic (PPK), Real Time Kinematic (RTK) and Network Real Time Kinematic (NRTK) (Li et al., 2015). The accuracy of GNSS is 10–20 mm (Dow et al., 2009). With lighter equipment and easier operation, these GNSS techniques can save labour and time in collecting the same amount of modelling data as TS (Mieczysław, 2013).

In recent years, due to being non-contact, rapid, accurate and complete, Terrestrial Laser Scanning (TLS) has been increasingly used to build three-dimensional models (Parrish et al., 2016). The positioning accuracy of TLS is of the order of millimetres (Staiger, 2003). The laser scanner is integrated with a computing device to save the acquired point information and also to control the scanning patterns. The operation of the laser scanner is almost fully automatic which leaves little room for operating error as human influence plays a less important role in the surveying process (Ersilia et al., 2012).

Most recently, Unmanned Aerial Systems (UAS), variously referred as Remotely Piloted Aircraft Systems (RPAS), Unmanned Aerial Vehicles (UAV's), "Aerial Robots" or simply "drones", have enabled high-quality data to be gathered quickly and easily (Casella et al., 2014; Turner et al., 2016). UAS platforms are typically grouped into two main categories: rotary UAS and fixed-wing UAS (Gomez and Green, 2017). Comparing both types, rotary UAS has more complex mechanics, which result in lower speeds and shorter flight ranges while fixed-wing UAS have a simpler structure providing more stable platforms. Furthermore, fixed-wing UAS enable longer flight duration and higher speeds, which are more suitable for aerial surveys over larger areas.

UAS, integrated with modern digital camera technology, breaks the time and space constraint allowing a study site to be remotely surveyed in a significantly reduced time using the imagery acquired (Smith et al., 2009; Colomina and Molina, 2014). UAS imagery, using Structure from Motion (SfM) processing techniques, has created a new opportunity for photogrammetry to create 3D surface models from the large number of overlapping photographs (Hodgson et al., 2013). To maintain the spatial accuracy of the data, the overlapping area for each two images should be at least 60%, making sure sufficient shared points can be recognised by the software for map construction (Zelizn,

2016). A multispectral camera mounted on a UAS allows both visible and multispectral imagery to be captured that can be used for characterizing land features, vegetation health and function (Fernández-Guisuraga et al., 2018). UAS is also a user-friendly and scalable methodology albeit with the requirement of specialized software and with restrictive image collection conditions such as high wind speed and poor light intensity (Bemis et al., 2014). For the management of UAS, different countries have different mandatory requirements, established by their national aviation authorities. And particular operating licenses and insurances may be required before operating an UAS (Tomasello et al., 2016).

LiDAR, TLS and UAS technologies are capable of creating digital topographic models of coastal dune complexes. There are three different types of digital topographic model, *viz.* Digital Surface Model (DSM), Digital Terrain Model (DTM) and Digital Elevation Model (DEM). A DSM represents the natural and built features on the Earth's surface (Crapoulet et al., 2016). A DTM is defined as an array of orderly values that are used to describe the spatial distribution of various properties of the earth's surface, for example, topographic information, natural resource and environment information, and economic information (Liang et al., 2012).When the DTM is used only to describe and express spatial information, such as terrain relief and elevations, it is also called a DEM (Liang et al., 2012). A DTM is a bare-earth raster grid referenced to a vertical datum (Hutchinson and Gallant, 1999). By filtering out non-ground points, *e.g.* building and vegetation cover in a DSM, a bare-earth DTM is created.

TLS and UAS technologies create DSMs of a study site as the ground features are not filtered. LiDAR use pules of laser light to measure range. A single pulse can generate a

number of returns such that the first return can be used to create a DSM and last return can be used to create a DTM.

The objective of this research was to compare three high-end methods, *viz.* LiDAR, TLS and UAS technology, for topographic modelling of a coastal dune complex with particular reference to the Brittas-Buckroney dune complex (Fig.3.1) in Co. Wicklow, Ireland. By comparing the efficacy of these different methods of spatial data collection, with respect to accessibility, cost, convenience and data quality, the advantages and disadvantages of these methods are considered in the context of topographic modelling of coastal dune complexes. The results can provide reference information for others involved in topographic modelling of similar environments.

Fig.3.1 Morphology of the Brittas-Buckroney dune complex.

3.4 Study site

The Brittas-Buckroney dune complex (Fig.3.2) is located *c.* 10 km south of Wicklow town on the east coast of Ireland and comprises two main sand dune systems, *viz.* Brittas Bay and Buckroney Dunes (NPWS, 2013). The study site for this research is Buckroney Dunes. The area of the Buckroney dune complex is *c.* 60 ha.

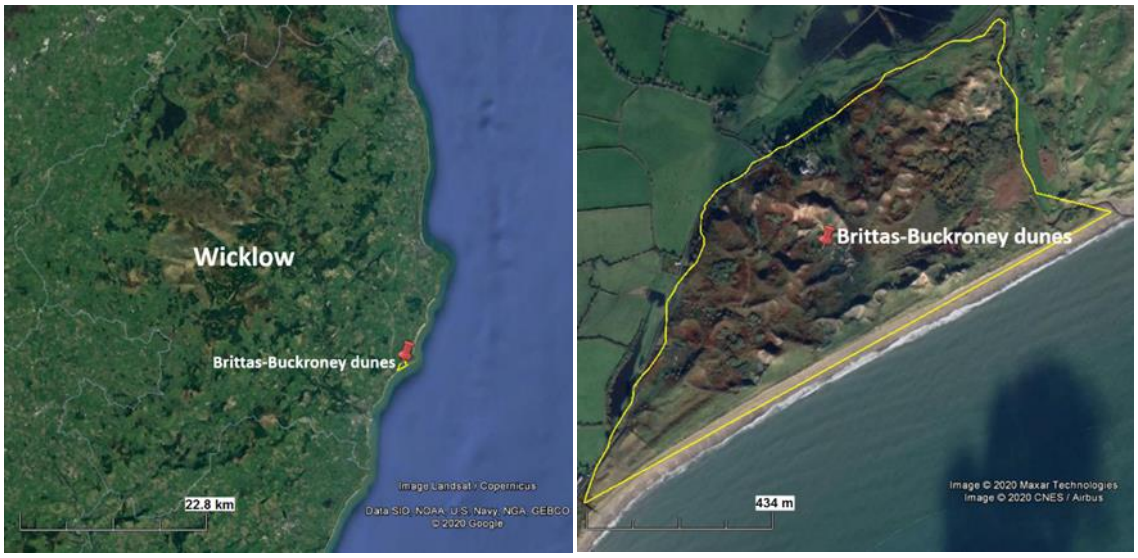

(a) (b)

Fig.3.2 Study site (a) general location and (b) Brittas-buckroney Dunes.

Within this site, ten habitats listed on the EU Habitats Directive are present, including two priority habitats in Ireland, *viz.* fixed dune and decalcified dune heath (NPWS, 2013). This site also contains good examples of different dune types. At the northern part of Buckroney dune complex, there are some representative parabolic dunes, while embryonic dunes mostly occur at the southern part. Meanwhile, the site is notable for the presence of well-developed plant communities.

With land acquisition in recent years, the marginal areas of the dune system have been reclaimed as farmland. The increasing anthropogenic activities at the dune system, such as farming and recreation activities, have brought pressure to the dune ecosystems development, with hazards like soil erosion, flooding and habitat loss. Proper

environmental management is required to ensure the continued survival of this coastal habitat and to maintain the diversity and stability of the ecosystem on this site and accurate topographic modelling is considered a prerequisite for such management.

3.5 Methodology

This study considered three different surveying methods to gather spatial data for the Brittas-Buckroney dune system. These were LiDAR data acquired from the NMA, and two on-site data collection technologies, *viz.* TLS and UAS.

3.5.1 Data acquisition

3.5.1.1 LiDAR

LiDAR data of the study site were available from OSi. The Lidar scanner used by OSi was an airborne Leica ALS50 (OSI, 2017). This scanner emits 150,000 pulses every second creating a point cloud of millions of pixels collected in X, Y, Z (easting, northing and elevation). After capturing the raw point cloud each point is then classified into different layers, such as ground, buildings and vegetation. The final outputs are of high accuracy and provide vertical accuracies between 0.15 m to 0.25 m.

In this research, the acquisition date of the dataset was 28/04/2011. The data file contained the Easting, Northing and Elevation information for each point recorded in the Irish Transverse Mercator (ITM) coordinate system. The horizontal spatial resolution of the data was 0.5 m and the vertical accuracy was 0.5 m (OSI, 2017).

3.5.1.2 TLS

A Topcon GLS2000 TLS (Fig.3.3) captures point cloud data with the scan rate of 120,000 pulses per second with an accuracy of 3.5 mm up to 150 m distance. The scanner has a

170° wide-angle camera and the scan range over 350 m. The field view of the scanner is 360° horizontally, and 320° vertically. A complete 3D model of an object such as sand dune typically required several scans from different locations which are subsequently registered together. These scans are captured at predetermined ground control points (GCPs) to enable precise geolocation.

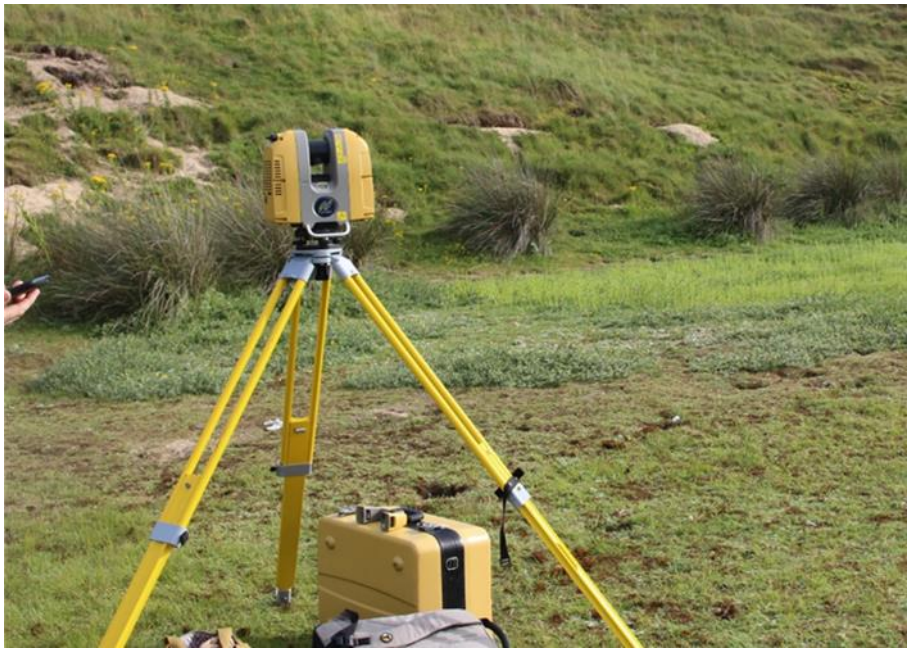

Fig.3.3 Topcon GLS2000 surveying on-site.

The coordinate positions of GCPs used in the TLS survey of the study area were measured using a Trimble 5800 GNSS receiver recording in the ITM coordinate system. The data from a TLS survey is in the form of a point cloud. All points within the point cloud have X, Y, and Z coordinate and laser return intensity values. The points were in an XYZIRGB format, representing X, Y, Z coordinate, return intensity, and Red, Green, Blue colour values taken from the on-board digital camera.

3.5.1.3 UAS

A SenseFly eBee UAS (Fig.3.4 (a)) was used to capture images of the study site. The SenseFly eBee UAS can cover up to 12 km2 in a single automated mapping flight, while flights over smaller areas, at lower altitudes, can acquire images with a ground sampling distance of down to 1.5 cm per pixel. The resulting point cloud, with GCPs used for georeferencing, can achieve horizontal and vertical accuracy of 3 cm – 5 cm, while the resulting point cloud without GCPs has absolute horizontal and vertical accuracy of 1 m−5 m.

Thirty-two GCPs were established around the study site to georeference the data from the UAS. These were marked as white crosses identifiable in the images captured by the UAS (Fig.3.4 (b)). The GCPs were in the ITM coordinate system and positions were determined using a Trimble 5800 GNSS receiver connected to the Trimble VRS commercial NRTK system.

(**a**) (**b**)

Fig.3.4 (a) SenseFly eBee UAS surveyed on-site (b) GCPs set on site for UAS surveying.

To maintain the high quality of the captured imagery, and considering the 20 min - 25 min battery life for a single flight of the UAS, the study site was divided into three sections, North, Centre and South. Settings for each flight included 70% overlap along lines and 60% side-lap between lines, flight height of 120 m and flight times of *c.* 20 min optimizing the data capture time with respect to battery life. In the three sections, the number of images collected by the UAS flight was 212, 209, and 149 respectively for the North, Centre and South sections.

3.5.2 Data processing

The raw datasets from LiDAR and TLS were point clouds, whereas UAS captured numerous overlapping images. By matching different images captured by UAS, a point cloud of the ground surface was generated by SfM technology. Point clouds from the LiDAR, TLS and UAS surveys then were used to generate DSMs for further study. To process the collected datasets, specific software was required in each case. Fig.3.5 outlines the processing steps of datasets acquired by LiDAR, TLS and UAS.

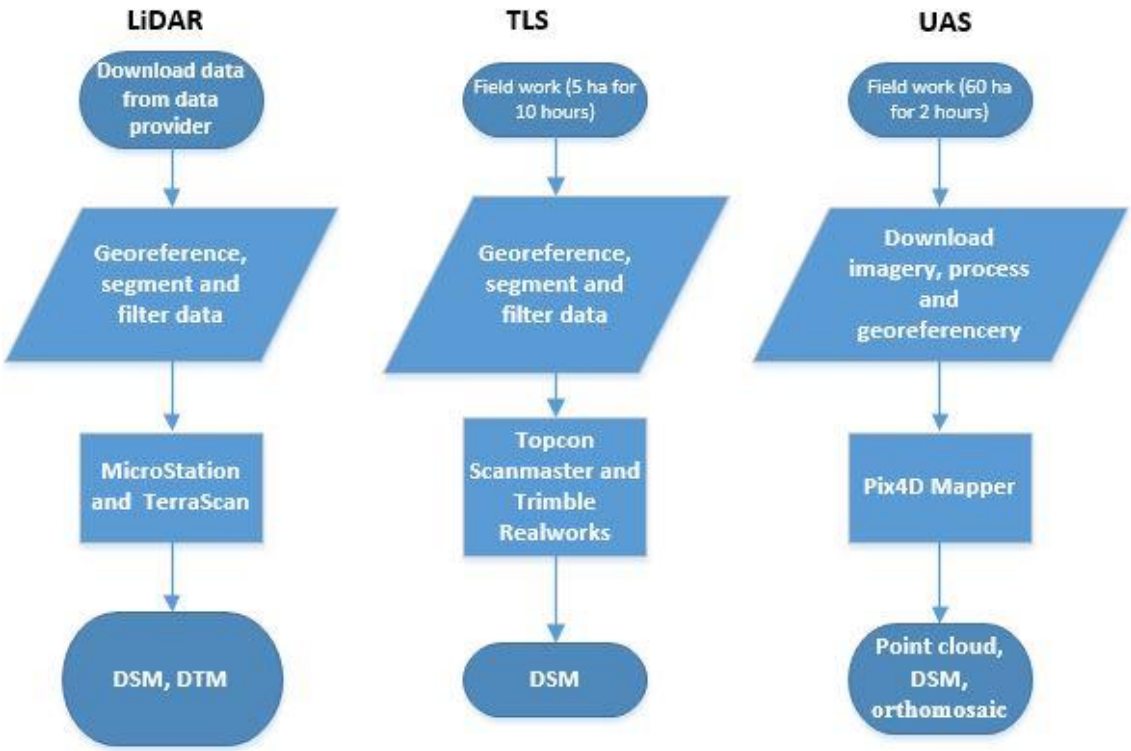

Fig.3.5 Flowchart of data processing from LiDAR, TLS and UAS technologies.

3.5.3 Model comparison

DSMs were generated from the datasets collected by the three different methods, i.e. LiDAR, TLS and UAS. Although it was not practical to create a 3D model for the whole study site by TLS technology, the model created from TLS data was used as reference data for an accuracy assessment of the models generated by both the LiDAR and the UAS data. Single point accuracy based on TLS collection is 0.003 m (Topcon Corporation, 2014). Models based on LiDAR and UAS technology were compared with the single dune model created by TLS data via CloudCompare software. The calculated offset between the models represented the accuracy of the models created by LiDAR and UAS.

3.6 Outcomes

The results show the topographic models of the Buckroney dune system created using the three surveying technologies, *viz.* LiDAR, TLS and UAS.

3.6.1 LiDAR

The LiDAR data is commonly segmented by using different filters to extract the ground surface or the above-ground features. Considering the first returns of laser light, DSM (Fig.3.6) and contour models of the site from LiDAR data were produced. The spatial resolution of the models was 0.2 m. In the DSM, the colour variation from blue to red represents elevation in the range − 0.89 m – +24.39 m.

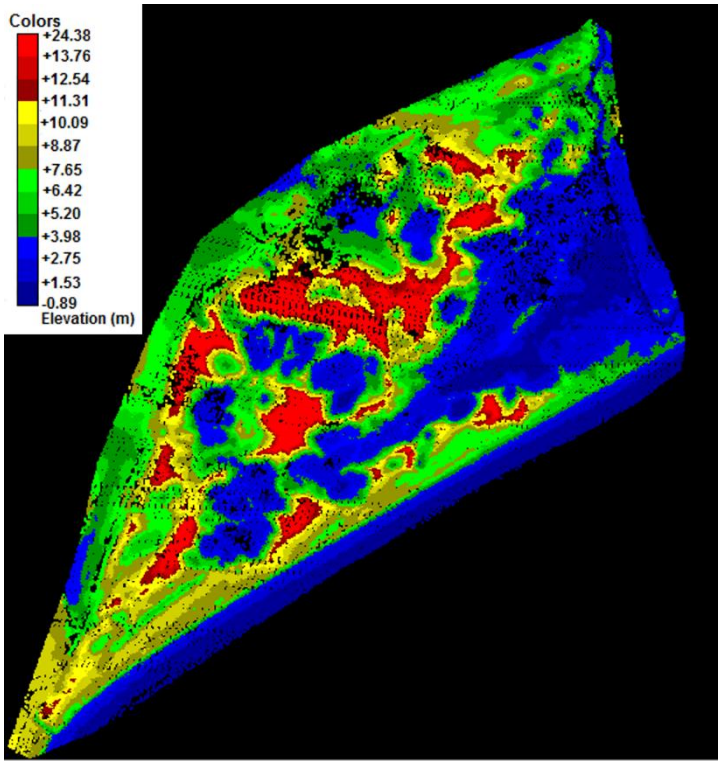

Fig.3.6 Digital Surface Model (DSM) of Buckroney dune complex processed by LiDAR data.

3.6.2 Terrestrial Laser Scanner

From the TLS data, a higher resolution DSM of the selected dune in the white rectangle in Fig.3.7 was created. The resolution of the model was 1 cm. This model was georeferenced to the ITM coordinate system by reference to three GCPs. TLS can collect multiple return signals from a target. The data presented in Fig.3.8 used the first return signals to create the DSM.

(**a**) (**b**)

Fig.3.7 Selected dune system (a) imagery of the selected dune system (b) 3D model of selected dune produced by TLS technology.

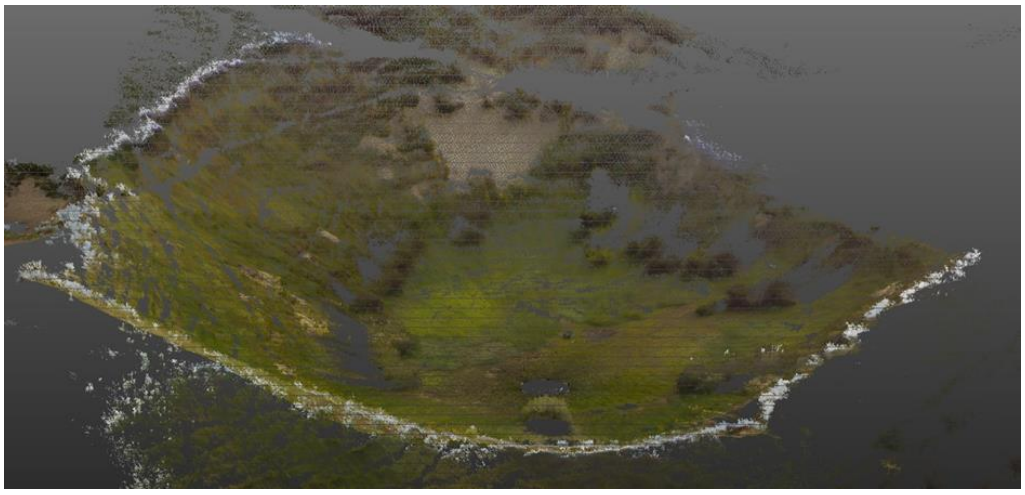

Fig.3.8 DSM of selected dune produced by TLS technology.

3.6.3 UAS

Using a dense image matching process, geo-referenced 3D point clouds, orthomosaics, DSMs, contour lines, and textured mesh models were generated for the study site from the UAS imagery. These outcomes were referenced to the ITM grid coordinate system, with a spatial resolution of 0.034 m and a spatial accuracy of 0.035 m when checked against 10 GCPs.

Pix4D software was used for the processing and a 3D point cloud of the study site was generated from the overlapping images. The orthomosaic (Fig.3.9) is a mosaic image adjusted for topographic relief, lens distortion, and camera tilt so it can be used to scale true distances. This high resolution orthomosaic is a useful product suitable for land feature classification and volumetrics analysis. The DSM (Fig.3.10) when combined with the position of land features, can provide the basic morphological data for environmental modelling. Environmental models can then contribute to the exploration and identification of important processes at coastal dune complexes, for example, dunes formation, structure changes to dunes and vegetation, aeolian and other environmental influences on morphology.

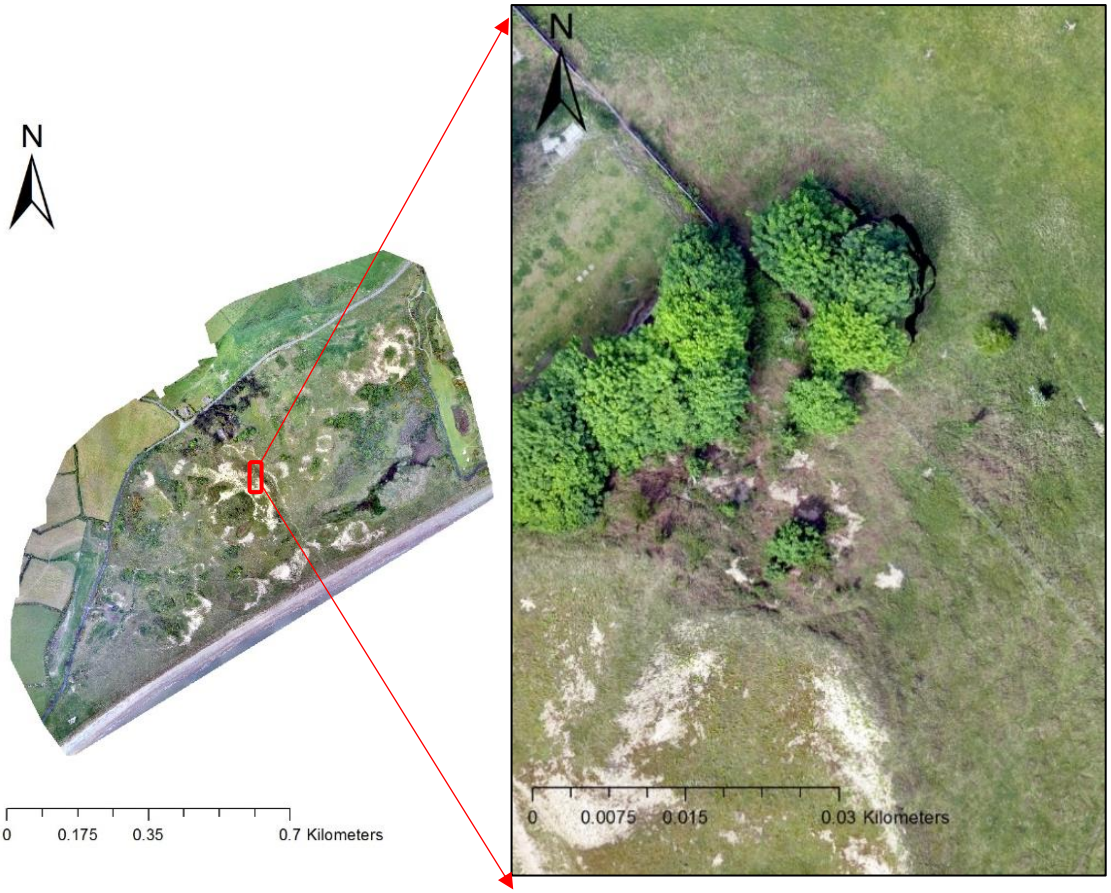

Fig.3.9 Orthomosaic model of the study site with a detailed extract.

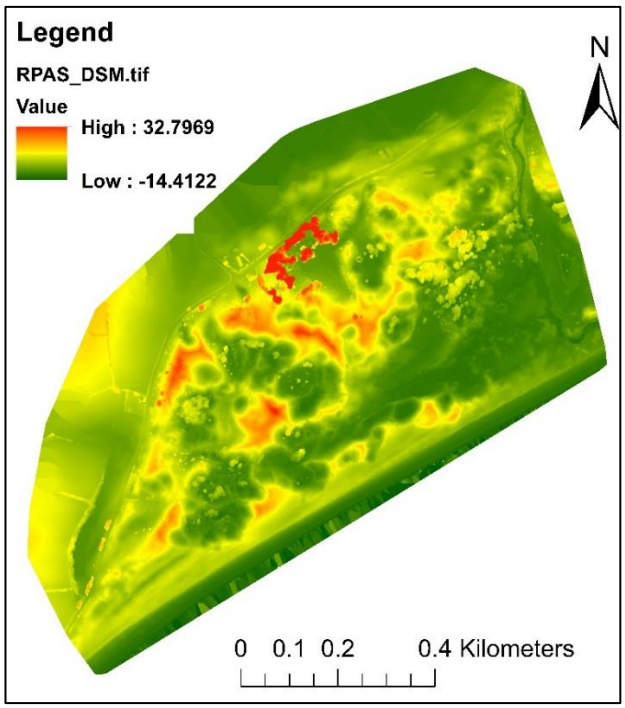

Fig.3.10 DEM of study site.

3.7 Analysis

Based on the accuracy for a single point measurement of 0.003 m, and allowing for a typical error budget, the estimated accuracy for the TLS model is ±0.010 m. Thus, the TLS model (Fig.3.8) was used as the reference model for a comparison with the LiDAR model (Fig.3.6) and the UAS model (Fig.3.10). A spatial accuracy assessment was carried out using package cloud-to-cloud separation estimation in the CloudCompare software package. The offset between TLS model and LiDAR model was 0.27 m and standard deviation was 0.18 m (Fig.3.11). The offset between TLS based model and UAS model was 0.11 m and standard deviation was 0.18 m (Fig.3.12).

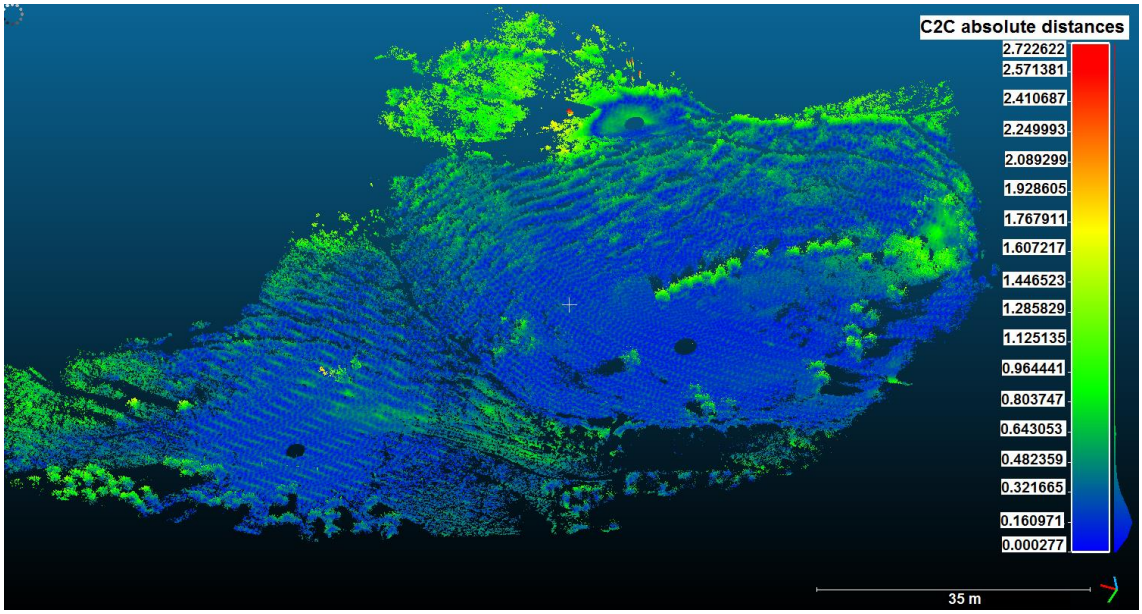

Fig.3.11 Offset between TLS based model and LiDAR based model.

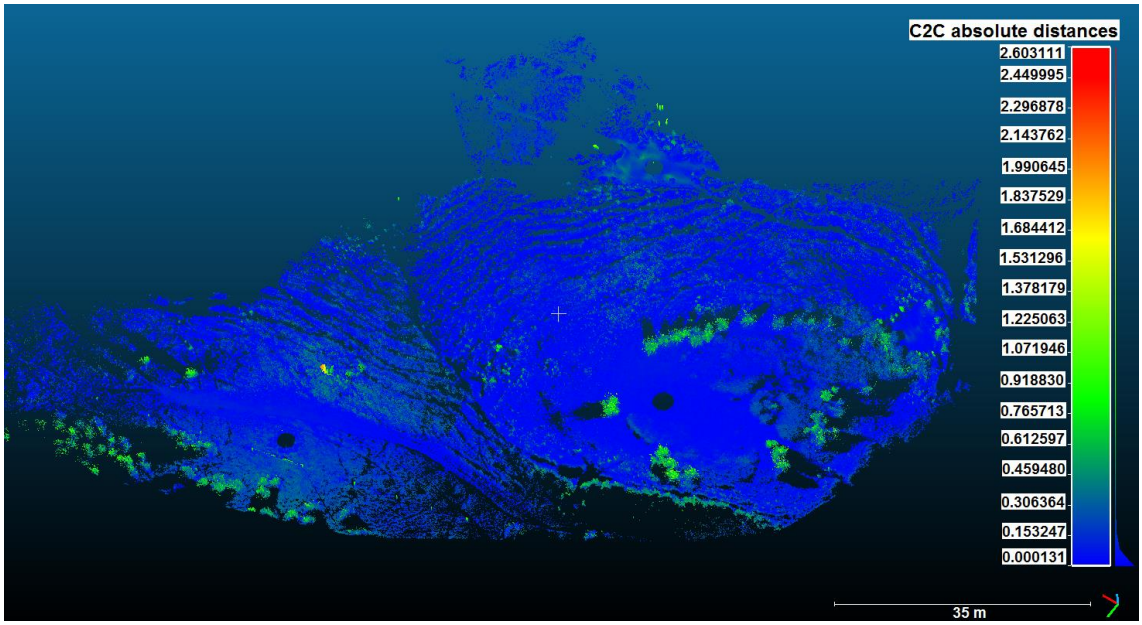

Fig.3.12 Offset between TLS based model and UAS based model.

LiDAR, TLS and UAS are all options for generating DSMs of a small coastal dune complex. However, the resolution, coverage and labour investment of these three methods vary. Based on this study, Table 3.1 compares the three methods considered for topographic models.

Table 3.1 Comparison of LiDAR, TLS and UAS for DSM generation of study site.

		LiDAR	**TLS**	**UAS**
Data acquisition	Area coverage	High	Low	Medium
	Cost	€250 per square kilometre	About €21,000	About €10,000
	Expertise level required	Competent	Proficient	Competent
	Data collection time om-site	No field work	7 hours field work for a single dune including mobilisation and establishment of GCPs	8 hours field work for 60 ha site including mobilisation and establishment of GCPs

	Weather dependencies	Not influenced by weather change	Limited by precipitation	Limited by precipitation and wind
	Flexibility	No flexibility	Flexibility	High flexibility
	Collected dataset	Point cloud	Point Cloud	Georeferenced imagery
Data processing	Software	MicroStation and TerraScan	Topcon Scanmaster and Trimble Realworks	Pix4D Mapper
Outcomes	Outcome packages	DSM, DTM	DSM	3D point cloud, DSM, orthomosaic image
	Resolution	0.2 m	0.003 m	0.034m
	Accuracy	0.3 m	0.010 m	0.1 m

Based on these accuracy assessment figures (Figs.3.11 and 3.12) and further comparison between the models (Table 3.1), UAS was considered as the better choice for the topographic modelling of this 60 ha coastal dune complex for this particular study.

3.8 Conclusion

In this study, three surveying methods for data collection were explored for topographic modelling of the 60 ha Buckroney coastal dune complex in Ireland, *viz.* LiDAR data, TLS and UAS. Using both existing LiDAR data and UAS technology, it was possible to complete the high resolution topographic modelling of the site within one day. In this timescale, TLS was only capable of generating a topographic model of a single dune within the study site. However, this model was of high resolution (0.01 m) and high accuracy (0.010 m) and was used as the reference model for an accuracy assessment of the models created by LiDAR and UAS. The results show the model based on UAS data has higher resolution (0.034 m) and higher accuracy (0.11 m) than the model generated from the LiDAR dataset. The UAS solution also provided more up-to-date and flexible data for modelling. Data collection using UAS was completed in one day for a 60 ha study

site which demonstrated the efficiency of the UAS survey method in dune complex areas. As the UAS surveyed remotely, it eased the difficulties of access through dunes areas with deep slopes and difficult vegetation.

However, notwithstanding the many benefits and advantages of UAS technology in modelling, it still has some challenges with dune complexes surveying. UAS is unable to create DTMs of coastal dune complexes as it lacks bare earth data in areas of dense vegetation. UAS is also sensitive to certain environmental conditions, such as wind, precipitation, low light. Although the use of UAS can save significant time at the on-site data collecting stage, more time is required for data processing. Preliminary items need to be take into consideration as well, such as arranging permits to fly and training under UAS regulations from the relevant aviation authority.

3.9 References

Acosta, A., Carranza, M.L., Izzi, C.F., 2005. Combining land cover mapping of coastal dunes with vegetation analysis. Applied Vegetation Science 8, 133-138.

Andrews, B., Gares, P.A., Colby, J.D., 2002. Techniques for GIS modelling of coastal dunes. Geomorphology 48, 1–3, 289–308.

Bemis, S.P., Micklethwaite, S., Turner, D., James, M.R., Akciz, S., Thiele, S.T., Bangash, H.A., 2014. Ground-based and UAV-Based photogrammetry: A multi-scale, high-resolution mapping tool for structural geology and paleoseismology. Journal of Structural Geology 69, 163-178.

Bolivar, L., Carter, W., Shrestha, R., 1995. Airborne laser swath mapping aids in assessing storm damage. Florida Engineering, 26–27.

Casella, E., Rovere, A., Pedroncini, A., Mucerino, L., Casella, M., Alberto, L., Firpo, M. 2014. Coastal and Shelf Science Study of wave runup using numerical models and low-altitude aerial photogrammetry : A tool for coastal management. Estuarine, Coastal and Shelf Science 149, 160–167.

Clark, J.R., 1977. Coastal environment management. Wiley, Chichester, UK.

Colomina, I., Molina, P., 2014. Unmanned aerial systems for photogrammetry and remote sensing : A review. ISPRS Journal of Photogrammetry and Remote Sensing 92, 79–97.

Crapoulet, A., Héquette, A., Levoy, F., Bretel, P., 2016. Using LiDAR Topographic Data for Identifying Coastal Areas of Northern France Vulnerable to Sea-Level Rise. Journal of Coastal Research 75, 1067-1071.

Curr, R.H.F., Koh, A., Edwards, E., Williams, A.T., Daves, P., 2000. Assessing anthropogenic impact on Mediterranean sand dunes from aerial digital photography. Journal of Coastal Conservation 6, 15-22.

D'iorio, M., Jupiter, S.D., Cochran, S.A., Potts, D.C., 2007. Optimizing remote sensing and GIS tools for mapping and managing the distribution of an invasive mangrove (Rhizophora mangle) on South Molokai, Hawaii. Marine Geodesy 30, 1–2, 125–144.

Dow, J.M., Neilan, R.E., Rizos, C., 2009. The international GNSS service in a changing landscape of global navigation satellite systems. Journal of Geodesy 83, 191–198.

Ersilia, O., Constantin, C., Marius, S., 2012. Terrestrial Laser Scanner Surveying Versus Total Station Surveying for 3D Building Model Generation. Mathematical Modelling in Civil Engineering 4, 168–178.

Fernández-Guisuraga J.M., Sanz-Ablanedo E., Suárez-Seoane, S., Calvo, L., 2018. Using unmanned aerial vehicles in Postfire vegetation survey campaigns through large and heterogeneous areas: opportunities and challenges. Sensors 18, E586.

Gomez, C., Green, D.R., 2017. Small unmanned airborne systems to support oil and gas pipeline monitoring and mapping. Arabian Journal of Geosciences 10, 202.

Grebby, S., Cunningham, D., Tansey, K., Naden, J., 2014. The impact of vegetation on lithological mapping using Airborne Multispectral Data: A case study for the North Troodos Region, Cyprus. Remote Sensing 6, 10860–10887.

Hodgson, A., Kelly, N., Peel, D., 2013. Unmanned Aerial Vehicles (UAVs) for Surveying Marine Fauna : A Dugong Case Study. PLOS ONE 8, 11, e79556.

Hutchinson, M.F. and Gallant, J.C., 1999. "Representation of Terrain." In Geographical Information Systems: Principles and Technical Issues, edited by Longley PA, Goodchild MF, Maguire DJ, and Rhind DW, 105–124, 2nd edition. New York: John Wiley & Sons.

Lee, J., Park, J., Choi, J., 2013. Evaluation of Sub-aerial Topographic Surveying Techniques Using Total Station and RTK-GPS for Applications in Macrotidal Sand Beach Environment. Journal of Coastal Research, Special Issue No. 65, 535–541.

Li, X., Zhang, X., Ren, X., Fritsche, M., Wickert, J., Schuh, H., 2015. Precise positioning with current multi-constellation global navigation satellite systems: GPS, GLONASS. Galileo and BeiDou Scientific Reports 5, 8328.

Liang, S., Li, X., Wang, J., 2012. Advanced Remote Sensing. Terrestrial Information Extraction and Applications, 1st Edition, Chapter 2. Academic Press.

Lucas, N.S., Shanmugam, S., Barnsley, M., 2002. Sub-pixel habitat mapping of a coastal dune ecosystem. Applied Geography 22, 3, 253–270.

MacLeod, M., Pereira da Silva, C., Cooper, J.A.G., 2002. A Comparative Study of the Perception and Value of Beaches in Rural Ireland and Portugal: Implications for Coastal Zone Management. Journal of Coastal Research 18, 1, 14-24.

McGovern, E.A., Holden, N.M., Ward, S.M., Collins, J.F., 2002. The radiometric normalization of multi-temporal Thematic Mapper imagery of the midlands of Ireland- a case study. International Journal of Remote Sensing 23, 4, 751-766.

McKenna, J., MacLeod, M., Cooper, A., O'Hagan, A.M., Power, J., 2005. Land tenure type as an underrated legal constraint on the conservation management of coastal dunes: examples from Ireland. Area 37, 3, 312–323.

Mieczysław, B., 2013. Study of Reliable Rapid and Ultrarapid Static GNSS Surveying for Determination of the Coordinates of Control Points in Obstructed Conditions. Journal of Surveying Engineering ASCE, 188–194.

NPWS (National Parks & Wildlife Service), 2013. Site Synopsis: Buckroney-Brittas Dunes and Fen SAC. NPWS site documents, 000729_Rev13.Doc.https://www.npws.ie/protected-sites/sac/000729

Olbert, A.I., Comer, J., Nash, S., Hartnett, N., 2017. High-resolution multi-scale modelling of coastal flooding due to tides, storm surges and rivers inflows. A Cork City example. Coastal Engineering 121, 278–296.

OSI (Ordnance Survey Ireland), viewed at Feb 2017. Highly Accurate Digital Terrain Models (DTM) or Digital Surface Models (DSM). OSI online document.https://www.osi.ie/wp-content/uploads/2015/05/Lidar_prod_overview.pdf

Parrish, C.E., Dijkstra, J.A., Jarlath, P.M.O.N., Mckenna, L., 2016. Post-Sandy Benthic Habitat Mapping Using New Topobathymetric Lidar Technology and Object-Based Image Classification. Journal of Coastal Research, IS 76,200–209.

Rapinel, S., Clement, B., Magnanon, S., Sellin, V., Laurence, H., 2014. Identification and mapping of natural vegetation on a coastal site using a Worldview-2 satellite image, Journal of Environmental Management 144, 236–246.

Schneider, T.D., Panich, L.M., 2008. Total Station Mapping: Practical Examples from Alta and Baja California. Journal of California and Great Basin Anthropology 28, 2, 2327-9400.

Smith, M.J., Chandler, J., Rose, J., 2009. High spatial resolution data acquisition for the geosciences: kite aerial photography. Earth Surface Process, Landforms 34, 155-161.

Staiger, R., 2003. Terrestrial Laser Scanning Technology, Systems and Applications. 2nd FIG Regional Conference in Marrakech, Morocco December 2-5, 2003.

Timm, B.C. and McGarigal, K., 2012. Fine-scale remotely-sensed cover mapping of coastal dune and salt marsh ecosystems at Cape Cod National Seashore using Random Forests. Remote Sensing of Environment 127, 106–117.

Tomasello, F., Ducci, M., Bell, J., 2016. Safe integration of drones into airspace. European Parliament's Committee on Transport and Tourism (TRAN), IP/B/TRAN/IC/2016-104.

Topcon Corporation, 2014. GLS-2000: Compact high-speed 3D Laser scanner. P/N:7010-2152 Rev.B TF 8/14.

Turner, I.L., Harley, M.D., Drummond, C.D., 2016. UAVs for coastal surveying. Coastal Engineering 114, 19–24.

Westley, K., McNeary, R., 2014. Assessing the Impact of Coastal Erosion on Archaeological Sites: A Case Study from Northern Ireland. Conservation and Management of Archectiture Sites 16, 3, 185–211.

Woolard, J.W., Colby, J.D., 2002. Spatial characterization, resolution, and volumetric change of coastal dunes using airborne LIDAR: Cape Hatteras, North Carolina, Geomorphology 48, 269–287.

Zelizn, V., 2016. Use of low-cost UAV photogrammetry to analyze the accuracy of a digital elevation model in a case study. Measurement 91, 276–287.

Chapter 4

DEVELOPMENT OF METHODLOGIES FOR THE APPLICATION OF UAS-MOUNTED MULTISPECTRAL SENSOR DATA FOR AUTOMATIC VEGETATION CLASSIFICATION AND ABUNDANCE MAPPING OF A COASTAL DUNE COMPLEX

4.1 Prologue

Chapter 3 focused on comparing and optimizing high-end surveying methodologies to produce topographic mapping for coastal dune complexes with particular reference to the Brittas-Buckroney dune complex in Co. Wicklow, Ireland (Element 1). To achieve the overall aim of this project, which is to develop environmental modelling for coastal dune complexes to contribute to effective conservation strategies, another two elements were included as follows:

Element 2 - Automatic vegetation classification and abundance mapping of a coastal dune complex using UAS-mounted multispectral sensor data.

Element 3 - Environmental modelling for vegetation and non-vegetation changes at coastal dune complexes for coastal environmental management.

This chapter focuses on Element 2, *viz.* vegetation mapping of coastal dune complex using multispectral sensor mounted on UAS. Initial outcomes from this element of the research were orally represented at two international conferences, the Conference of Irish Geographers at Maynooth University, May 10-12th, 2018 and "Innovative Sensing - From Sensors to Methods and Applications" International Society of Photogrammetry and Remote Sensing (ISPRS) symposium, Karlsruhe Institute of Technology, Germany, 9th to 12th of October 2018. The final results were published in the Remote Sensing Journal (2019), Volume 11, in a paper entitled "Coastal Dune Vegetation Mapping Using a Multispectral Sensor Mounted on an UAS". This paper, as published, is reproduced in Chapter 4.

4.2 General information

Abstract: Vegetation mapping, identifying the type and distribution of plant species, is important for analysing vegetation dynamics, quantifying spatial patterns of vegetation evolution, analysing the effects of environmental changes and predicting spatial patterns of species diversity. Such analysis can contribute to the development of targeted land management actions that maintain biodiversity and ecological functions. This paper presents a methodology for 3D vegetation mapping of a coastal dune complex using a multispectral camera mounted on an unmanned aerial system with particular reference to the Buckroney dune complex in Co. Wicklow, Ireland. Unmanned aerial systems (UAS), also known as unmanned aerial vehicles (UAV) or drones, have enabled high-resolution and high-accuracy ground-based data to be gathered quickly and easily onsite. The Sequoia multispectral sensor used in this study has green, red, red edge and near-infrared wavebands, and a regular camer with red, green and blue wavebands (RGB camera), to capture both visible and near-infrared (NIR) imagery of the land surface. The workflow of 3D vegetation mapping of the study site included establishing coordinated ground control points, planning the flight mission and camera parameters, acquiring the imagery, processing the image data and performing features classification. The data processing outcomes included an orthomosaic model, a 3D surface model and multispectral imagery of the study site, in the Irish Transverse Mercator (ITM) coordinate system. The planimetric resolution of the RGB sensor-based outcomes was 0.024 m while multispectral sensor-based outcomes had a planimetric resolution of 0.096 m. High-resolution vegetation mapping was successfully generated from these data processing outcomes. There were 235 sample areas (1 m × 1 m) used for the accuracy assessment of the classification of the vegetation mapping. Feature classification was conducted using nine different classification strategies to examine the efficiency of multispectral sensor data for vegetation and contiguous land cover mapping. The nine classification strategies

included combinations of spectral bands and vegetation indices. Results show classification accuracies, based on the nine different classification strategies, ranging from 52% to 75%.

Keywords: coastal dune; vegetation mapping; UAS; multispectral sensor; classification strategies

4.3 Introduction

Coastal dune fields are at the transition between terrestrial and marine ecosystems and are highly-valued, natural resources for providing drinking water, mineral resources, recreation, ecoservices and desirable land for development (Frosini et al., 2012). These natural resources provide food and habitation for aquatic and terrestrial organisms and, also, offer human settlement and recreation spaces. Activities at the coastal zone area can contribute to local and national economic development in areas like aquaculture, fisheries and tourism, and the area also has an important function to control erosion and flooding, thus protecting and maintaining environmental functions (Fenu et al., 2012). In recent years, increasing tourism and development in the coastal dune area in the southeast of Ireland have resulted in increased pressure on the environment, resulting in issues including soil erosion, flooding and habitat loss (McKenna et al., 2007).

Vegetation at coastal dune complexes has a strong impact on dune morphology and dynamics as it can influence sand transport (Sabatier et al., 2009). Vegetation is also a critical environmental component of the coastal ecosystem for food production, resource conservation, nutrient cycling and carbon sequestration (Woo et al., 1997; Kuplich, 2006). High-resolution vegetation mapping of coastal dune complexes, with accurate distribution and population estimates for different functional plant species, can be used to analyse vegetation dynamics, quantify spatial patterns of vegetation evolution, analyse

the effects of environmental changes on vegetation and predict spatial patterns of species diversity (Vaca et al., 2011). Such information can contribute to the development of targeted land management actions that maintain biodiversity and ecological functions.

This research involved the generation of 3D vegetation mapping of a coastal dune complex at Buckroney in Co. Wicklow, Ireland, using a multispectral sensor mounted on an unmanned aerial system (UAS) (Fig.3.1). The research presents a workflow for 3D vegetation mapping of a coastal dune complex, including establishing ground control points (GCPs), planning the flight mission and camera parameters, acquiring the imagery, processing the image data and performing digital features classification. The process illustrates the efficiency of image data collection and the high-resolution of the vegetation mapping of the site using a multispectral camera mounted on a UAS. Classification accuracy also needs to be considered and some research also quoted an overall classification accuracy of 65% as the minimum acceptable for reliable vegetation mapping (NPS, 2018). To examine the efficiency of multispectral sensors for vegetation mapping, classification was conducted based on nine different classification strategies, including different combinations of wavebands and spectral indices.

4.4 Background

Traditionally, field survey has been the most commonly used method for vegetation mapping (Yu et al., 2000). However, this method is time-consuming, expensive, and limited in spatial coverage (Song et al., 2007). Satellite remote sensing, in contrast, offers a potentially more efficient means of obtaining data. Each vegetation community has a unique spectral response in multispectral satellite image data which is a function of the characteristic species composition (Verbesselt et al., 2010; Qi et al., 2013). Satellite-based hyperspectral data can be a useful tool for vegetation mapping on a regional scale but, in

the context of species level classification, it is limited to homogeneous stands of the same species because of limited spatial resolution, *e.g.*, 30 m of EO1 Hyperion images, and low signal to noise ratio (Kozhoridze et al., 2016).

Airborne remote sensing provides higher spatial resolution data than satellite remote sensing for coastal dune complexes mapping. Such higher resolution is more suitable for coastal dune inspection and monitoring (Launeau et al., 2018). Light detection and ranging (LiDAR) is an active remote sensing technique measuring the return time of a laser pulse backscattered by a target as an echo signal whose intensity is proportional to the reflectance properties of the target (Baltsavias, 1999). Classical LiDAR records discrete echoes in real-time but may not distinguish targets that are too close to each other. The minimum target separation is typically 0.4 m in airborne LiDAR (Launeau et al., 2018). Lidar data is often available from national mapping agencies (NMAs), such as Ordnance Survey Ireland (OSi) who quote spatial resolutions and vertical accuracies in rural areas of 0.5 m and 0.5 m respectively (OSi, 2018). However, LiDAR data from NMAs is of limited use for vegetation mapping of coastal dune areas because of the relatively coarse spatial resolution, poor vegetation classification potential and fixed acquisition dates.

In recent years, there has been a significant advance in exploring the capabilities of small UAS (Unmanned Aerial Systems) as part of vegetation research (Anderson and Gaston, 2013; Kaneko and Nohara, 2014; Pajares, 2015; Weil et al., 2017). UAS, variously referred as Remotely Piloted Aircraft Systems (RPAS), unmanned aircraft vehicles (UAV), "Aerial Robots" or simply "drones", enable on-site data collection for vegetation mapping (Turner et al., 2016). In comparison with other remote sensing platforms, UAS typically have a lower operating height which enables the collection of higher spatial

resolution in a small area (Venturi et al., 2016). UAS also have flexible revisit times whereas the availability of other remote sensing data is limited in acquisition date and coverage depending on national commission. UAS also provide the possibility for data acquisition of inaccessible areas or hazardous environments. The collected images are processed by specialized software, for example Pix4D or Agisoft, which utilize Structure from Motion (SfM) technology and dense image matching. Importing a wide variety of suitable imagery and control data to the software, a georeferenced 3D model can be constructed. Fig.4.1 shows a workflow for photogrammetry-based 3D construction based on Bemis's research (Bemis et al., 2014).

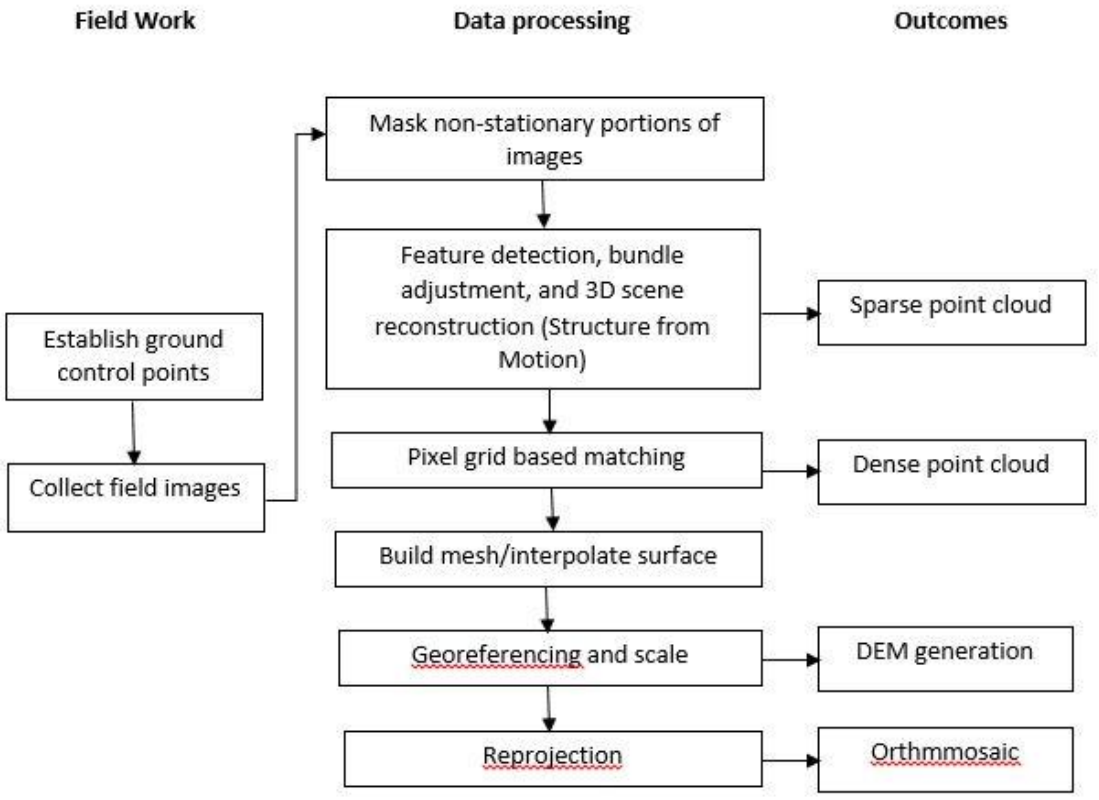

Fig.4.1 Photogrammetry-based 3D construction workflow of UAS technology.

Structure from Motion (SfM) for UAS-collected data processing is a technique that has emerged in the last decade to construct photogrammetry-based 3D models (Tonkin and

Midgley, 2016). The critical element for implementation of photogrammetry to 3D mapping using SfM is the collection of numerous overlapping images of the study area (Uysal et al., 20015). From each pair of overlapping pictures, SfM can calculate the unique coordinate position (x, y, z or Easting, Northing, Elevation) of a set of particular points presented in both images. To maintain the accuracy of the mapping, the overlapping area for each two images should be at least 60%, ensuring sufficient shared points can be recognised by software for the map construction. To generate a 3D model, many thousands of matching object and textural features are automatically detected in multiple overlapping images of the ground surface, from which a high density point cloud with 3D coordinate positions is derived.

A multispectral camera mounted on a UAS allows both visible and multispectral imagery to be captured that can be used for characterizing land features, vegetation health and function. The Parrot Sequoia multispectral sensor has green (530-570 nm), red (640-680 nm), red edge (730-740 nm) and near infrared (770-810 nm) wavebands and a RGB camera (400 nm to 700 nm) (Ren et al., 2017). Colour, structure and surface texture of different land features can influence the reflectance pattern of the wavebands (Fernández-Guisuraga et al., 2018). By analysing these spectral reflectance patterns, different earth surface features can be identified. This process is known as classification and it is usually carried out by digital image processing using a variety of classification algorithms.

Image processing is also capable of discriminating vegetation by calculating different visible-based or multispectral data-based spectral indices. For example, the Normalized Differential Vegetation Index (NDVI), which relates the reflectance of land features at near infrared and red wavebands, is widely used to differentiate green vegetation areas from other land features, such as water and soil (Gini et al., 2012). The index ranges from

-1 to 1, with 0 representing the approximate value of no vegetation (Silleos et al., 2006). There are other spectral indices that can be calculated from multispectral bands and are used for vegetation mapping, Weil et al. listed six of these related with normal red, green and blue wavebands (RGB) camera-based bands and four multispectral bands (Table 4.1) (Weil et al., 2017).

Table 4.1 Spectral indices calculated from four multispectral bands for vegetation mapping.

Spectral indices	**Formula**	**Explanation**
Relative Green	$\frac{Green}{(Red + Green + Blue)}$	The relative component of green, red and blue bands over the total sum of all camera bands. Less affected from scene illumination conditions than the original band value.
Relative Red	$\frac{Red}{(Red + Green + Blue)}$	
Relative Blue	$\frac{Blue}{(Red + Green + Blue)}$	
NDVI	$\frac{NearInfrared - Red}{Nearinfrared + Red}$	Relationship between the NIR and red bands indicates vegetation condition due to chlorophyII absorption within red spectral range and high reflectance within the NIR range.
gNDVI	$\frac{NearInfrared - Green}{Nearinfrared + Green}$	Improvement of NDVI, accurate in assessing chlorophyll content.

GRVI	$\frac{Green - Red}{Green + red}$	Relationship between the green and red bands is an effective index for detecting phenophases.

Overhead imagery of natural terrain typically includes shading and weaker reflectance from shaded areas complicates the classification of vegetation communities. Various image pre-processing methods have been developed to minimize the effects of shadows on image classification. These methods include band ratios *e.g.* (Helmer et al., 2000; Huang and Cai, 2009), additional topographic data (*e.g.* Liu et al., 2002), and topographic correction (*e.g.* Tokola et al., 2001; Cuo et al., 2010). Band ratios can minimize changes in solar illumination caused by variations in slope and aspect (Elvidge and Lyon, 1985). Research has also demonstrated that simulated NDVI is resistant to topographic effects at all illumination angles (Song and Woodcock, 2003). The normalized difference moisture index (NDMI) and tasseled cap wetness have also been used to classify forest types (Wilson and Sader, 2002). The use of digital elevation models (DEM) in vegetation classification in mountainous regions has also proven useful in improving the classification accuracy, if the distribution of vegetation is determined by altitude (Franklin et al., 2002). Topographic correction models have also been applied to Landsat images and have been shown to increase classification accuracies (Gao and Zhang, 2009).

4.5 Study site

The Brittas-Buckroney dune complex (Fig.4.2) is located c. 10 km south of Wicklow town on the east coast of Ireland and comprises two main sand dune systems, *viz.* Brittas Bay and Buckroney Dunes (NPWS, 2018). The study site for this research is Buckroney Dunes, which is managed by the Irish National Park & Wildlife Service. The area of the

Buckroney dune complex is *c.* 40 ha. Within this site, ten habitats listed on the EU Habitats Directive are present, including two priority habitats in Ireland, *viz.* fixed dune and decalcified dune heath (NPWS, 2018). This dune system also contains good examples of other dune types. At the northern part of Buckroney dune complex, there are some representative parabolic dunes, while embryonic dunes mostly occur at the southern part.

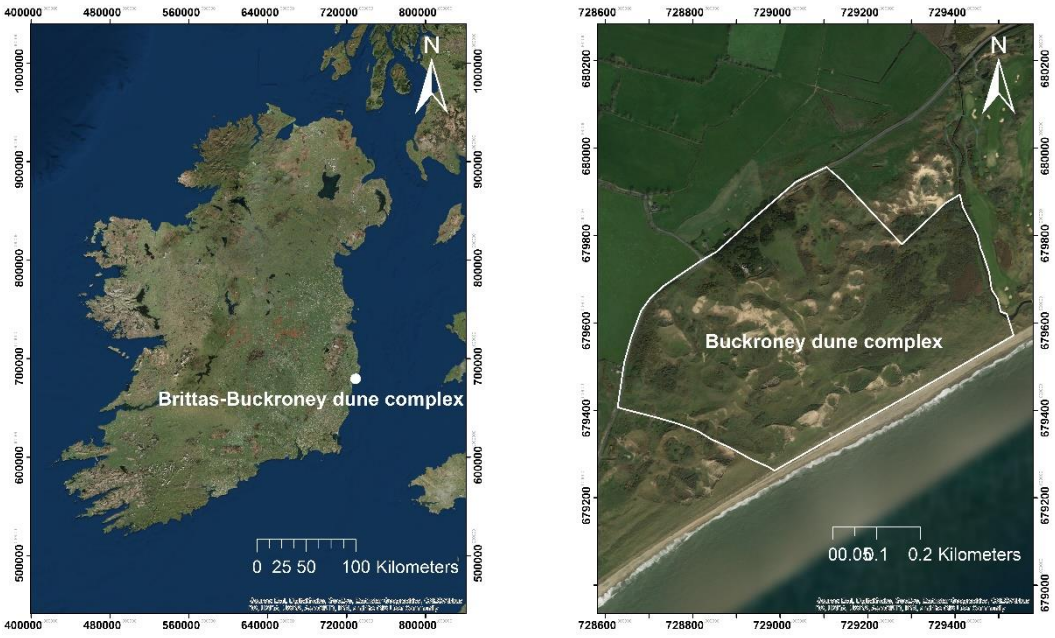

(**a**) (**b**)

Fig.4.2 Study site (a) general location and (b) site details.

The site is notable for the presence of well-developed plant communities (Gao and Zhang, 2009). Mosses, such as Tortula ruraliformis (*Syntrichia ruralis* subsp. *ruraliformis*), *Rhytidiadelphus triquetris*, and *Homalothecium lutescens* and lichens (*Cladonia spp., Peltigera canina*), are frequently found in this dune complex. Sharp Rush (*Juncus acutus L.*) dominates south of the inlet stream to the fen area at the north of the dune complexes, and in small areas elsewhere within the Buckroney dune complex. The main dune ridges are dominated by European marram grass (*Ammophila arenaria (L.) Link*). Gorse (*Ulex*

europaeus L.)) is also present at the back of the dunes. To the west, a dense swamp of Common Reed (*Phragmites australis (Cav.) Trin. ex Steud.*) is present. There are extensive areas of Rusty Willow (*Salix cinerea* subsp. *oleifolia Macreight*) scrub throughout the dune complex.

(**a**)

(**b**)

(**c**)

(**d**)

(**e**) (**f**)

Fig.4.3 Plant species at site (a) Mosses land; (b) Sharp rush (*J. acutus*); (c) European marram grass (*A. arenaria*); (d) Gorse (*U. europaeus*) (e) Common reed (*P. australis*); (f) Rusty willow (*S. cinerea* subsp. *oleifolia*).

With land acquisition in recent years, the marginal areas of the dune system have been reclaimed as farmland. The increasing anthropogenic activities at the dune system, such as farming and recreation activities, have brought pressure on the development of the dune ecosystem, with hazards like soil erosion, flooding and habitat loss. Accurate and high resolution 3D vegetation mapping can contribute to an understanding of the natural processes that impact the coastal dune complex and can help with the development of targeted land management policies.

4.6 Methodology

The UAS platform used was a DJI Phantom 3 Professional, which has 4 rotors, a central body containing the electronic components and landing gear that sustains the entire structure (Fig.4.4). The UAS is powered by a lithium polymer battery that allows a flight time up to 25 min. The multispectral sensor used in this study was a Parrot Sequoia which

is comprised of five individual cameras and a sun sensor. The cameras consist of a 16 MP RGB camera and four 1.2 MP multispectral cameras that record in the green, red, red edge and near infrared wavebands. The camera cluster is mounted under the central body of the UAS and a sun sensor is positioned above the central body as seen in Fig.4.4. The field work for this study was conducted in February 2018.

Fig.4.4 Sequoia multispectral sensor mounted on a DJI Phantom 3 Pro UAS.

4.6.1 Field work

4.6.1.1 Ground Control points

Field surveying with the UAS started with establishing ground control points (GCPs) across the study site whose Irish Transverse Mercator (ITM) coordinates were determined using a Trimble GNSS receiver connected to the Trimble VRS NRTK system (Fig.4.5). This system can reach 2 cm spatial and 5 cm vertical accuracy for point measurement (Trimble positioning service site, 2019). These GCPs were used at the processing stage to georeference the 3D models generated from the data. In this study, 20 GCPs, marked

as white crosses on-site, were recorded. To ensure visibility in the captured images, open, flat and relatively bare ground locations were selected for the GCPs.

Fig.4.5 GCPs set on site for UAS surveying.

4.6.1.2 Flight mission planning

Pix4DCapture software provided a solution for flightpath design for the UAS surveying project while separate Parrot Sequoia software was used to set the multispectral sensor recording parameters. For this study, the parameters of the flight mission were set as shown in Table 4.2 (a) and (b).

Table 4.2 (a) Parameters set for UAS flight mission.

Flight height	**Overlapping along line**	**Overlapping between lines**	**Estimated flight time**	**Maximum flight speed**
80 m	80%	75%	10 min	10 m/s

Table 4.2 (b) Parameters set for multispectral sensor mounted on UAS.

Capture mode	Interval distance	Image resolution	Bit depth
GPS-controlled	15 m	1.2 Mpx	10-bit

4.6.1.3 Radiometric calibration

Radiometric calibration was required to convert the multispectral raw imagery data to absolute surface reflectance data thereby removing the influence of different flights, dates, and weather conditions. The collection of solar irradiance data for each flight is required for radiometric calibration. Imaging of a white balance card (Fig.4.6), captured before each flight, and provided an accurate representation of the amount of light reaching the ground at the time of capture. The balance card containing a grey square and Quick Response (QR) codes around it. The large grey square in the centre of the balance card is a calibrated "panel" that can be used to calibrate the reflectance values as every balance card has been tested to determine its reflectance across the spectrum of light captured. The captured balance card images provided absolute reference information which was applied to each image individually for the collection of repeatable reflectance data over different flights, dates, and weather conditions.

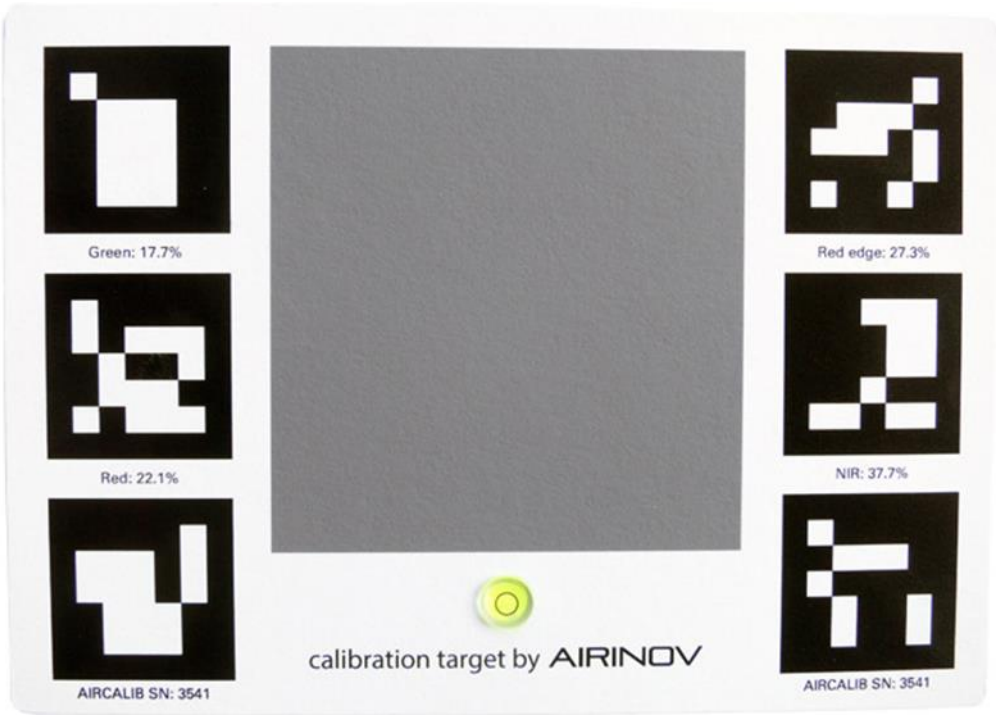

Fig.4.6 The balance card used for radiometric calibration.

4.6.1.4 Other considerations

After setting the flight parameters and reflectance calibration, a number of other items were considered before launching the UAS to ensure a safe and effective flight. These included weather conditions, backup battery, SIM card for image storage and UAS controller charge. In case of an emergency, the flight could be terminated manually from the controller. In consideration of the maximum 25 min battery life for a single flight of the UAS, the study site of about 40 ha was divided into three overlapping flying events.

4.6.2 Data processing

Overlapping imagery data collected by the UAS was processed with Pix4D software to generate geo-referenced orthomosaics, DSMs, contours, 3D point clouds and textured mesh models in various formats. As the image database of this research was large, a computer with seven cores (i7), 32 GB of Random-access Memory (RAM) and 1.5 TB

storage was used to process and save the files. The procedure is highly automated but required over 70 processing hours for the whole study site. The RGB imagery and multispectral imagery were processed in two separate projects. The RGB project required GCP position information to refer the project in the ITM coordinate system. Images of the calibration target were used for radiometric calibration and to remove the brightness difference in the multispectral bands project. Other processing options were customized to select the proper scale and format for the resulting data. A quality assessment report for each processing step was generated and stored.

4.6.3 Classification

From the orthomosaic model generated from the captured imagery, areas with dominated plant spices, including Pasture, Rusty Willow, Gorse, Sharp Rush, Marram, Common Reed and Mosses land, were presented. Based on this orthomosaic map, 1 m × 1 m ground truth samples were selected for classification to 12 different land features, including 7 vegetation species plus road, beach, stream, sand and built area. There were 280 samples identified for ground truth information. Forty-five ground truth samples among the 280 were used as training for a supervised classification. In this study, supervised classification using the maximum likehood classification algorithm was used for vegetation mapping with 12 land features identification.

To examine the efficacy of the multispectral sensor for vegetation mapping, classifications were conducted based on the classification strategies shown in Table 4.3. Classifications using these different strategies, were applied using the same training samples and the same check samples for accuracy assessment.

Table 4.3 Band combination for nine different classification strategies.

Classification strategy	Band combinations in each classification strategy
Three wavebands from RGB camera	Red + Green + Blue (1)
Four wavebands from Multispectral sensor	Green + Red + Red edge + NIR (2)
Seven available multispectral wavebands	Red + Green + Blue (from RGB) + Green + Red + Red edge + NIR (from multispectral) (3)
Eight wavebands combinations	Red + Green + Blue (from RGB) + Green + Red + Red edge + NIR (from multispectral) + Relative Green (4)
	Red + Green + Blue (from RGB) + Green + Red + Red edge + NIR (from multispectral) + Relative Red (5)
	Red + Green + Blue (from RGB) + Green + Red + Red edge + NIR (from multispectral) + Relative Blue (6)
	Red + Green + Blue (from RGB) + Green + Red + Red edge + NIR (from multispectral) + NDVI (7)
	Red + Green + Blue (from RGB) + Green + Red + Red edge + NIR (from multispectral) + gNDVI (8)
	Red + Green + Blue (from RGB) + Green + Red + Red edge + NIR (from multispectral) + GRVI (9)

4.7 Results and discussion

4.7.1 Data processing

The imagery was processed using Pix4D software which generated a 3D point cloud (Fig.4.7), an orthomosaic model (Fig.4.8), a DSM from the RGB imagery (Fig.4.9), and a NDVI index map (Fig.4.10) which was generated from the multispectral imagery.

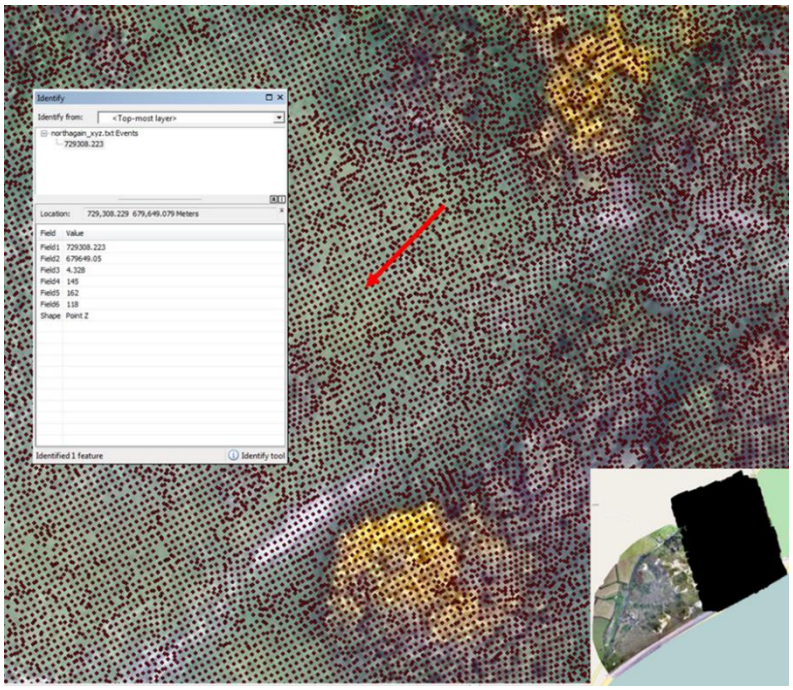

Fig.4.7 A sample of the 3D point cloud for the north section of study site.

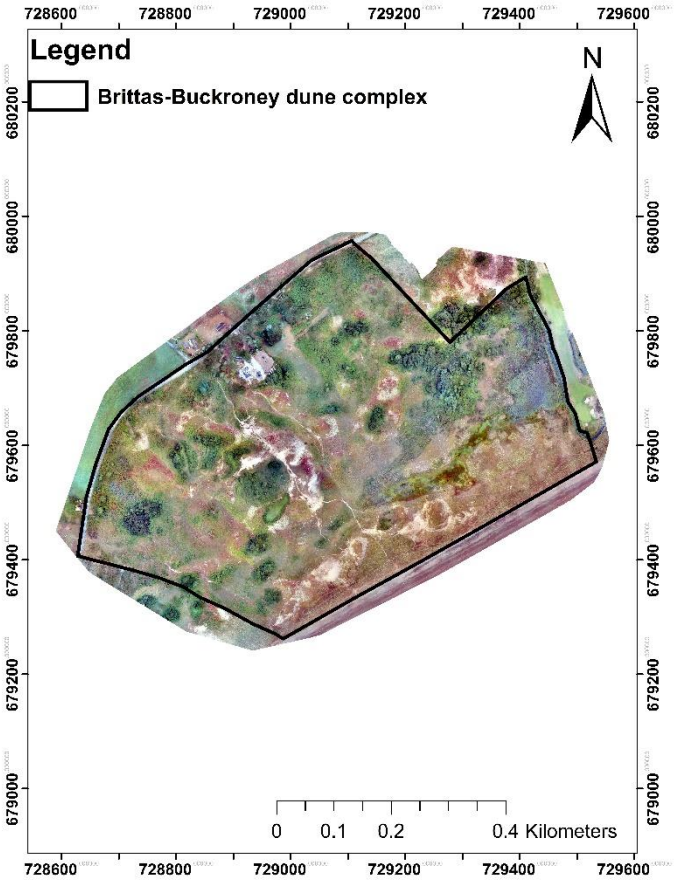

Fig.4.8 Orthomosaic model of the study site.

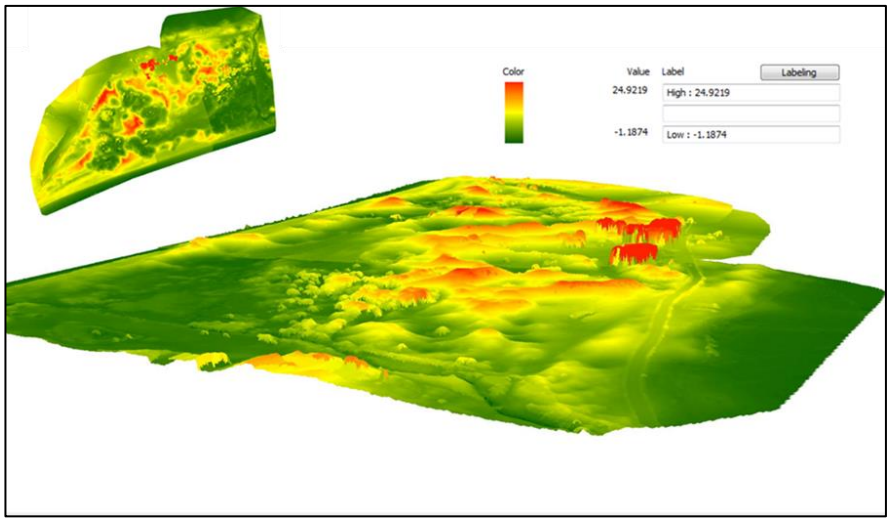

Fig.4.9 The view of DSM of the study site.

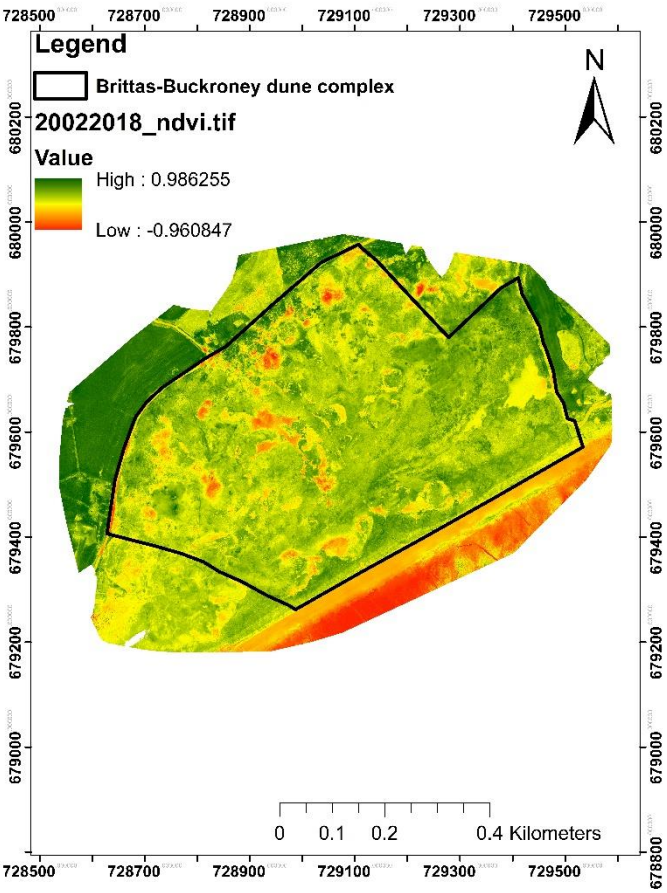

Fig.4.10 NDVI map of the study site.

In addition, seven individual multispectral waveband orthomosaics (red, green, blue from normal RGB camera and red, green, red edge, near infrared from multispectral sensor) of the site were created. These results were all referenced to the Irish Transverse Mercator (ITM) grid coordinate system. Ground sample distance (GSD) in a digital imagery of the ground from air is the distance between pixel centers measured on the ground. Outcomes from the RGB imagery had a GSD of 0.029 m and a georeferenceing Root-Mean-Square (RMS) error of 0.111 m.

Georeferencing of multispectral imagery by reference to GCPs is not supported within the Pix4D software. Multispectral imagery is georeferenced by reference to the on-board autonomous GNSS data included in the Exchangeable Image File Format (EXIF) files.

Six GCPs were identified in the outcome models and used as check point for outcome accuracy assessment. The multispectral imagery had a spatial resolution of 0.096 m and a georeferencing accuracy of 0.798 m.

4.7.2 Spectral analysis

From the orthomosaic model generated from the captured imagery, eight dominant vegetation areas, including Pasture, Rusty Willow, Gorse, Sharp Rush, Marram, Common Reed and Mosses land, and other four significant contiguous land cover types were identified on the site, *viz.* road, beach, stream, sand and built area. Spectral patterns for these 12 types were analysed in the available seven wavebands, *viz.* green, red, NIR and red edge from the multispectral sensor and red, green, blue wavebands extracted from RGB imagery. Fig.4.11 shows the spectral patterns of the twelve land cover types using these seven available wavebands.

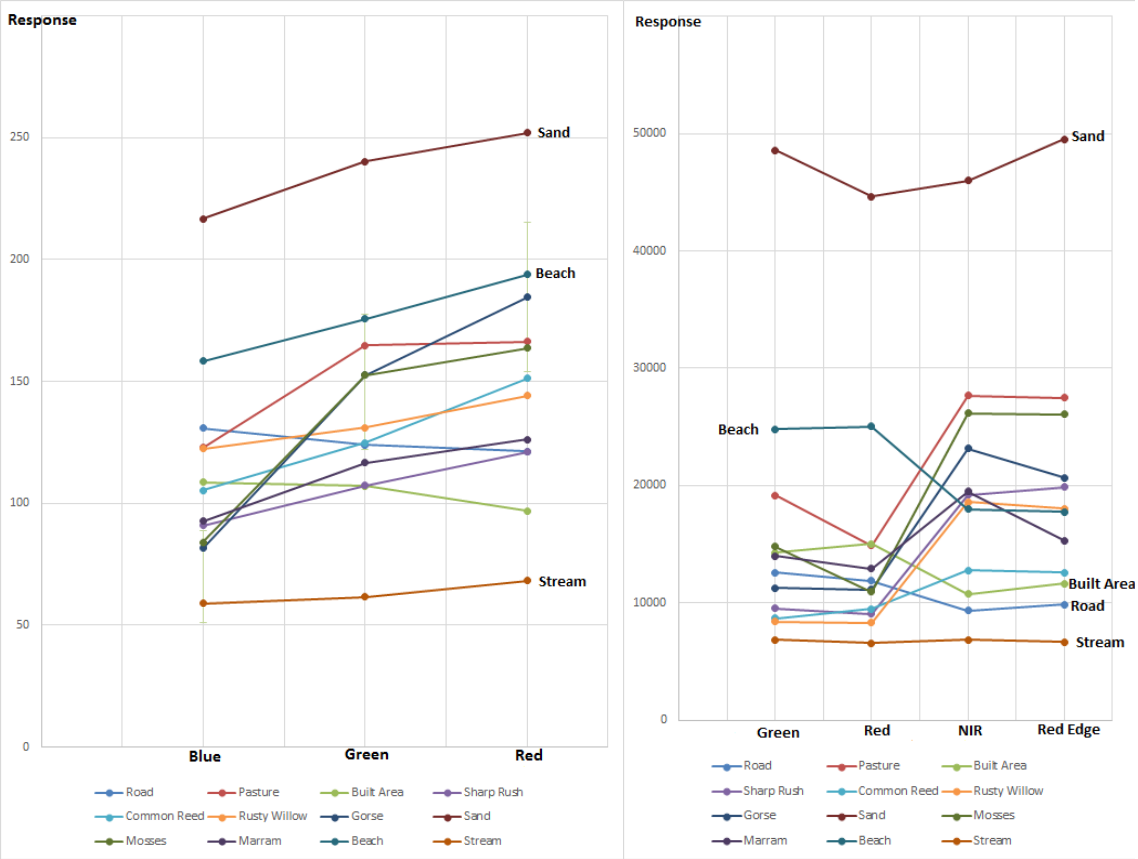

(**a**) (**b**)

Fig.4.11 Response of training samples in wavebands from (a) Blue, green and red wavebands extracted from RGB camera; (b) Green, red, NIR and red edge wavebands from multispectral sensor

As can be seen in Fig.4.11, "sand" and "stream" have significantly different responses under these seven available wavebands from the RGB camera and the multispectral sensor, which make them separable in the land feature classification. "Beach" has a distinctly separate response from other land cover types in the blue waveband extracted from the RGB camera and the red wavebands from the multispectral sensor, which means "beach" could be classified by considering the spectral pattern in only these two wavebands. Other land cover types have less separated responses in these available

wavebands which make it more difficult to spectrally differentiate them. Thus, separable response value in available wavebands from the RGB camera and the multispectral sensor can only be used to identify “sand”, “stream” and “beach”, other land cover features are hard to classified using response values in available wavebands.

Fig.4.11 also shows that vegetation land cover features have quite disparate spectral patterns in the RGB-derived bands but similar spectral patterns in the four wavebands of the multispectral sensors. The multispectral sensor-derived patterns all feature low responses at green and red wavebands and relatively higher responses at NIR and red edge wavebands. Non-vegetation land cover features do not follow this pattern and do not exhibit similar characteristic spectral patterns. Therefore, the characteristic spectral pattern of vegetation land features in the multispectral sensor-derived bands can be used to distinguish and separate vegetation and non-vegetation land features in the site.

In general, land cover features have characteristic spectral responses, in terms of both pattern and response value, which can be used as a basis for land cover features classification.

4.7.3 Classification accuracy

In this study, to examine the efficiency of multispectral sensor at vegetation mapping, accuracies of classifications were compared using different classification strategies (as shown in Table 4.3), including a combination of different multispectral wavebands and vegetation indices, calculated by multispectral wavebands. Classification accuracy was calculated by comparing the ground truth information and classified information in 245 samples through matrix analysis as seen in Table 4.4. Fig.4.12 shows the vegetation map of the site as the result of classification.

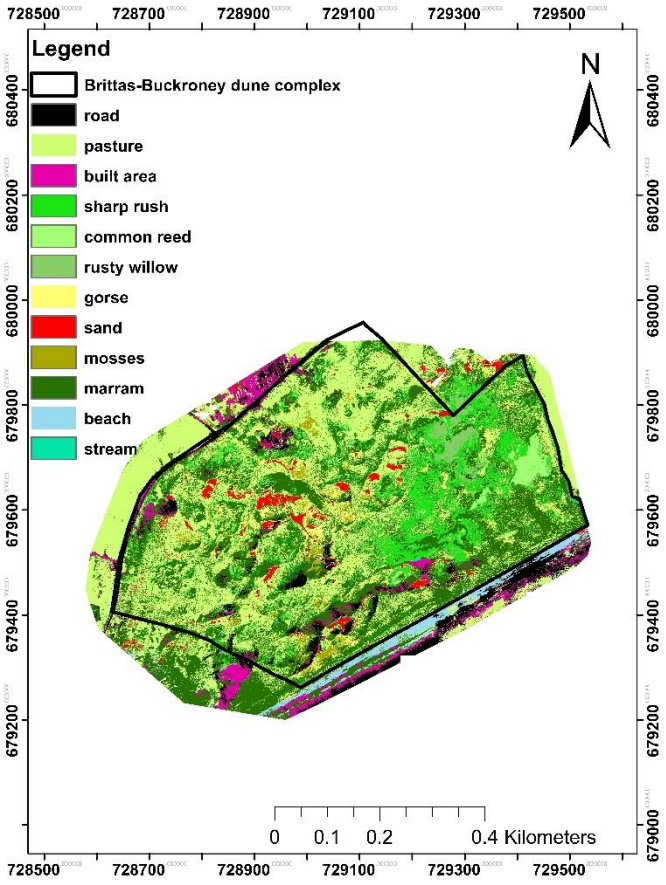

Fig.4.12 Vegetation mapping of study site.

Table 4.4 Sample matrix analysis for accuracy assessment.

		Classified data										
		Road	Built Area	Sand	Stream	Beach	Pasture	Sharp Rush	Common Reed	Rusty Willow	Gorse	Mosses Land	Marram
Ground truth data	Road	13	3	1		4							1
	B_A	2	16	3									
	Sand			16	2						1		2
	Str		1		17	2							1

Beach	1	14												
Past			16											
S_R				14										
C_R				1	15		5		2				1	
R_W				1			8							
Gorse				2			1		16		1			
M_L			3	1			1				17			
Mar			1	1	5		5		1		2		15	

Through the matrix, the accuracies based on different classification strategies (in Table 4.3) were calculated (Fig.4.13). 3RGB means the classification layer is the combination of red, green and blue wavebands from RGB camera, as seen in Table 4.3 (1); 4MTB means the classification layer is the combination of green, red, re edge and near infrared from multispectral sensor, as seen in Table 4.3 (2); 7MTB means the classification layer is the combination of all available multispectral wavebands, as seen in Table 4.3 (3); 8MTB_DSM, 8MTB_RG, 8MTB_RR, 8MTB_RB, 8MTB_NDVI, 8MTB_gNDVI, 8MTB_GRVI and 8MTB_NI were represented by (4), (5), (6), (7), (8), (9) in Table 4.3 respectively.

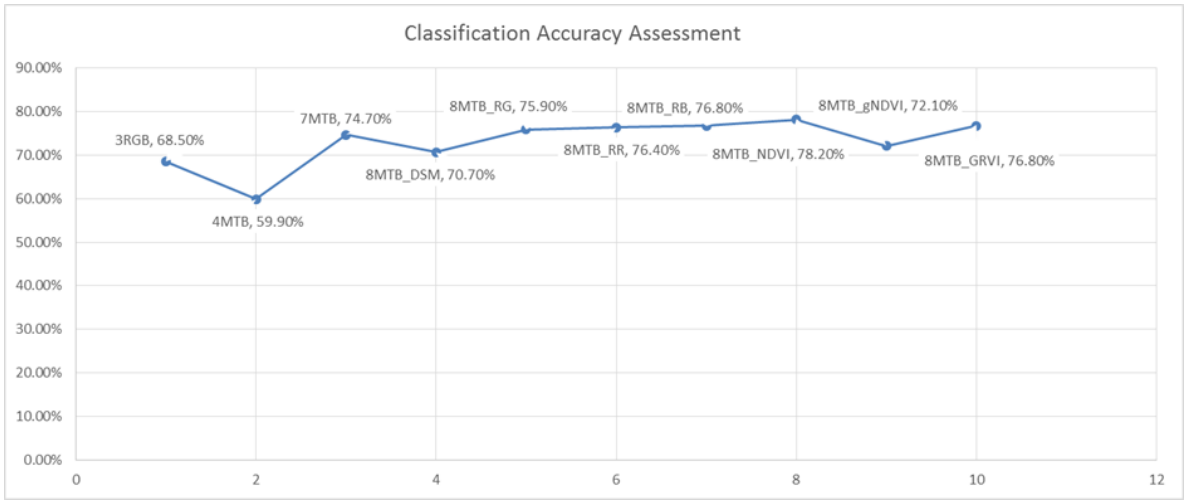

Fig.4.13 Classification accuracy based on different strategies.

The classification accuracy results (Fig.4.13) illustrate that multispectral sensor waveband data can help to improve the accuracy as, for example, the classification accuracy based on 7MTB is higher than that based on 3RGB. Adding more wavebands from multispectral sensor provides more reflectance information for classification and may help to improve the classification accuracy, such as 8MTB_RG (76%), 8MTB_RR (76%), 8MTB_RB (77%), 8MTB_NDVI (78%) and 8MTB_GRVI (77%) has higher accuracy than 7MTB (74%).

However, adding more reflectance information from the combination of wavebands did not always translate to an improvement in the classification accuracy. For example, 8MTB_DSM (71%) and 8MTB_gNDVI (72%) have lower accuracies than 7MTB (74%).

The classification accuracy of different classification strategies may also be influenced by image resolution. The multispectral sensor and RGB camera have different resolutions, being 1.2 Megapixels (MP) and 16MP respectively. This may lead to the classification accuracy of 4MTB (60%), from the multispectral sensor data, being lower

than 3RGB (69%) from RGB camera data. Although a lower spatial resolution can have a smoothing effect that can, sometimes, lead to a higher classification accuracy.

In addition, the RGB camera contains three non-discrete spectral bands, whereas the multispectral sensor has four discrete spectral bands. As seen in Fig.4.14, non-discrete spectral bands have a distinctly curved response and each band has considerable overlap in the wavelength range, whereas the discrete spectral bands of the multispectral sensor have an even response without overlap (MicaSense Knowledge Base site, 2018). This should result in the multispectral wavebands providing more reliable reflectance patterns for land feature classification.

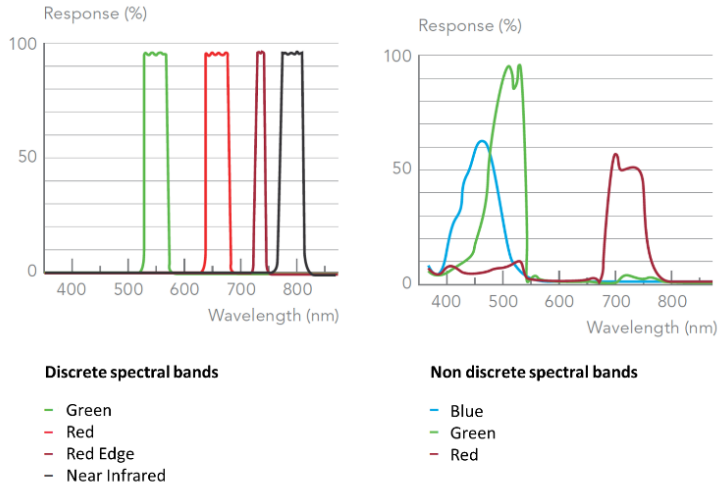

Fig.4.14 Wavelength and response of discrete and non-discrete spectral bands.

4.8 Conclusions

High-resolution vegetation and contiguous land cover mapping was successfully generated from imagery captured using a Sequoia multispectral sensor mounted on a UAS. The highest classification accuracy (78%) was achieved using eight spectral bands which included the three wavebands from the RGB camera, the four wavebands from the

multispectral sensor and the NDVI index. Whereas using the three wavebands from the RGB camera and the four wavebands from the multispectral sensor, in combination, achieved a classification accuracy of 75%. Classification accuracy using only the four multispectral wavebands, was lower than the accuracy using the three wavebands of the RGB camera. Factors including image resolution, number of wavebands used, spectral separability and index type may contribute to the observed different classification accuracies using different classification strategies.

This research also highlighted an effective option for on-site surveying, significantly reducing the hazards and workload for the development of vegetation maps and DEM's of a study area. Using the multispectral sensor resulted in data captured from a wider range of wavebands than an RGB camera alone, with better resolution and accuracy than other conventional remote sensing technologies, enabling the generation of dense 3D point clouds, and orthomosaic models, DEM and NDVI index maps. In these outcomes, vegetation distribution and elevation changes over the Buckroney dune complex were represented clearly. The classification results also illustrated the high accuracy achieved for identifying different vegetation and contiguous land cover.

However, notwithstanding the many benefits and advantages of UAS and multispectral technology in vegetation mapping, the technology still has some challenges with respect to dune complex surveying. One issue is the permission, licensing, training required and restrictions to areas of UAS flight from the relevant aviation authority. As different countries have varying legislation controlling UAS use, it is recommended to be well-informed about the limitations on UAS use before the start of any UAS project. Although the use of a UAS platform can save much time at the on-site data collecting stage, a considerable amount of time is required for data processing. Furthermore, compared to

other conventional survey methods, UAS is less robust as it is significantly impacted by environmental factors such as wind, precipitation and poor light conditions.

4.9 References

Anderson, K., Gaston, K.J., 2013. Lightweight unmanned aerial vehicles will revolutionize spatial ecology. Frontiers in Ecology and the Environment 11, 138–146.

Baltsavias, E.P., 1999.Airborne laser scanning: Existing systems and firms and other resources. ISPRS Journal of Photogrammetry and Remote Sensing 54, 164–198.

Bemis, S.P., Micklethwaite, S., Turner, D., James, M.R., Akciz, S., Thiele, S.T., Ali, H., 2014. Ground-based and UAV-based photogrammetry: a multi-scale, high- resolution mapping tool for structural geology and paleoseismology, Journal of Structural Geology 69, 163–178.

Cuo, L., Vogler, J.B. Fox, J.M., 2010. opographic normalization for improving vegetation classification in a mountainous watershed in Northern Thailand. International Journal of Remote Sensing 31, 3037–3050.

Elvidge, C., Lyon, R., 1985. Influence of rock–soil spectral variation on the assessment of green biomass. Remote Sensing of Environment 17, 265–279.

Fenu, G., Cogoni, D., Ferrara, C., Pinna, M.S., Bacchetta, G., 2012. Relationships between coastal sand dune properties and plant community distribution: The case of Is Arenas (Sardinia). Plant Biosystems 146, 3, 586–602

Fernández-Guisuraga, J.M., Sanz-Ablanedo, E., Suárez-Seoane, S., Calvo, L., 2018. Using Unmanned Aerial Vehicles in Postfire Vegetation Survey Campaigns through Large and Heterogeneous Areas: Opportunities and Challenges. Sensors 18, 2, 1-17.

Franklin, S.E., Lavigne, M.B., Wulder, M.A., McCaffrey, T.M., 2002. Large-area forest structure change detection: an example. Canadian Journal of Remote Sensing 28, 588–592.

Frosini, S., Lardicci, C., Balestri, E., 2012. Global Change and Response of Coastal Dune Plants to the Combined Effects of Increased Sand Accretion (Burial) and Nutrient Availability. PLOS ONE 7, 10, e47561.

Gao, Y.N., Zhang, W.C., 2009. A simple empirical topographic correction method for ETM plus imagery. International Journal of Remote Sensing 30, 9, 2259–2275.

Gini, R., Passoni, D., Pinto, L., Sona, G., 2012. Aerial images from an UAV system: 3d modeling and tree species classification in a park area. Int. Arch. Photogram. Remote Sensing Spatial Information Science 39, B1, 361–366.

Helmer, E.H., Brown, S., Cohen, W.B., 2000. Mapping montane tropical forest successional stage and land use with multi-date Landsat imagery. International Journal of Remote Sensing 21, 2163–2183.

Huang, Q.H., Cai, Y.L., 2009. Mapping karst rock in Southwest China. Mountain Research and Development 29, 14–20.

Kaneko, K., Nohara, S., 2014. Review of effective vegetation mapping using the UAV (Unmanned Aerial Vehicle) method. International Journal of Geographical Information Science 6, 733.

Kozhoridze, G., Orlovsky, N., Orlovsky, L., Blumberg, D.G., Golan-Goldhirsh, A., 2016. Remote sensing models of structure-related biochemicals and pigments for classification of trees. Remote Sensing of Environment 186, 184–195.

Kuplich, T.M., 2006. Classifying regenerating forest stages in Amazonia using remotely sensed images and a neural network. Forest Ecology and Management 234, 1–9.

Liu, Q.J., Takamura, T., Takeuchi, N., Shao, G., 2002. Mapping of boreal vegetation of a temperate mountain in China by multitemporal LANDSAT imagery. International Journal of Remote Sensing 23, 3385–3405.

Launeau, P., Giraud, M., Ba, A., Moussaoui, S., Robin, M., et al., 2018. Full-Waveform LiDAR Pixel Analysis for Low-Growing Vegetation Mapping of Coastal Foredunes in Western France. Remote Sensing 10, 669.

McKenna, J., O'Hagan, A.M., Power, J., Macleod, M., Cooper, A., 2007. Coastal dune conservation on an Irish commonage: Community-based management or tragedy of the commons. The Geographical Journal 173, 2, 157–169.

MicaSense Knowledge Base site, accessed on 12/05/2018. What spectral bands does the Sequoia camera capture? Available Online: https://support.micasense.com/hc/en-us/articles/217112037-What-spectral-bands-does-the-Sequoia-camera-captur.

NPS (National Park Service) by NatureServe, access on 26/03/2018. Accuracy Assessment: Cowpens National Battlefield Vegetation Map (A NatureServe Technical Report). Available online: https://irma.nps.gov/DataStore/DownloadFile/575467.

NPWS (National Parks & Wildlife Service) (site documents), access on 14/05/2018. Site Synopsis: Buckroney-Brittas Dunes and Fen SAC. Available online: https://www.npws.ie/protected-sites/sac/000729.

OSi (Ordnance Survey Ireland), access on 20/02/2018. Highly Accurate Digital Terrain Models (DTM) or Digital Surface Models (DSM). Available online: https://www.osi.ie/wp-content/uploads/2015/05/Lidar_prod_overview.pdf.

Pajares, G., 2015. Overview and current status of remote sensing applications based on unmanned aerial vehicles (UAVs). Photogrammetric Engineering and Remote Sensing 81, 281–329.

Qi, X.K., Wang, K.L., Zhang, C.H., 2013. Effectiveness of ecological restoration projects in a karst region of southwest China assessed using vegetation succession mapping. Ecological Engineering 54, 245–253.

Ren, X., Sun, M., Zhang, X., Liu, L., 2017. A Simplified Method for UAV Multispectral Images Mosaicking. Remote Sensing 9, 9, 1-21.

Sabatier, F., Anthony, E.J., Hquette, A., Suanez, S., Musereau, J., Ruz, M.H., Regnauld, H., 2009. Morphodynamics of beach/dune systems: Examples from the coast of France. Géomorphologie 15, 3–22.

Silleos, N.G., Alexandridis, T.K., Gitas, I.Z., Perakis, K., 2006. Vegetation indices: advances made in biomass estimation and vegetation monitoring in the last 30 years. Geocarto International 21, 4, 21–8.

Song, C.H., Schroeder, T.A., Cohen, W.B., 2007. Predicting temperate conifer forest successional stage distributions with multitemporal Landsat Thematic Mapper imagery. Remote Sensing of Environment 106, 228–237.

Song, C.H., Woodcock, C.E., 2003. Monitoring forest succession with multitemporal Landsat images: factors of uncertainty. IEEE Transactions on Geoscience and Remote Sensing 41, 2557–2567.

Tokola, T., Sarkeala, J., Linden, M.V.D., 2001. Use of topographic correction in Landsat TM-based forest interpretation in Nepal. International Journal of Remote Sensing 22, 4, 551–563.

Tonkin, T.N., Midgley, N.G., 2016. Ground-control networks for image based surface reconstruction: an investigation of optimum survey designs using UAV derived imagery and structure-from-motion photogrammetry, Remote Sensing 8, 9, 786.

Trimble positioning service site, access on 23/07/2019. Trimble RTX Frequently Asked Question. Available online: https://positioningservices.trimble.com/wp-content/uploads/2019/02/Trimble_RTX_Frequently_Asked_Questions.pdf.

Turner, I.L., Harley, M.D., Drummond, C.D., 2016. UAVs for coastal surveying, Coastal Engineering 114, 19–24.

Uysal, M., Toprak, A.S., Polat, N., 2015. DEM generation with UAV Photogrammetry and accuracy analysis in Sahitler hill, Measurement 73, 539–543.

Vaca, R.A., Golicher, D.J., Cayuela, L., 2011. Using climatically based random forests to downscale coarse-grained potential natural vegetation maps in tropical Mexico. Applied Vegetation Science 14, 388-401.

Verbesselt, J., Hyndman, R., Newnham, G., Culvenor, D., 2010. Detecting trend and seasonal changes in satellite image time series. Remote Sensing of Environment 114, 106–115.

Venturi, S., Di Francesco, S., Materazzi, F., Manciola P., 2016. Unmanned aerial vehicles and Geographical Information System integrated analysis of vegetation in Trasimeno Lake, Italy. Lakes and Reservoirs: Research and Management 21, 5–19.

Weil, G., Lensky, I., Resheff, Y., Levin, N., 2017. Optimizing the Timing of Unmanned Aerial Vehicle Image Acquisition for Applied Mapping of Woody Vegetation Species Using Feature Selection. Remote Sensing 9, 11, 1-25.

Wilson, E.H., Sader, S.A., 2002. Detection of forest harvest type using multiple dates of Landsat TM imagery. Remote Sensing of Environment 80, 385–396.

Woo, M.K., Fang, G.X., DiCenzo, P.D., 1997. The role of vegetation in the retardation of soil erosion. Catema 29, 2, 145–159.

Yu, L.F., Zhu, S.Q., Ye, J.Z., Wei, L.M., Chen, Z.G., 2000. A study on evaluation of natural restoration for degraded karst forest. Scientia Silvae Sinicae 36, 6, 12–19 (in Chinese).

Chapter 5

ENVIRONMENTAL MODELLING FOR VEGETATION AND NON-VEGETATION CHANGES AT COASTAL DUNE COMPLEXES

5.1 Prologue

Chapter 3 and Chapter 4 of this dissertation focused comparing and optimizing high-end surveying methods to produce topographic mapping, and then producing vegetation mapping, based on UAS-mounted multispectral sensor data, for coastal dune complexes with particular reference to the Brittas-Buckroney dune complex in Co. Wicklow, Ireland. To achieve the overall aim of this project, which was to develop environmental modelling for coastal dune complexes to contribute to the effective conservation strategies, a further element, Element 3, was designed as follows:

Element 3 - Environmental modelling for vegetation and non-vegetation changes at coastal dune complexes for coastal environmental management.

This chapter focuses on Element 3 above and forms the basis of a research paper entitled 'Development of environmental models for a coastal dune complex using drone-mounted multispectral sensor data' which has been submitted to the Ocean & Coastal Management Journal and is currently under review. The research paper, as submitted, is reproduced in Chapter 5.

5.2 General information

Abstract: Increasing human activities and global climate changes threaten ecosystem maintenance at coastal zones, resulting in issues including soil erosion, flooding and habitat loss. Environmental modelling was developed to identify and explore important processes at coastal zones, which can contribute to more effective coastal management and conservation. This study presents the process of environmental modelling of a coastal dune complex with particular reference to the Buckroney dune complex in County Wicklow, Ireland. As part of the study, a methodology was developed for monitoring land

feature changes concerning for vegetation health, density and distribution using a multispectral sensor mounted on a drone. Based on spectral analysis of the captured multispectral data, a vegetation index was created, referred to as the 'Buckroney index (BKI)'. This BKI value represented the health and density of vegetation, and has demonstrated good performance at distinguishing vegetation features from non-vegetation features. By monitoring the BKI value of vegetation features at the site over a vegetation growing season, a mathematical model was established that simulates vegetation growing processes related with time-series environmental parameters, *viz.* temperature, rainfall, wind, solar radiation, evaporation, pressure, humidity, cloud, visibility, sun hours and UV index. The average accuracy of the mathematical model was 92% and the model showed that the most significant time-series parameters affecting vegetation during the 10 months of monitoring were wind, temperature and UV index. In addition, a distribution model was developed that represented the probability of non-vegetated land-cover occurrence on the site related to position-related environmental parameters, namely slope, aspect, elevation and nearest distance to pathways. Further analysis of the non-vegetated distribution model showed that elevation and distance from pathlines had weights of importance of 60% and 20% respectively, while slope and aspect represented the remaining 20% of importance in effecting non-vegetation occurrence in the coastal dune systems over the observed period of the study. The mathematical model of vegetation changes and the predictive non-vegetation distribution model contributed to better understanding the vegetation growing process and finding high-risk areas for non-vegetation feature occurrence, indicating sand exposure or soil erosion areas in the site. These results were helpful for coastal environmental management in protecting areas of high ecological value and minimizing the impacts of non-vegetated exposure, often associated with soil erosion at coastal dune complexes.

Keywords: Coastal dune complexes; drone; multispectral sensor; vegetation features; non-vegetated features area; environmental parameters; mathematical model; distribution model.

5.3 Introduction

Coastal zones comprise 2% of the earth's land area (Acosta et al., 2005). They are the transition areas between the marine and terrestrial environments and dune complex is one of the main structures at these coastal zones (Lucas et al., 2002). These coastal zones play an essential role in the preservation of coastal ecosystem stability and biological diversity as they provide drinking water, mineral resources, offer habitats for unique flora and fauna communities, control soil erosion and flooding, and protect nearby natural and build systems from other environmental hazards (Clark, 1997; Andrews et al., 2002).

In recent years, increasing tourism and development in the coastal dune area of coastal zones has resulted in increased pressure on the environment, resulting in issues including soil erosion, flooding and habitat loss (Phillips and Jones, 2006; Martinez et al., 2016). Preservation and effective management of coastal zones requires a full understanding of the key processes that control their dynamic morphology (Mitasova et al., 2005; Payo et al., 2017). However, coastal zones are difficult to study because of the complex relationships linking topography, hydrology, aeolian processes and sand movement throughout the system (Andrews et al., 2002; Payo et al., 2017). A better understanding of these areas can be developed using a modelling approach to explore and identify the important processes at coastal zones, for example, sand dunes development and how vegetation, aeolian activity and other environmental variables affect morphological changes (Alhajraf, 2004; Zhang et al., 2010; Xia and Dong, 2016).

In Ireland, coastal erosion rates at 'soft' (sediment-dominated) coasts average 0.2–0.5 m/y, commonly rising to 1–2 m/y on some southern and eastern coasts (Devoy, 2008). Current total rates of land loss for Ireland from erosion and flooding have been estimated to be approximately 1.6 km^2/y, concentrated in about 300 sites (Devoy, 2008).

This research involves modelling of a coastal dune complex at Buckroney in County Wicklow, Ireland (Fig.3.1), which is managed by the Irish National Parks & Wildlife Service (NPWS) and presents a methodology for monitoring the occurrence of vegetation and non-vegetated landscape changes at the site over 10 months using a multispectral sensor mounted on a drone. To represent the health and density of vegetation, and to distinguish vegetation from non-vegetated features at the site, a vegetation index, called the 'Buckroney Index' (BKI), was developed. The first objective of this study is the development of a mathematical modelling that relates monthly mean BKI values for vegetated areas with time-series parameters, namely temperature, rainfall, wind, solar radiation, evaporation, pressure, humidity, cloud, and UV index. Building an understanding of system dynamics in this way greatly aids our understanding of the vegetation processes at the site. A second objective of this study was to develop a distribution model mapping the non-occurrence of vegetation related to position dependent parameters, *viz.* slope, aspect, elevation and distance to pathways, which can indicate areas with an increased potential for sediment exposure and associated soil erosion. By analysing the mathematical model and predicted non-vegetation distribution model, the most significant environmental parameters governing the processes of vegetation growth and the non-occurrence of vegetation, can be identified. These outputs can contribute to a better understanding of coastal environmental management processes and can help towards the protection of area of heightened ecological importance and vulnerability.

5.4 Background

In order to represent the eco-geomorphological character of the coastal region at Buckroney it is necessary to establish a geo-referenced model that addresses the dynamics of both vertical and horizontal changes in the dune terrain (Krueger, 2011). The use of a three dimensional (3D) modelling representation provides greater understanding of the inherent dynamics in the system, especially when the processes to be simulated are strongly characterized by three-dimensionality in terms of its geometry. For example, a detailed 3D model can represent the geo-structural characterization of the surface of coastal dune system and can also support deterministic analyses aimed at assessing dune stability.

In modelling environmental systems, one of the most widely used type of model is the mathematical simulation model (Hardisty et al., 1993; Hanson et al., 2003; Mendoza et al., 2017), which is a description of a system using mathematical concepts and language to help explain process and function in environmental systems (Stive et al., 1997; Walkden and Hall, 2011; Kobayashi, 2016). Mathematical models have been applied to the modelling of post-storm beach accretion and recovery and gravel beach variability (Pender and Karunarathna, 2013). An example of mathematical modelling tool, Xbeach, is widely used for beach and dune erosion, specifically designed for small-scale (project-scale) coastal applications which can be used for morphology modelling (Roelvink et al., 2009).

Vegetation modelling on coastal dune complexes is important as vegetation has a strong impact on dune morphology and dynamics and can influence sediment transport (Sabatier et al., 2009). Vegetation is also a critical environmental component of the coastal ecosystem for food production, resource conservation, nutrient cycling, and carbon

sequestration (Woo et al., 1997; Kuplich, 2006). Vegetation models of coastal dune complexes, with accurate distribution and population estimates for different functional plant species, can be used to analyse vegetation dynamics, quantify spatial patterns of vegetation evolution, analyse the effects of environmental changes on vegetation, and predict the spatial patterns of species diversity (Vaca et al., 2011; Zhang et al., 2012; Moriondo et al., 2013). Vegetation distribution modelling has developed over recent decades and is increasingly used for predictions of occurrences of species within applied ecology or the potential occurrences of soil erosion areas (Guisan and Zimmermann, 2000; Drew et al., 2011; Yackulic et al., 2013). Such information can contribute to the development of targeted land management actions that maintain biodiversity and ecological functions (Miller et al., 2007; Weber, 2011; Hemsing and Bryn, 2012).

Coastal vulnerability assessment is an established methodology for the identification of sensitive coastal zones, and incorporates a wide range of discipline including physical and urban geography for territorial planning, economics and environmental management (ISDR, 2004; Serafim et al., 2019).Vulnerability assessment has increasingly been used to generate data on threats or risks, as a component in the decision-making process (Bankoff et al., 2003; Ciccarelli et al., 2017). Belperio et al. (2001) considered elevation, exposure, aspect, and slope as the significant physical parameters for assessing the coastal vulnerability of a coastal zone with respect to sea-level rise and concluded that coastal vulnerability is strongly correlated with elevation and exposure and a regional-scale, distributed, coastal process modelling may be suitable in assessing coastal vulnerability to sea-level rise in tide-dominated, sedimentary coastal regions. A case study of the Xiamen coast in China, using a multi-criteria index for coastal vulnerability assessment (*e.g.* erosion) (Zhu et al., 2019), showed that 52% and 31% of the Xiamen coast exhibited medium vulnerability and high vulnerability areas, respectively, to coastal erosion. The

coastal erosion vulnerability of artificial coasts was significantly higher than those of natural coasts. And the research showed this difference was mainly controlled by the coastal slope and coastal buffer ability compared to other seven considered parameters, *viz.* coastal geomorphology, coastal natural habitats, significant wave height, storms, values of roads and buildings, population activity and GDP per capita and fiscal revenue (Zhu et al., 2019).

As coastal zones include multiple landforms, the modelling should consider the interactions between the component landforms, for example, beaches and dune complexes (Payo et al., 2017). This is difficult as the interactions are complicated and not fully understood. At this stage, researchers have found solutions by using model-to-model interfaces, integrating several software suits to develop component models in the same platform. Significant development has been achieved in this field in the last decade, especially by the Open Modelling Interface (OpenMI) and Community Surface Dynamics Modelling System (CSDMS) (Gregersen et al., 2005; Jackson et al., 2013; Hutton et al., 2014). They both aim to improve insight by linking various different models together to explore broader system processes and interactions.

5.5 Study site

The Brittas-Buckroney dune complex (Fig.4.2) is located c. 10 km south of Wicklow town on the east coast of Ireland and comprises two main sand dune systems, *viz.* Brittas Bay and Buckroney Dunes. The study site for this research is Buckroney Dunes which is managed by the Irish National Parks & Wildlife Service. The area of the Buckroney dune complex is *c.* 40 ha. Within this site, ten habitats listed on the EU Habitats Directive are present, including two priority habitats in Ireland, *viz.* fixed dune and decalcified dune heath. This dune system also contains good examples of other dune types. At the northern

part of the Buckroney dune complex, there are some representative parabolic dunes, while embryonic dunes mostly occur at the southern part (NPWS, 2018).

The site is notable for the presence of well-developed plant communities (NPWS, 2018). Mosses are frequently found in this dune complex, while Sharp Rush (*J. acutus*) dominates south of the inlet stream to the fen area at the north of the dune complex, and in small areas elsewhere within the Buckroney dune complex. The main dune ridges are dominated by Marram (*Ammophila arenaria*), while Gorse (*Ulex europaeus*) is also present at the back of the dunes. To the west, a dense swamp of Common Reed (*Phragmites australis*) is present. There are also extensive areas of Rusty Willow (*Salix cinerea subsp. oleifolia*) scrub throughout the dune complex (NPWS, 2018).

With the land acquisition in recent years, marginal areas of the dune system have been reclaimed as farmland. Increasing anthropogenic activities within the dune system, such as farming and recreational activities, have increased pressure on the development of the dune ecosystem, with issues including soil erosion, flooding and habitat loss.

5.6 Methodology

This research used data from a multispectral sensor mounted on a drone for monitoring changes in land features over the growing season, from February 2018 to November 2018. Monthly climate data of time-series environmental parameters, *viz.* temperature, rainfall, wind, solar radiation, evaporation, pressure, humidity, cloud, and UV index, were obtained from Ireland's national meteorological service, Met Éireann (https://www.met.ie/), and monthly climate averages were obtained from World Weather Online (https://www.worldweatheronline.com/). Data on position-related environmental parameters, *viz.* slope, aspect, elevation and distance to pathlines, were generated from a Digital Surface Model (DSM) of the site which was created from drone imagery. Using

these datasets, a series of analytical protocols were developed to synthesis an environmental model to predict changes of vegetated and non-vegetated features in coastal dune complex.

5.6.1 Data acquisition

The drone platform used in this research was a DJI Phantom 3 Professional, which has four rotors, a central body containing the electronic components and landing gear that sustains the entire structure (Fig.4.4). The drone was powered by a lithium polymer battery that allowed a maximum flight time of 25 min. The multispectral sensor used in this study was a Parrot Sequoia which was comprised of five individual cameras and a sun sensor. The cameras consisted of a 16 MP RGB sensor and four 1.2 MP multispectral sensors that record in green (0.530–0.570 μm), red (0.640–0.680 μm), red edge (0.730–0.740 μm) and near-infrared (NI) (0.770–0.810 μm) wavebands. The camera cluster was mounted under the central body of the drone and a sun sensor was positioned above the central body as seen in Fig.4.4. The sun sensor provided real-time corrections for variations in illumination during a sortie. The field work for this study was conducted monthly during the period from February to November in 2018.

Overlapping imagery data collected by the UAS was processed with Pix4D software to generate geo-referenced orthomosaics, DSMs, contours, 3D point clouds and textured mesh models in various formats. As the image database of this research was large, a computer with seven cores (i7), 32 GB of RAM amd 1.5 TB storage was used to process and save the files. The procedure is highly automated but required over 70 processing hours for the whole study site. The RGB imagery and multispectral imagery were processed in two separate projects. The RGB project required GCP position information to refer the project in the Irish Transverse Mercator (ITM) coordinate system. Images of

the calibration target (Fig.4.6) were used for radiometric calibration and to remove the brightness difference in the multispectral bands project. Other processing options were customized to select the proper scale and format for the resulting data. A quality assessment report for each processing step was generated and stored.

5.6.2 Spectral analysis for vegetation and non-vegetation mapping

An essential part of this study was vegetation mapping showing vegetation areal extent, health and density, and non-vegetation mapping representing the areal extent of sand exposure in the site. The spectral characteristics of relevant land cover features were required as ground-truth data for subsequent automatic, spectral classification-based mapping to separate vegetated and non-vegetated areas. Spectral libraries are collections of spectral patterns of homogeneous land-cover materials based on field measurements and they provide an accessible alternative source of the required spectral characteristics. Compared to on-site observation, the use of spectral libraries saves both time and effort, particularly when seasonal changes of vegetated features need to be considered. Although finding a perfect match between relevant land-cover types on the ground and in the spectral libraries is generally unrealistic, similar land features in the spectral libraries can still provide useful data for vegetation mapping using spectral-based classification methods

In this research, the spectral libraries of the U.S. Geological Survey (USGS) and the ECOSTRESS spectral library of the California Institute Technology were used. These spectral libraries provided reflectance patterns over a wide spectral range from 0.2 μm to 3 μm, which containing the spectral range (0.5 μm to 0.8 μm) of multispectral sensor. Reflectance patterns of similar land-cover materials to those encountered in the study area, *e.g.* road, roof, sand (dune area), sea water, yellow flower, and different coastal grass

types, including golden grass, grass with 90% dry and 10% green, grass with 80% dry and 20% green, grass with 70% dry and 30% green, grass with 60% dry and 40% green, grass with 50% dry and 50% green, grass with 40% dry and 60% green, and grass with 95% green, were selected.

5.6.3 Parameters for environmental modelling

An essential element for environmental modelling is to identify and estimate the environmental parameters which characterize the model and, hence, to simplify the model structure (Hardisty, 1993). In this research, monthly vegetation and non-vegetation feature changes at the study site, over the study period, were influenced by different environmental parameters. These parameters were considered to be divided into two general types, time-series parameters which change with time, and position-series parameters which change with location. In this research, 12 different time-series parameters were considered, *viz.* rainfall, soil temperature, wind, evaporation, solar radiation, temperature, pressure, humidity, cloud, visibility, UV index and sun hour, and four position-series parameters were considered, *viz.* aspect, slope, elevation and distance to pathlines. These parameters data can obtained from Ireland's national meteorological service, Met Éireann, and from World Weather Online. Monthly data of these environmental parameters were based on the nearest meteorological station built at Arklow, which is about 10 km from the study site (the Buckroney dune complex).

5.6.4 Development of environmental models

In this research, observing and monitoring changes in vegetated and non-vegetated features of the study site were conducted using a multispectral sensor mounted on a drone. The acquired imagery (Fig.5.1) was used to create sequential maps of the land surface showing the extent of vegetation and changes reflecting the quality and composition of

that vegetation over time including the occurrence of bare ground (non-vegetated land). Through spectral analysis, the spectral characteristics of vegetation and non-vegetation features were identified and used to separate the land features for the generation of vegetation map and non-vegetation maps.

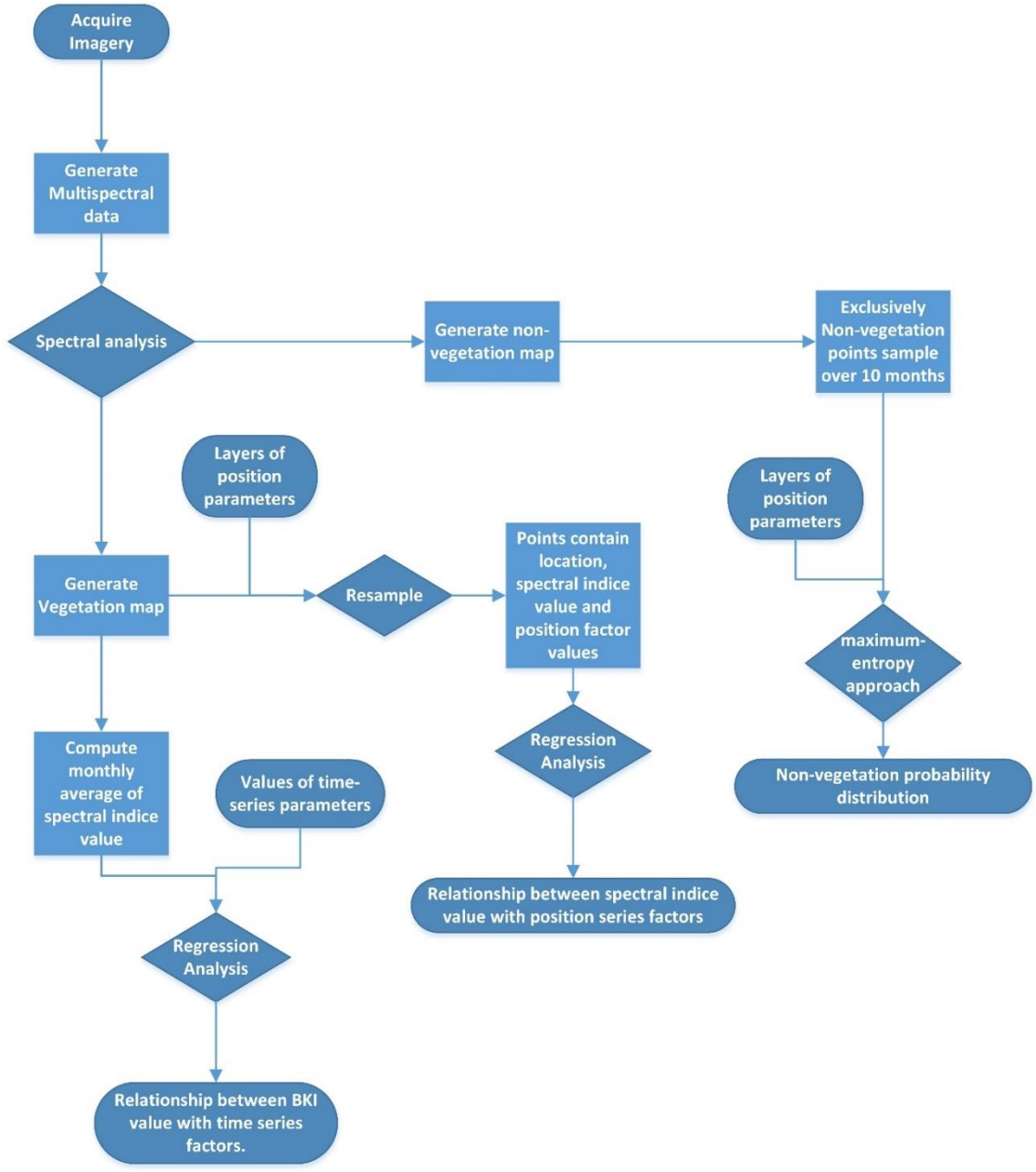

Fig.5.1 Flowchart of environmental modelling processes in this research

Maps of the vegetated surface areas were generated during the ten month observation period by spectral analysis. There are some existing spectral indices that can be calculated from multispectral bands and are widely used for vegetation mapping. These spectral indices can represent the growing status of vegetation shown as spatial response to chlorophyll level. Weil et al. (2017) listed six such indices that relate to the camera-based RGB spectral bands and four multispectral bands (Table 5.1). In this research, monthly spectral index value were computed and used as a vegetation growth index. Regression analysis was used to find the time-series parameters which have impacts on vegetation land feature changes and to simulate the relationship between monthly spectral index values and the time-series environmental parameters, leading to a mathematical model for vegetation features changes (Fig.5.1).

Table 5.1 Spectral indices calculated from wavebands of multispectral sensor.

Spectral indices	**Formula**	**Explanation**
Relative Green	$\frac{Green}{(Red + Green + Blue)}$	The relative component of green, red and blue bands over the total sum of all camera bands. Less affected from scene illumination conditions than the original band value.
Relative Red	$\frac{Red}{(Red + Green + Blue)}$	
Relative Blue	$\frac{Blue}{(Red + Green + Blue)}$	
NDVI	$\frac{Near - infrared - Red}{Near - infrared + Red}$	Relationship between the Near-infrared (NIR) and red bands indicates vegetation condition due to chlorophyll absorption within red spectral range and high reflectance within the NIR range.
gNDVI	$\frac{Near - infrared - Green}{Near - infrared + Green}$	Improvement of NDVI, more accurate in assessing chlorophyll content.

GRVI	$\frac{Green - Red}{Green + red}$	Relationship between the green and red bands is an effective index for detecting phenophases.

Maps of the non-vegetated surface areas were generated during the ten month observation period. Maximum-entropy techniques were used to find the relationship between the position of non-vegetated areas and position-related parameters. Maximum-entropy techniques provide the probability distribution to construct descriptive and predictive models of biological systems. Based on their conceptual simplicity and mathematical reliability, maximum-entropy techniques are often used in complex biological networks with large experimental data sets (Phillips et al., 2004). For maximum-entropy analysis in this research, a dataset was created of georeferenced non-vegetated areas occurrence localities as sample areas and another dataset was created that contained monthly values of position-related environmental parameters, such as aspect, slope, elevation, and distance to pathlines obtained from the digital surface data of the site. Maximum-entropy analysis of these two datasets was aimed at identifying the regions within the site with environmental parameters which satisfied the requirements for the occurrence of non-vegetation features. Accordingly, a model of the geographic distribution, over the study period, of the non-vegetation features at the site, *e.g.* exposed sand, was developed. This distribution model predicts where non-vegetated areas are more likely to occur within the site. These areas are indicative the sand exposure and related erosion area. A further outcome of maximum-entropy analysis was a measure of the influence of the different position-related environmental parameters referred-to as the ‘percent contribution’ and ‘permutation importance’. ‘Percent contribution’ represents the contribution of each environmental parameter to the output model while ‘permutation importance’ represents the importance of environmental parameters in the output model (De Martino et al., 2018).

5.7 Result

Imagery from multispectral sensor mounted on drone were all referenced to the ITM grid coordinate system. Ground sample distance (GSD) represens the distance between pixel centres as measured on the ground. The RGB imagery had a GSD of 0.029 m and a georeferencing root mean square (RMS) error of 0.111 m. From the RGB drone imagery of the study area, a 3D point cloud, an orthomosaic model and a DSM were produced using the Pix4D software package. Fig.5.2 shows the orthomosaic model of the site for the 20th of February 2018. Similar orthomosaic models were produced for each of the other months included in the study.

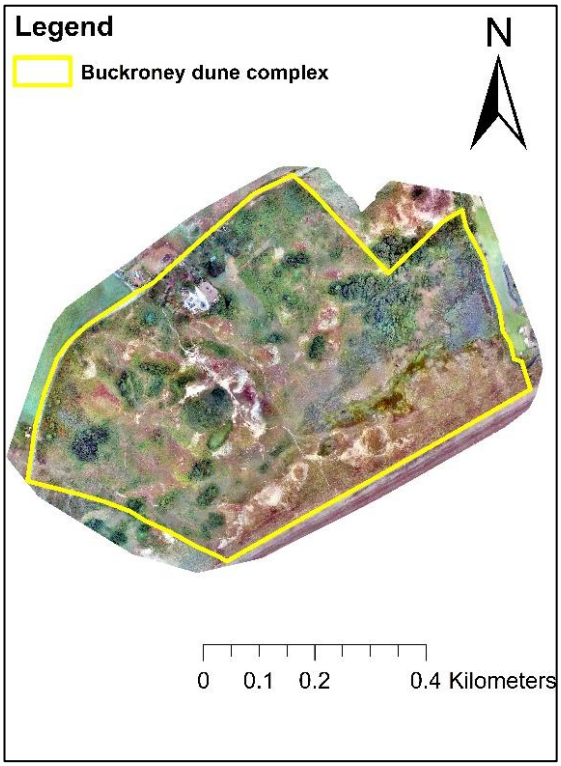

Fig.5.2 Orthomosaic model of the study site from captured RGB imagery.

Georeferencing of multispectral imagery by reference to the ground control points (GCPs) is not supported within the Pix4D software. Multispectral imagery is georeferenced by reference to the on-board autonomous GNSS data included in the

imagery EXIF files. Six GCPs were identified in the outcome models and used as check points for outcome accuracy assessment. The multispectral imagery had a spatial resolution of 0.096 m and a georeferencing accuracy of 0.798 m.

Resulting from the spectral analysis, a new spectral index, referred-to as 'BKI', was developed to indicate vegetation health and density and to distinguish vegetated and non-vegetated features in the site. An explanation of the BKI index is given in the following section 5.1. Based on the outcome of the processing of acquired imagery and monitoring of BKI changes, a mathematical model was developed to represent the relationship between vegetation changes and time-series environmental parameters (shown in section 5.2). Another distribution model was also developed to predict the occurrence of non-vegetated features and their relationship with the position-related parameters within the site (shown in section 5.3).

5.7.1 BKI Vegetation Index

Fig.5.3 shows the reflectance of the different land features, related to coastal dune land cover, that were selected for analysis from the spectral libraries. These land features are road, roof, sand (dune area), sea water, yellow flower, and different grass types *viz.* golden grass, grass with 90% dry and 10% green, grass with 80% dry and 20% green, grass with 70% dry and 30% green, grass with 60% dry and 40% green, grass with 50% dry and 50% green, grass with 40% dry and 60% green, and grass with 95% green.

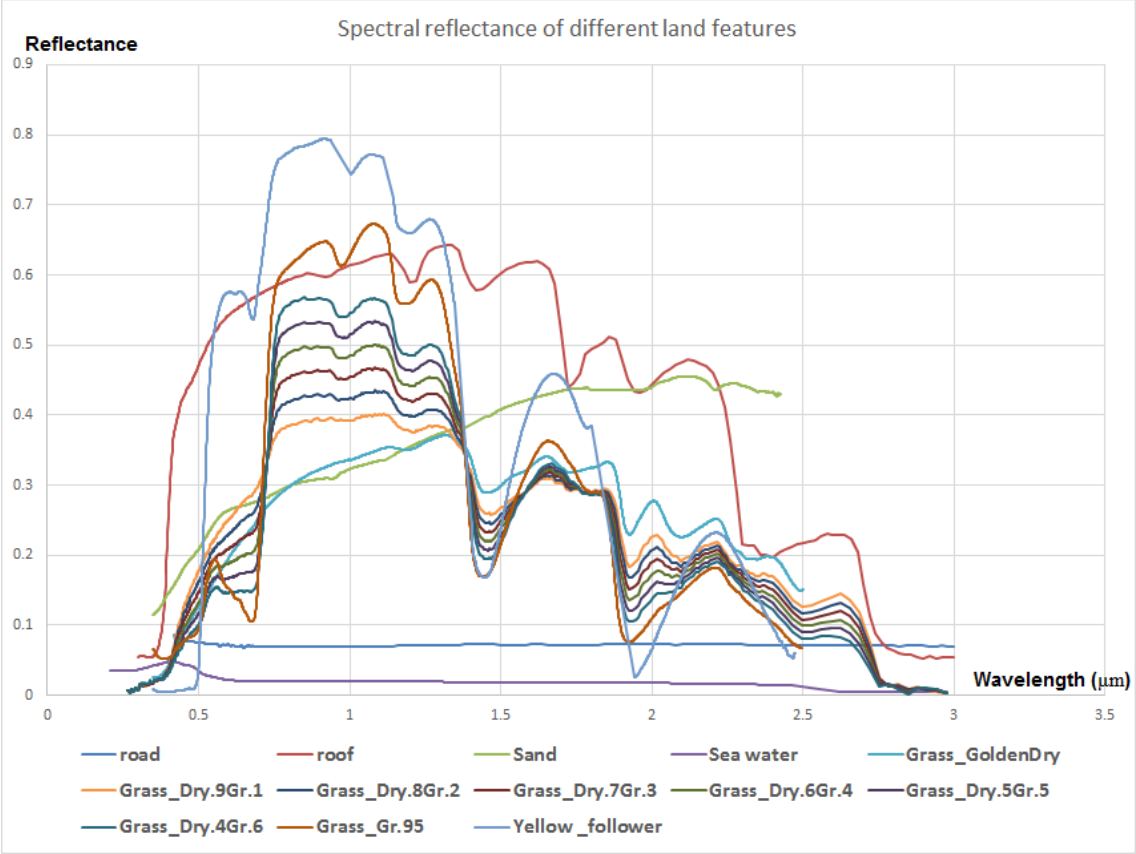

Fig.5.3 Spectral reflectance of land features related with study site.

In Fig.5.3, it can be seen that vegetated features have similar spectral reflectance patterns, while non-vegetated features have alternative spectral reflectance patterns. The difference of reflectance values between the red waveband (0.64 - 0.68 μm) and the near-infrared (NIR) waveband (0.77 - 0.81 μm), can be used to distinguish vegetated and non-vegetated land features, as non-vegetation land feature have a reduced difference between red and NIR wavebands, while vegetated features have an increased difference value between red and near-infrared. Each vegetated and non-vegetated land feature material has a unique difference value between these two wavebands and this property can be used for vegetation mapping classification.

The new spectral index, named 'Buckroney index' (BKI), relates the red and near-infrared wavebands by evaluating the reflectance difference values between these two wavebands

and up-scaling the difference value by mathematical method. BKI was created to indicate the health and density vegetation features at the coastal dune complex and to distinguish vegetation and non-vegetation land features. This new index was created as follows:

$$BKI = \frac{(NIR - R)}{(NIR + R)/2} \times 100 \quad (1)$$

where NIR and R are the reflectance values of the near-infrared and red wavebands respectively.

A BKI distribution map of the study site was created with values ranging from -196 to 198 (Fig.5.4). As BKI is a development of NDVI, it has the same ability to indicate vegetation health (shown as spectral response to chlorophyll level) and density (representing vegetated coverage). Green, with higher index values, represents healthy and dense vegetation while red represents grey, reduced or no vegetation features. Furthermore, BKI can be used to distinguish vegetated and non-vegetated features in the site as a primary element for the subsequent environmental modelling of the study area.

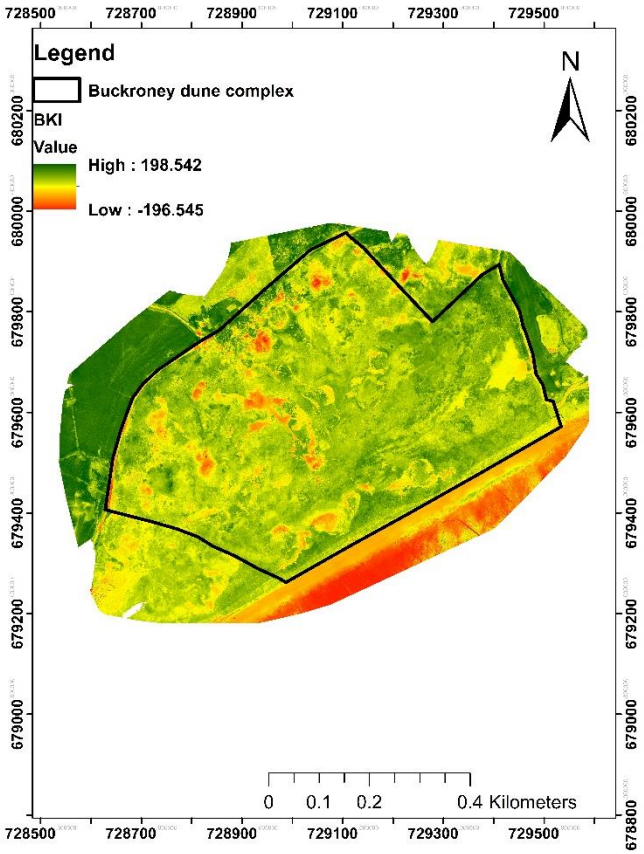

Fig.5.4. BKI map of study site.

In this study, to examine the efficiency of BKI for distinguishing vegetated and non-vegetated features, the accuracies, using different spectral indices, of identifying vegetated and non-vegetated area were compared with existing spectral indices listed in Table 5.1. The accuracy of identifying vegetated and non-vegetated area was calculated by comparing the ground truth versus classified information in 245 samples (1 m × 1 m) through matrix analysis. These samples were selected in the orthomosaic model generated from the captured imagery, including eight dominant vegetated areas (pasture, rusty willow, gorse, sharp rush, marram, common reed and mosses land), and another four non-vegetated area (road, beach, stream, sand and built area) on the site. Fig.5.5 shows the comparison of the accuracy of different vegetation indices for distinguishing vegetated and non-vegetated area.

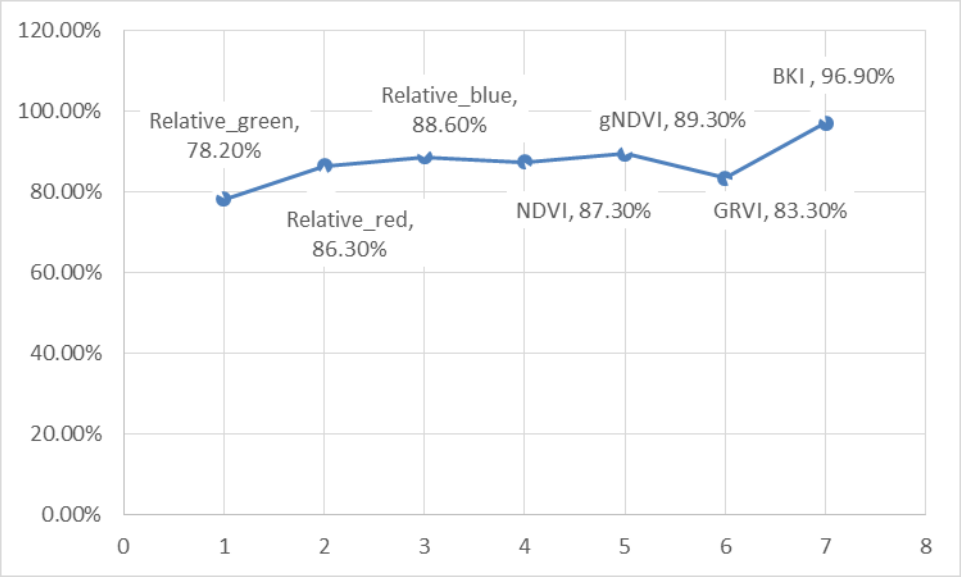

Fig.5.5. Accuracy comparison of different vegetation indices for distinguishing vegetated and non-vegetated area.

The result (Fig.5.5) shows that BKI index has better performance at distinguishing vegetated and non-vegetated area than other spectral indices in this study.

For further analysis the function of the BKI index in vegetation mapping, the spectral patterns of 45 ground truth samples (1 m × 1 m) were examined and the results are shown in Fig.5.6.

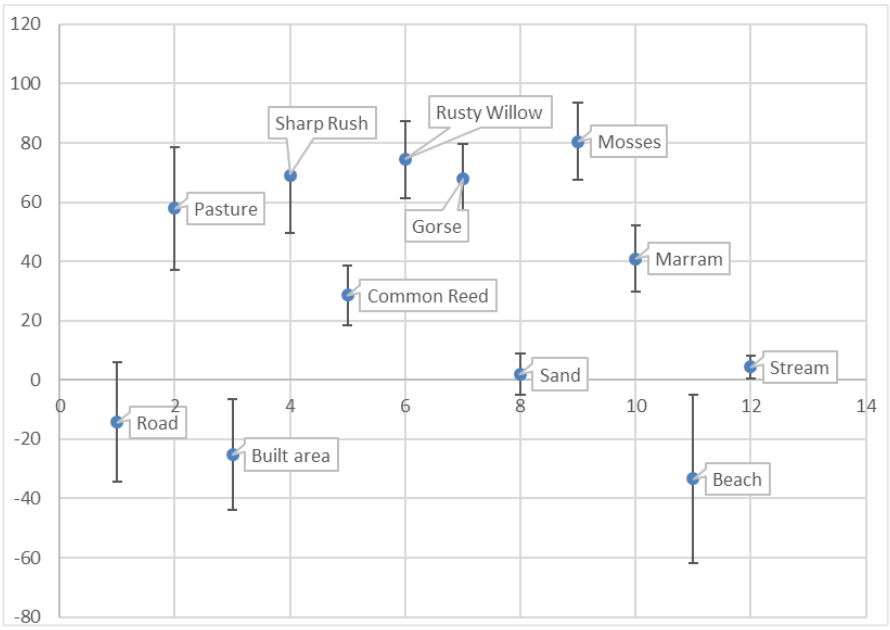

Fig.5.6. BKI value of training samples in the site.

Fig.5.6 shows that BKI values below 10 represented non-vegetation land features, while BKI values above 10 represented vegetation species. Thus, the BKI can be used to distinguish vegetated and non-vegetated land features at the study site. By observing and monitoring the same sample area over a 10 month period (February-November 2018) which included the full growing season, the BKI value has also been linked to the growth status of the vegetation, *viz.* density and health. A higher BKI value represents healthier and denser vegetated land features in summer, while a lower BKI value represents grey and sparse vegetation land features in winter.

5.7.2 Mathematic modelling of vegetated area changes

Data for 12 time-series environmental parameters (Table 5.2) were collected based on monthly climate averages from both Met Éireann, Ireland's national meteorological service, and World Weather Online, which provides global weather forecast and other weather-related content.

Table 5.2 Monthly data of 12 time-series parameters at the study site from February to November 2018.

Time-series Parameters	**Feb**	**Mar**	**April**	**May**	**June**	**July**	**Aug**	**Sep**	**Oct**	**Nov**
Rainfall (mm)	45.6	134.9	96.95	26.15	8.75	46.2	48.6	64.1	57.7	167.8
Soil_Temp (°C)	3.2	3.6	8	12.7	17.7	18.9	15.9	12.7	9.5	7.4
Wind (kmph)	26.4	23.9	20.5	16.5	14.1	14.4	16.8	21.4	21.7	27.6
Evaporation (mm)	29.1	44.45	73.7	117.75	150.1	138.1	99.5	69.95	40.55	23.9
Solar_radiation (Joules/cm2)	15353	22566	36908	57924	69256	59395	43122	32934	20464	7352
Temp (°C)	3.9	4.6	8.35	11.55	14.85	16.65	15.4	12.5	9.8	8.55
Pressure (mb)	1016.9	1001.7	1012.5	1018.1	1019.6	1016.5	1015.6	1019.6	1017.9	1007.1
Humidity (%)	74	82	84	83	80	82	82	79	78	81
Cloud (%)	48	68	53	38	37	45	51	45	47	70
Visibility (Km)	9.1	8.1	9.2	10.2	9.7	10.5	9.3	9.6	9.9	9.2
UV_Index	1	2	3	4	5	5	4	4	2	2
Sun_hour (h)	148.5	137.5	204.5	286.5	281.5	269.5	230.5	237.5	156	88

To monitor vegetation changes at the site, BKI maps for each month from February to November were generated by processing the multispectral data captured from the drone. From these BKI maps, point samples with BKI values over 10, which represent the vegetation features, were selected. Then ArcMap software was used to generate the mean BKI value of each month for the vegetation areas (Table 5.3). Comparison of the mean BKI value from February to November represented the vegetation health and density changes in the site over the period of the study which includes the growing season. Monthly BKI value (Table 5.3) were considered as the response values in the vegetation change modelling.

Table 5.3 Mean BKI value of each month from Feb to Nov 2018.

Month	**Mean BKI Value**
Feb	92.83
Mar	91.82
Apr	130.83
May	132.74
Jun	154.31
Jul	135.4
Aug	147.65
Sep	134.27
Oct	123.47
Nov	110.68

Multiple regression analysis comparing monthly BKI values with monthly data of the 12 time-series parameters, *viz.* rainfall, soil temperature, wind, evaporation, solar radiation, temperature, pressure, humidity, cloud, visibility, UV index and sun hour, was undertaken and the R^2 values are shown in Table 5.4.

Table 5.4 R^2 values for BKI changes with different time-series parameters.

Time-series Parameters	**R^2(%)**
Rainfall	35
Soil_temp	82
Wind	70
Evaporation	60
Solar_radiation	61
Temp	82
Pressure	40
Humidity	15
Cloud	41
Visibility	39
UV_index	76
Sun_hour	62

As shown in Table 5.4, 'Soil_temp' and 'Temp' both had the highest R^2 of 82%, which suggests parameters 'Soil_temp' and 'Temp' have correlation with the BKI value changes during the observation months. However, the result of the regression analysis of 'Soil_temp' and 'Temp' showed that R^2 was 98%, which indicated that these two variables had closely correlation, which means they effect the model in the similar way. However, in the model, considered parameters should have no correlation. Accordingly, only 'Temp' was chosen as a parameter in the result model, as 'Temp' has slightly higher R^2 value than 'Soil_temp'. The other two parameters, 'Wind' and 'UV_index', have higher R^2 values than other time-series parameters, which suggests their fitted regression models are closer to the observed data. By considering the accuracy and the concise

structure of the modelling, the three most significant time-series parameters, *viz.* 'Temp', 'Wind' and 'UV_index', were selected as parameters for vegetation index changes in the site.

Using the three parameters from above, a linear model was created that related with the response variable (BKI value). Equation (2) shows the resulting model.

$$BKI = 108.4 - 0.97 \times Wind + 1.28 \times UVindex + 3.08 \times Temp \quad (2)$$

The R^2 of this result model is 84%, which means that the model explains 84% the variability of the observed data.

In this research, the leave-one-out cross-validation method was used to provide an accuracy assessment of the BKI predictive model. This method is used to estimate how accurately a predictive model performs in practice and requires a training dataset for establishing modelling and a validation dataset for the accuracy test. Each round of leave-one-out cross-validation generated a predictive model omitting one sample and this excluded sample was used as validation data for the accuracy test. In this research, the predicted model related 'Temp', 'Wind' and 'UV_index' to BKI values at the site. Ten months of data were obtained so ten rounds of leave-one-out cross-validation were conducted. The results of the ten rounds of leave-one-out cross-validation are shown in Table 5.5.

Table 5.5 Accuracy assessment of the BKI determination model.

Month	**Observed BKI Value**	**Calculated BKI Value**	**Accuracy (%)**
Feb	92.83	98.04	94.4

March	91.82	109.092	81.2
April	130.83	114.5495	87.6
May	132.74	132.995	99.8
June	154.31	143.215	92.8
July	135.4	159.993	81.8
August	147.65	142.784	96.7
September	134.27	128.085	95.4
October	123.47	115.425	93.5
November	110.68	109.832	99.2

As shown in Table 5.5, the model (2) of the relationship between BKI and 'Temp', 'Wind' and 'UV_index' has a high average accuracy of 92%. This result also suggests that increasing 'Wind' can cause a reduction of the BKI value, while higher 'Temp' and 'UV_index' can lead to improvements of BKI value.

Regression analysis between position-series parameters and BKI values resulted in very low R^2, around 0.1%, which means BKI value does not have an obvious correlation with position-series parameters, *viz.* slope, elevation, aspect and distance to pathlines.

5.7.3 Non-vegetated spatial distribution modelling

To develop the distribution model of the non-vegetation area at the site, the location of non-vegetated features and other environmental parameters (*viz.* slope, aspect, elevation and distance to pathlines) in the geographical region of interest needed to be defined. Firstly, pixels with BKI values below 10 were selected from the monthly BKI map using ArcMap software. Analysing these monthly BKI maps from February to November, the points with non-vegetated features in this ten-month duration were sampled with each sample point containing information including location and BKI value. Datasets of

aspect, slope, and elevation of the site were generated from the DSM using imagery captured by the drone. The distance to the pathlines for each sample point was calculated based on the captured imagery from the drone. In general, sample point information, including geographic location, BKI value, aspect, slope, elevation and distance to pathlines, were generated as shown in Table 5.6. MaxEnt software applied Maximum-entropy techniques were used to study the non-vegetated sample points datasets, in order to identify the range of the position-related parameters which satisfied the requirements for the occurrence of non-vegetation features. Accordingly, datasets of position-related parameters over the site were analysed and resulted in the distribution geographical model (Fig.5.7) predicting the non-vegetation occurrence at the site.

Table 5.6 A sample of non-vegetation points information.

Point Number	**Easting (m)**	**Northing (m)**	**BKI**	**Distance From Pathlines (m)**	**Aspect (º)**	**Slope (º)**	**Elevation (m)**
1	729101.1	679954.1	-27.6	303.5	143.4	28.6	9.0
2	729103.9	679954.1	-7.7	304.9	52.8	4.2	8.6
3	729095.6	679951.3	-27.3	298.3	153.3	28.4	9.2
4	729098.3	679951.3	-25.6	299.7	124.2	3.0	8.9
5	729101.1	679951.3	-21.8	301.1	157.2	10.5	8.7
6	729103.9	679951.3	-12.9	302.6	107.8	20.7	8.3
7	729090.0	679948.5	-29.6	293.1	299.6	1.4	9.0
8	729092.8	679948.5	-30.7	294.5	133.9	8.8	9.0

9	729095.6	679948.5	-26.1	295.9		136.6	7.6	8.7
10	729098.3	679948.5	-5.8	297.3		180.6	15.7	8.6

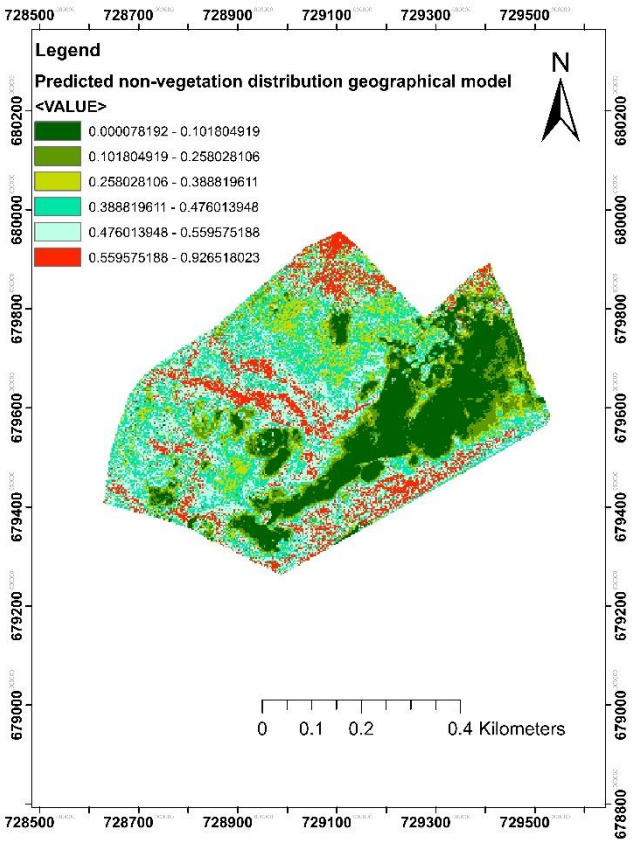

Fig.5.7 Predicted non-vegetation distribution geographical model.

As the predicted non-vegetation distribution geographical model shown in Fig.5.7, the value 0-1 represents the probability of non-vegetated features occurrance in the site. Red colours, with higher values, show areas with conditions which has higher probability for occurrence of non-vegetated areas, while green colours, with lower values, show areas with a lower probability for non-vegetation occurrence. This map can be used to define a highlight areas at risk to soil erosion and vegetation loss at the coastal dune complex. Fig. 5.7 also shows the position of areas with dense and healthy vegetation, shown in dark

green, and so identify areas that may need to be focused on in terms of conservation needs in order to maintain the ecosystem of coastal dune complex.

Table 5.7 represents the 'percent contribution' and 'permutation importance' of different variables in the model as the result of the maximum-entropy analysis. 'Percent contribution' represents the contribution of each position-related parameter to the distribution model while 'permutation importance' represents the importance of the position-related parameters in the distribution model.

Table 5.7 'Percent contribution' and 'permutation importance' of different variables in the predicted non-vegetation distribution geographical model.

Variable	Percent contribution	Permutation importance
Elevation	75.3	60.9
Distance to the pathlines	14.7	20.8
Aspect	5.7	9.5
Slope	4.4	8.8

As shown in Table 5.7, 'elevation' is the most important parameter (weight value 61%) to effect the non-vegetation distribution model. The variable 'distance to the pathlines' has an influence on the non-vegetation distribution model as well, with weight 21%, while variables 'aspect' and 'slope' have the lowest impact on the non-vegetation distribution model, with weight of 9.5% and 8.8% respectively. These results demonstrate that areas with high elevation and close to pathlines are risk areas with a high probability for non-vegetation occurrence and associated erosion. To protect these high-risk areas, one effective method is to re-plan the pathlines in the site to avoid the high elevation areas, thus helping to reduce the probability of vegetation erosion and the occurrence of bare ground and associated susceptibility to erosion.

5.8 Conclusion

In conclusion, a multispectral sensor mounted on a drone was used to monitor the distribution of vegetation, the topographic profile and geospatial character of changes in the Buckroney coastal dune complex over a 10 month period from February to November 2018. A BKI index was created to represent vegetation health and vegetation density in a growing season and the index can also be used to distinguish vegetated and non-vegetated features in the study site. A mathematical model was developed for mapping vegetation changes using the primary time-series environmental parameters at Buckroney coastal dune complex over the study period. The mathematical model also suggested 'Temp', 'Wind', and 'UV_index' were the most significant time-series parameters for BKI value changes. Higher 'Temp' and 'UV_index' can increase monthly BK Index value of vegetation area, while higher 'Wind' can decrease monthly BK Index value of vegetation area.

A predicted non-vegetation distribution geographical model was also established, showing the high-risk areas for non-vegetation occurrence. This non-vegetation distribution model illustrated that 'elevation' and 'distance from pathlines' were the most important parameters effecting non-vegetation occurrence, typically representing sand exposure and erosion areas in the site. These results can contribute to coastal environmental management to protect the vegetation areas and reduce soil erosion at the coastal dune complex.

This research illustrated the efficiency of image data collection and the high-resolution mapping of the site using a multispectral camera mounted on a drone, significantly reducing the hazards and workload for data collection related to the development of vegetation maps and DSMs of a study area. Notwithstanding the many benefits and

advantages of drone and multispectral technology in vegetation mapping, the technology still has some challenges with respect to dune complexes surveying including weather dependency.

5.9 Reference

Acosta, A., Carranza, M.L., Izzi, C.F., 2005. Combining land cover mapping of coastal dunes with vegetation analysis. Applied Vegetation Science 8, 133-138.

Alhajraf, S., 2004. Computational fluid dynamic modeling of drifting particles at porous fences: Environmental Modelling & Software 19. 163–170.

Andrews, B., Gares, P.A., Colby, J.D., 2002. Techniques for GIS modeling of coastal dunes. Geomorphology 48, 1–3, 289–308.

Bankoff, G., Frerks, G., Hilhorst, D., 2003. Mapping Vulnerability: Disasters, Development and People, chapter 3. London, Earthscan Publishers.

Belperio, T., Bourman, B., Bryan, B., Harvey, N., 2001. Distributed process modeling for regional assessment of coastal vulnerability to sea-level rise. Environmental Modeling and Assessment 6, 1, 57–65.

Ciccarelli, D., Pinna, M.S., Alquini, F., Cogoni, D., Ruoco, M., Bacchetta, G., Sarti, G., Fenu, G., 2017. Development of a coastal dune vulnerability index for Mediterranean ecosystems: A useful tool for coastal managers? Estuarine, Coastal and Shelf Science, 187, 84-95.

Clark, J.R., 1977. Coastal environment management. John Wiley & Sons, New Jersey, U.S., ISBN 0471158542.

De Martino, A., De Martino, D., 2018. An introduction to the maximum entropy approach and its application to inference problems in biology. Heliyon 4, e00596. (doi: 10.1016/j .heliyon.2018.e00596)

Devoy, R.J.N., 2008. Coastal Vulnerability and the Implications of Sea-Level Rise for Ireland. Journal of Coastal Research 24, 325-341.

Drew, C.A., Wiersma, Y.F., Huettmann, F., 2011. Predictive species and habitat modelling in landscape ecology: concepts and applications. Springer: Berlin, German, 2011.

Gregersen, J.B., Gijsbers, P.J.A., Westen, S.J.P., Blind, M., 2005. OpenMI: the essential concepts and their implications for legacy software. Advances in Geosciences 4, 37–44.

Guisan, A., Zimmermann, N.E., 2000. Predictive habitat distribution models in ecology. Ecological Modelling 135, 147–186.

Hanson, H., Aarninkhof, S., Capobianco, M., Jimenez, J., 2003. Modelling of coastal evolution on yearly to decadal time scales. Journal of Coastal Research 19, 790–811.

Hardisty, J., Taylor, D.M., Metcalfe, S.E., 1993. Computerised Environmetal Modelling: A Practical Introduction Using Excel. John Wiley & Sons: New Jersey, US, 1993.

Hemsing, L.Ø., Bryn, A., 2012. Three methods for modelling potential natural vegetation (PNV) compared: a methodological case study from south-central Norway. Journal of Geography 66, 11–29.

Hutton, E.W., Piper, M.D., Peckham, S.D., Overeem, I., 2014. Building sustainable software-the CSDMS approach. arXiv Preprint, 4106.

ISDR (International Strategy for Disaster Reduction), 2004. Living with Risk: a Global Review of Disaster Reduction Initiatives. World Meteorological Organization and the Asian Disaster Reduction Center, Geneva, pp. 429, 2004.

Jackson, D.W.T., Cruz-Avero, N., Smyth, T.A.G., Hernández-Calvento, L., 2013. 3D airflow modelling and dune migration patterns in a mobile coastal dune field. Journal of Coastal Research 65, 1301-1306.

Kobayashi, N., 2016. Coastal sediment transport modeling for engineering applications. Journal of Waterway Port Coastal and Ocean Engineering-ASCE 142, 03116001.

Krueger, C.P., Soares, C.R., Huinca, S.C.M., Leandro, D., Goncalves, R.M., 2011. Satellite positioning on the coast of the Paran´a, Brazil. Journal of Coastal Research, SI (64), 1352–1356.

Kuplich, T.M., 2006. Classifying regenerating forest stages in Amazonia using remotely sensed images and a neural network. Forest Ecology and Management 234, 1–9.

Lucas, N.S., Shanmugam, S., Barnsley, M., 2002. Sub-pixel habitat mapping of a costal dune ecosystem. Applied Geography 22, 3, 253–270.

Martinez, M.L., Silva, R., Mendoza, E., Odériz, I., 2016. Coastal Dunes and Plants: An Ecosystem-Based Alternative to Reduce Dune Face Erosion. Journal of Coastal Research 75, 303-307.

Mendoza, E., Odériz, I., Martínez, M.L., Silva, R., 2017. Measurements and modelling of small scale processes of vegetation preventing dune erosion. Journal of Coastal Research 77, 19-27.

Mitasova, H., Overton, M., Harmon, R.S., 2005. Geospatial analysis of a coastal sand dune field evolution: Jockey's Ridge, North Carolina. Geomorphology 72, 204-221.

Miller, J., Franklin, J., Aspinall, R., 2007. Incorporating spatial dependence in predictive vegetation models. Ecological Modelling 202, 225–242.

Moriondo, M., Jones, G.V., Bois, B., Dibari, C., Ferrise, R., Trombi, G., Bindi, M., 2013. Projected shifts of wine regions in response to climate change. Climatic Change 119, 825–839.

NPWS (National Parks Wildlife Service), 2018. Site Synopsis: Buckroney-Brittas Dunes and Fen SAC (National Parks & Wildlife Service site documents). Available online: https://www.npws.ie/protected-sites/sac/000729. (access on 14/05/2018).

Payo, A., Favis-Mortlock, D., Dickson, M., Hall, J.W., 2017. Coastal Modelling Environment version 1.0: a framework for integrating landform-specific component models in order to simulate decadal to centennial morphological changes on complex coasts. Geoscientific Model Development 10, 2715–2740.

Pender, D., Karunarathna, H., 2013. A statistical-process based approach for modelling beach profile variability. Coastal Engineering 81, 19-29.

Phillips, S.J., Dud´ık, M., Schapire, R.E., 2004. A Maximum Entropy Approach to Species Distribution Modeling. Proceedings of the Twenty-First International Conference on Machine Learning, Banff, Canada, 2004, pages 655-662.

Phillips, M.R., Jones, A.L., 2006. Erosion and tourism infrastructure in the coastal zones: Problems, consequences and management. Tourism Management 27, 3, 517-524.

Roelvink, J.A., Reniers, A., van Dongeren, A., de Vries, J., McCall, R., Lescinski, J., 2009. Modelling storm impacts on beaches, dunes and barrier islands. Coastal Engineering, 56, 11-12, 1133-1152.

Sabatier, F., Anthony, E.J., Hquette, A., Suanez, S., Musereau, J., Ruz, M.H., Regnauld, H., 2009. Morphodynamics of beach/dune systems: Examples from the coast of France. Géomorphologie 15, 3–22.

Serafim, M.B., Siegle, E., Corsi, A.C., Bonetti, J., 2019. Coastal vulnerability to wave impacts using a multi-criteria index: Santa Catarina (Brazil). Journal of Environmental Management 230, 21–32.

Stive, M.J.F., Ruol, P., Capobianco, M., Buijsman, M., 1997. Behaviour oriented model for the evaluation of long-term lagooncoastal dynamic interaction along the Po River Delta. Coastal Dynamics – Proceedings of the International Conference, American Society Civil Engineers, Plymouth, UK, June 1997, 903–912.

Vaca, R.A., Golicher, D.J., Cayuela, L., 2011. Using climatically based random forests to downscale coarse-grained potential natural vegetation maps in tropical Mexico. Applied Vegetation Science 14, 388-401.

Walkden, M.J., Hall, J.W., 2011. A mesoscale predictive model of the evolution and management of a soft-rock coast. Journal of Coastal Research 27, 529–543.

Weber, T.C., 2011. Maximum entropy modeling of mature hardwood forest distribution in four U.S. states. Forest Ecology and Management 261, 779–788.

Weil, G., Lensky, I., Resheff, Y., Levin, N., 2017. Optimizing the Timing of Unmanned Aerial Vehicle Image Acquisition for Applied Mapping of Woody Vegetation Species Using Feature Selection. Journal of Remote Sensing 9, 1–5.

Woo, M.K., Fang, G.X., DiCenzo, P.D., 1997. The role of vegetation in the retardation of soil erosion. Catema 29, 2, 145–159.

Xia, J., Dong, P., 2016. A GIS add-in for automated measurement of sand dune migration using LiDAR-derived multitemporal and high-resolution digital elevation models. Geosphere 12, 4, 1316–1322.

Yackulic, C.B., Chandler, R., Zipkin, E.F., Royle, J.A., Nichols, J.D., Grant, E.H.C., Veran, S., 2013. Presence only modelling using MAXENT: when can we trust the inferences? Journal of Methods in Ecology and Evolution 4, 236–243.

Zhang, D., Narteau, C., Rozier, O., 2010. Morphodynamics of barchan and transverse dunes using a cellular automaton model. Journal of Geophysical Research 115, F03041.

Zhang, M.G., Zhou, Z.K., Chen, W.Y., Slik, J.W.F., Cannon, C.H., Raes, C.H., 2012. Using species distribution modelling to improve conservation and land use planning of Yunnan, China. Biological Conservation 153, 257–264.

Zhu, Z.T., Cai, F., Chen, S.L., Gu, D.Q., Feng, A.P., Cao, C., Qi, H.S., Lei, G., 2019. Coastal vulnerability to erosion using a multi-criteria index: A case study of the Xiamen coast. Sustainability 11, 93.

Chapter 6

CONCLUSION

Coastal dune complexes play an essential role in the maintenance of ecosystem as they can provide habitats for special flora and fauna, control soil erosion and flooding, and protect nearby properties. However, global climate change and increasing anthropogenic activities at coastal dune complexes have brought potential hazards, such as soil erosion, flooding and habitat loss. The conservation status of dune habitats along the Irish coastline is largely unsatisfactory, not achieving the requirements of the EU Habitats Directive as concluded by the Irish National Parks and Wildlife Service (NPWS). The study site at Buckroney dune complex, which is under the management of the Irish NPWS and includes ten habitats listed on the EU Habitats Directive, is similarly under pressure from environmental issues. Reliable and current spatial information related to the site was considered potentially helpful to the establishment of environmental models, which have significant relevance for the development of appropriate and effective conservation strategies for such coastal environments.

Within this project, environmental modelling for coastal dune complexes was developed to contribute to the development of effective environmental management with particular reference to the Buckroney dune complex in Co. Wicklow, Ireland. The research identified UAS technology as an optimal approach for the collection of high-resolution and high-accuracy geospatial data of the study area. The research also demonstrated that multispectral data acquired by a sensor mounted on a UAS platform could be used to develop high-resolution and high-accuracy functional vegetation abundance mapping of the dune complex and, in addition to monitor vegetation and non-vegetation changes over a growing season. Based on such data, a mathematical model was developed that simulated vegetation development related to time-series environmental parameters, such as temperature, rainfall, wind and solar radiation. The average accuracy of the mathematical model was 92%, predicting the vegetation growing status (represented by

a vegetation index value) according to the available values of time-series environmental parameters. The model was also used to establish that the most significant time-series parameters affecting vegetation growth during the 10 months of monitoring were wind, temperature and UV index. This model contributed to a better understanding of the interaction between vegetation growth and the time-series parameters. In addition, a distribution geospatial model was also developed that represented the probability of non-vegetated land-cover occurrence on the site related to position-related environmental parameters, namely slope, aspect, elevation and distance from pathlines. Further analysis of the non-vegetated distribution geospatial model demonstrated that elevation and distance from pathlines were more important than slope and aspect in effecting non-vegetation occurrence in the coastal dune system. The non-vegetation distribution geospatial model was used to identify higher erosion risk areas within the site. The mathematical model of vegetation changes and the predictive non-vegetation distribution model were designed to support coastal environmental management in protecting areas of high ecological value including minimizing the impacts of non-vegetated exposure which is often associated with increased soil erosion at coastal dune complexes.

As geospatial data collection methods for topographic modelling, both remote, small-scale survey data, *viz.* from aerial photogrammetry, optical satellite imagery, radar and LiDAR data, and ground-based, large-scale survey data, *viz.* from total station, RTK GPS, TLS and UAS were considered and critically compared in this research. The outcome demonstrated the efficacy and efficiency of UAS as a geospatial data gathering tool for topographic modelling of coastal zones in Ireland. LiDAR data was identified as a viable alternative. However the modelling based on UAS data had higher resolution (0.034 m) and higher accuracy (0.11 m) than the model from LiDAR dataset. UAS technology also provided more up-to-date and more flexible coverage data for modelling. Data collection

using UAS took one day for a 60 ha study site which demonstrated the efficiency of the UAS survey method in dune complex areas. As the UAS surveyed remotely, it eased the difficulties of access through dune areas with deep slopes and generally through difficult terrain.

The application of a multispectral sensor mounted on a UAS was studied for the generation of vegetation identification and distribution mapping of the study site. The multispectral sensor captured regular, wideband RGB imagery and, in addition, imagery in four narrow wavebands, *viz.* green, red, red edge and near-infrared (NIR). The captured imagery from each sortie was processed to generate a 3D point cloud, an orthomosaic model, a DSM, and an NDVI index map which was generated from the multispectral imagery. In addition, seven individual multispectral waveband orthomosaics (red, green, blue from normal RGB camera and red, green, red edge, NIR from the multispectral sensor) of the site were created. Based on these multispectral wavebands, six vegetation indices were calculated for discriminating vegetation, *viz.* Relative Green, Relative Red, Relative Blue, NDVI, gNDVI and GRVI.

The outcomes above were all referenced to the Irish Transverse Mercator (ITM) grid coordinate system. Ground sampling distance (GSD) in digital images of the ground surface, taken from the air, is the distance between pixel centres as measured on the ground. Outcomes from the RGB imagery had a GSD of 0.029 m and a georeferencing Root-Mean-Square (RMS) error of 0.111 m. The multispectral imagery had a spatial resolution of 0.096 m and a georeferencing accuracy of 0.798 m.

From the orthomosaic models eight dominant vegetation areas, including Pasture, Rusty Willow, Gorse, Sharp Rush, Marram, Common Reed and Mosses land, and another four significant contiguous land cover types were identified on the site, *viz.* road, beach,

stream, sand and built area. Land cover classification accuracy assessment was based on nine different classification strategies calculated by comparing ground truth information and classified information in 245 samples through matrix analysis. It was concluded form the classification accuracy assessment results that:

- Multispectral sensor waveband data can help to improve classification accuracy for vegetation mapping
- The numbers of wavebands used for classification influenced classification accuracy. For example, the inclusion of more waveband data from the multispectral sensor did not always translate to an improvement in classification accuracy.
- The classification accuracy of different classification strategies can also be influenced by the resolution of the captured imagery.
- Discrete spectral bands from the multispectral sensor provided more reliable reflectance patterns for land feature classification.

This research used UAS-based multispectral data to monitor vegetation and non-vegetation features changes at the studied coastal dune complex over a growing season from February 2018 to October 2018. Spectral analysis was used for land feature reflectance pattern assessment to find a solution for distinguishing vegetation and non-vegetation features, which can contribute to the monitoring of vegetation and non-vegetation feature changes at the study site. It was concluded that the difference of reflectance values between red (0.5-0.6 μm) and NIR (0.7- 0.8 μm) wavebands can be used to distinguish vegetation and non-vegetation land features. The non-vegetation land features had a smaller difference value between red and NIR wavebands, whereas vegetation species had a larger difference value between red and NIR wavebands. A new spectral index was developed that related the red and NIR wavebands based on evaluating

the difference reflectance value between these two wavebands and enlarging the difference value. The new index was created for distinguishing vegetation and non-vegetation land features at the coastal dune complex. This new vegetation index, named the 'BKI index', was created as follows:

$$BKI = \frac{NIR-R}{(NIR+R)/2} \times 100$$

where NIR and R is the reflectance value of near-infrared and red waveband respectively.

BKI values at the site ranged from -80 to 150, which, when applied, represented from red to green in the resulting index map. Green, with a higher index value, represented dense vegetation species while red represented less dense or no vegetation features. A BKI value below 10 represented the non-vegetation land features, while a BKI value above 10 represented vegetation species. The BKI index was shown to perform well at distinguishing vegetation and non-vegetation land features at the study site. The value of the BKI index also represented vegetation growth status. A higher BKI value represented healthy and dense vegetation land features, while a lower BKI value represented less than vigorous and sparse vegetation land features.

By analysis of the BKI mapping of the site from February to October 2018, a mathematic model (Equation 1) was developed, using regression analysis that represented the relationship between monthly mean BKI value and three determined environmental parameters, *viz.* 'Temp', 'Wind' and 'UV_index'.

$$BKI\ Value = 108.4 - 0.97 * Wind + 1.28 * UV_{index} + 3.08 * Wind \quad (1)$$

The R-square value, a statistical measure of how close the data are to the fitted regression line, of this result model was 84%.

Modelling accuracy assessment was conducted using the leave-one-out cross-validation method. The results showed that:

- The created mathematic model, relating BKI value of vegetation features and environmental parameters of 'Temp', 'Wind' and 'UV_index', had a high accuracy about 92%.
- Temperature, wind and UV index were more important environmental parameters for vegetation index value changes in the site than other time-series parameters, *viz.* rainfall, solar radiation, evaporation, pressure, humidity, cloud, visibility, sun hours.
- Increasing 'Wind' can reduce the BKI value while higher 'Temp' and 'UV_index' can help increase the BKI value, which means heavier wind may reduce the growth of vegetation while higher temperature and a higher UV index of solar light can help the growth of vegetation.

By monitoring the non-vegetation features distribution and changes from February 2018 to October 2018, a predictive non-vegetation distribution geospatial model was generated to determine the relationship of the occurrence localities of non-vegetation features to position-series environmental variables, *viz.* aspect, slope, elevation, distance to pathlines. From this analysis it was concluded that:

- Risk areas could be highlighted from the resulting model, relating the areas with soil erosion and vegetation loss issues at the coastal dune complex. These areas may need more attention for conservation in order to maintain the ecosystem development of the coastal dune complex.

- Elevation was the most important parameter (weight value 61%) to affect the non-vegetation distribution model. Also Distance to the Pathlines has some influence on the non-vegetation distribution model with a weight of 21%.
- Practical management strategies can be developed using this model. This has been discussed with officers from the NPWS who have shown great interest.

In conclusion, this research has shown that UAS technology was the most suitable option for geospatial data collection for coastal zones compared with other considered geospatial data resources. This research also highlighted an effective option for on-site surveying, significantly reducing the hazard and workload for the development of vegetation maps and DEM's of a study area. Using the multispectral sensor resulted in data captured from a wider range of wavebands than RGB camera, with better resolution and accuracy than other conventional remote sensing technologies, enabling the generation of dense 3D point clouds, and orthormosaic models, DEM and vegetation index maps. In these maps, vegetation distribution and elevation changes over the Buckroney dune complex were clearly represented. The classification result also illustrated the high accuracy achieved for identifying different land feature areas based on these maps.

This research also proved the possibility to monitor the distribution of vegetation, the topographic profile and geospatial character of changes at the Buckroney coastal dune complex from February 2018 to October 2018 using a multispectral sensor mounted on a UAS. The BKI index, a new vegetation index, was created in this research to represent vegetation health and vegetation density in a growing season and to separate the vegetation and non-vegetation features at the study site. A mathematical model was developed for mapping vegetation changes using the primary time-series environmental parameters at the study site over the study period. The mathematical model demonstrated

that ‘Temp’, ‘Wind’, and ‘UV_index’ were the most significant time-series parameters for BKI value changes. A predicted non-vegetation distribution geographical model was also established, showing the high-risk areas for non-vegetation occurrence, typically representing sand exposure and erosion areas in the site. These results can contribute to coastal environmental management to protect the vegetation areas and reduce soil erosion at the coastal dune complex.

As Buckroney dune complexes are under the management of the Irish NPWS, meetings with officers of NPWS have been conducted and suitable and efficacious management suggestions for the coastal zone have been discussed based on this research. For example, it was concluded that the existing fences constructed with wire and timber piles, and which were intended to protect valuable vegetation species, should be replaced by planted vegetation to reduce wind influence and, thus, support the vegetation growth. As ‘high elevation’ and ‘close to pathlines’ are high-risk parameters for sand exposure, it would be better to re-plan the pathlines for visitors to avoid high elevation areas thereby reducing the sand exposure risk at the site.

Notwithstanding that this research demonstrated the efficiency of UAS technology in capturing spatial datasets and these datasets were successfully used for vegetation mapping and environmental modelling of the study site, UAS technology still presented some limitation and challenges during this research. DTMs of coastal dune complexes, derived from UAS data, will not reflect the bare earth surface in areas of dense vegetation. UAS application in the field is also sensitive to environmental conditions, such as wind, precipitation and low light, which can lead to logistical and data quality challenges when monitoring in the field. Processing of UAS-based data requires more time compared to other remote small-scale data sources. Preliminary items also need to be taken into

consideration, such as arranging permits to fly and training under UAS regulations from the relevant aviation authority.

This research shows UAS-based multispectral data is a practical option for environmental modelling for the Buckroney dune complex. It provides reference information for similar research for environmental modelling for the coastal zone. Further research is required to assess the suitability of this methodology to other coastal dune complexes in Ireland and internationally. Furthermore, the applicability of the environmental modelling approach that was developed at Buckroney to other coastal dune complexes needs to be established.

Chapter 7

Appendix

UAV data for coastal dune mapping

Chen Suo[1], Eugene McGovern[2], Alan Gilmer [3]

Environmental Sustainability & Health Institute, Dublin Institute Technology, Dublin, Ireland
E-mails: [1]d15123973@mydit.ie; [2]eugene.mcgovern@dit.ie; [3]alan.gilmer@dit.ie

Abstract. High resolution topographic maps are critical for the development of rigorous and quantitative numerical simulation landscape models. These models can inform targeted land management actions that maintain biodiversity and ecological functions. Mapping functional vegetation communities to obtain accurate distribution and population estimates is an important element of landscape models and is a challenging task which requires a considerable investment in time and resources. A recent development in surveying technologies, Unmanned Aerial Vehicles (UAV's), also known as drones, has enabled high resolution and high accuracy ground-based data to be gathered quickly and easily on-site. The application of UAV's represents a new opportunity to survey relatively large areas in significantly less time compared to other on-site surveying methods, including GPS, robotic total stations and terrestrial laser scanners. The objective of this research is to use UAV technology to create topographical and vegetation mapping of coastal dune complexes with particular reference to the Brittas-Buckroney dune complex in Co. Wicklow. As the area of study site was about 60 hectares, it was divided into three sections, North, Centre and South. This paper presents the five steps to achieve the objective, setting ground control points, making an autonomous flight plan, flying the UAV for data collection, data processing and result analysis via ArcGIS. The final result, processed by specific software PIX4D, was a topographical map of the study site in the Irish Transverse Mercator coordinate system, with a resolution of 0.125 m and Root-Mean-Square (RMS) error 0.050 m. In conclusion, UAV technology provides new possibilities for mapping as it maximizes improvement of the data quality while reducing the investment in time and labour.

Keywords: coastal dune complexes, unmanned aerial vehicles, topographic maps.

Conference topic: Technologies of geodesy and cadastre.

Introduction

The coastal zone area is important at both the natural and the economic level. The coastal dune field is at the transition between the terrestrial and marine ecosystems which are highly-valued, natural resources for providing drinking water, mineral resources, recreation, eco-services and desirable land for housing development. These natural resources provide food and habitation for aquatic and terrestrial organisms and offer human settlement and recreation spaces as well. Activities at the coastal zone area can contribute to local and national economy development, in areas like aquaculture, fisheries and tourism, and the area also has an important function to control erosion and flooding thus protecting and maintaining environmental development. In recent years, increasing tourism and development in the coastal dune area of the South East of Ireland have resulted in increased pressure on the environment, resulting in issues including soil erosion, flooding and habitat loss.

High-resolution mapping of the topography and the vegetation communities across a dune field, in particular the mixture of different functional plant types such as pioneer versus succession species, is critical for the establishment of rigorous and quantitative numerical simulation landscape models. These models can inform targeted land management actions that maintain biodiversity and ecological functions. However, mapping functional vegetation communities to obtain accurate distribution and population estimates is a challenging task which requires a considerable investment in time and resources.

There are a number of sources of spatial data available for coastal dunes mapping. Satellite imagery provides remotely-sensed panchromatic, spectral and multispectral data, provided by national mapping agencies (NMA's), like Ordnance Survey Ireland (OSI) or the United States Geological Survey (USGS). NMA's can provide base topographical mapping from aerial photography with different ranges of resolutions. From USGS Earth Explorer, a base topographical map is available to download free with the resolution about 30 m. Higher resolution aerial topography maps can be bought from these NMA's or commercial companies. Although valuable, these data may not provide the resolution necessary for accurate numerical modelling of a dune complex. Recently, Digital Elevation Models with a higher resolution from

airborne laser scanning have been used for mapping. The airborne laser scanner can collect the database as point clouds and then use them to generate different kind of digital surface model, including 3D maps. A major limitation for this data source is that the cost for airborne laser scanner is quite high and the study site may not have been included in the areas covered by the NMA. Recent developments in surveying technology have enabled high resolution and high accuracy spatial data to be gathered on-site. These technologies include Total Station, robotic Total Stations and RTK GPS where coordinate positions of points are collected and then used to generate 2D maps based on the features at the collected points. This kind of 2D map has high accuracy and gives a clear representation about the position of particular land features. However, data collection by these technologies is time consuming and therefore may not be suitable for a relatively large study site with various land features. With significant progress in survey technologies, terrestrial laser scanners offer an option to collect point cloud data on-site from which to generate 3D models that accurately show elevation changes of a coastal dune complex.

Most recently, Unmanned Aerial Vehicles (UAV's), variously referred as UAS (Unmanned Aerial Systems), RPAS (Remotely-Piloted Aerial Systems), "Aerial Robots" or simply "drones" (Turner *et al.* 2016), have enabled high quality ground-based data to be gathered quickly and easily on-site. Most importantly, it is the evolution of technology for the transformation from imagery to point clouds to create digital surface model, including 3d map as well. The application of UAV's represents a new opportunity to survey relatively large areas in significantly less time compared to other on-site surveying methods. This paper presents the methodology and efficacy of using UAV's for ground data collection to create topographical and mapping of coastal dune complexes with particular reference to the Brittas-Buckroney dune complex in Co. Wicklow, Ireland.

Methodology

Brief overview of UAV technology

In recent decades, large-scale decades, photogrammetry was the primary method for the establishment of topographic maps and was widely used in traditional geologic field studies. UAV technology implemented in mapping reflect the evolution of methodology in photo-based 3D reconstruction, making a new possibility for photogrammetry to create 3D maps (Zelizn 2016). Mapping by UAV is also a user-friendly and scalable methodology with the requirement of the specialized software and restrictive image collection conditions. By the great progress in digital camera technology, a larger number of photos with better image quality can be collected in a short time in the field. UAV, integrated with modern digital camera technology, breaks the time and space constraint, allowing a study site to be remotely surveyed in a significantly reduced time with the result of a large number of high resolution and high accuracy images. In the camera model, it represents a 3D real world as a 2D image. Structure from Motion (SfM) is a technique that has emerged in the last decade to construct the photogrammetry-based three-dimensional model, creating 3D surface models from a large number of overlapping photographs. SfM was developed in the 1990's in the computer vision industry, impressive by its advances in both motion perception and automated feature-matching algorithms (Lowe 1999). SfM is effective if there is a high degree of overlap that captures the study area from a wide number of different positions and orientations. To generate the topographic map, many thousands of matching object and textural features are automatically detected in multiple overlapping images of the ground surface, from which a high density point cloud with 3D coordinate positions is derived. The critical element for implementation of photogrammetry to 3D maps is collection of numerous overlapping images (Uysal *et al*. 2015). From each two overlapping pictures, specialized software using SfM can calculate the unique coordinate position (x, y, z or Northing, Easting, Elevation) of a set of particular points presented in both images. To maintain the accuracy of the map, the overlapping area for each two images should be at least 60%, making sure enough shared points can be recognised by software for the map construction. 3D models can be generate by numerous overlapping images without user intervention. But in this way, the 3D models will be in an arbitrary coordinate system. In order to reference the 3D surface model to a real-world system, control points are used to transform all the points in the study area into the correct coordinate system (Tonkin, Midgley 2016). A minimum of three control points needs to be set at the maximum distance over all the study site. The coordinate position of these control points should be obtained and saved as reference for adjusting the whole study site to the correct coordinate system. UAV flight height and speed influence the resolution of collected imagery and are essential to be set in the flight plan to achieve the particular resolution requirement.

In field work, the first thing is to set a certain number of control points depending on the area of the study site. Then total station or Real Time Kinematic GPS technology is used to get the coordinate position of the control points. After this, UAV flight path, including flight height, overlapping percentage and flight

speed should be set according to the resolution requirement of the map and then the flight can be started to collect images (Smith *et al*. 2009). The collected images need to be processed by specialized software, for example Pix4D or Agisoft, which offers a powerful approach to conduct an accurate survey. Importing a wide variety of suitable imagery and control data to the software, a georeferenced 3D model can be effectively constructed. Figure 1 shows the workflow for photogrammetry-based 3D construction.

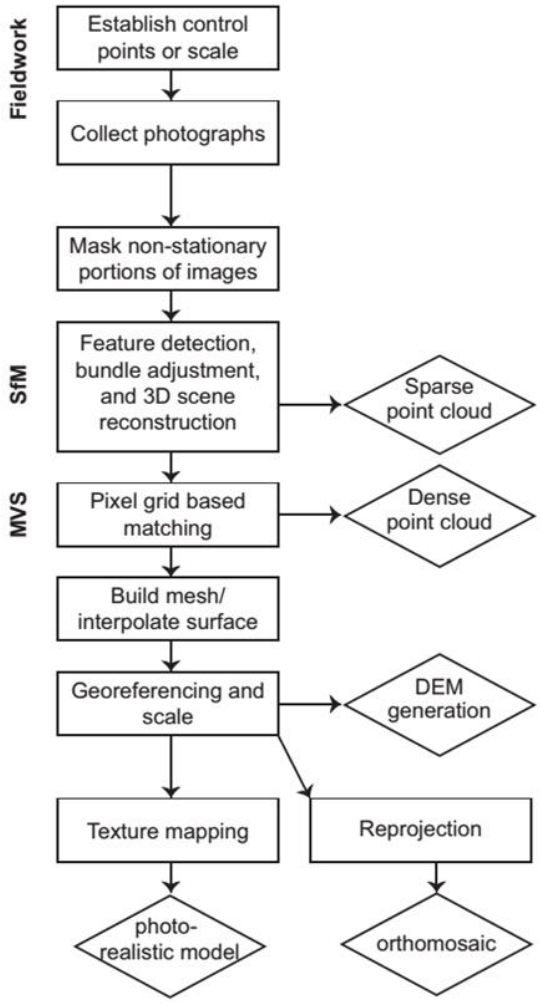

Fig. 1. Photogrammetry-based 3D construction workflow of UAV technology (Bemis *et al.* 2014)

Irish Aviation Authority for UAV

With the increasing use of UAV in Ireland, over 6,000 drones and model aircraft have been registered with the IAA in the past year. For the management of UAVs in Ireland, the Irish Aviation Authority (IAA) has a mandatory requirement for all owners to register drones weighing 1 kg or more to be involved in quality training on how to use the UAV properly. IAA also insists that users be aware of their responsibility and operate their UAV in a safe manner and in full compliance with the regulations. The primary emphasis is that the UAV cannot cause harm to people or property, or interfere with other forms of aviation. Moreover, UAV cannot fly over 120 m above ground level and should be within 300 m distance from the operator at all times. Before using the UAV, the operator should get the permission from the landowner for take-off and landing. IAA also has strict legislation to prohibit users to operate UAV's over an assembly of people or over urban area or in restricted areas (e.g. military installations, prisons, airport etc.). The authority may define areas within Air Traffic Services airspace, where small unmanned aircraft activity may take place without permission from the Authority. OpenAIP (www.openair.net) is a Worldwide aviation database to deliver free, current and precise navigational data about airports, airspaces, navigational aids, thermal hotspots and many other datasets. In order to fly UAV in a safe location, openAIP can be downloaded free of charge for private use to provide useful information about whether the survey area is in a restricted area. More information on the safe regulation of UAV's in Ireland can be found on the website (www.iaa.ie/drones) and UAV registration is accessible via the website also.

Generating 3D maps of the study site

Brittas-Buckroney Dunes, located about 10 km south of Wicklow town in Ireland (Fig. 2), comprises by two main sand dune systems, Brittas Bay and Buckroney Dunes, which are separted by the rocky headland of Mizen Head. The dunes have cut off the outflow of a small river at Mizen Head and a fen, Buckroney Fen, has developed on the site. Ten habitats listed on the EU Habitats Directive, including two priority habitats, occur within the study area. More background information as well as a detailed land cover map of this area are required to highlight the landscape features.

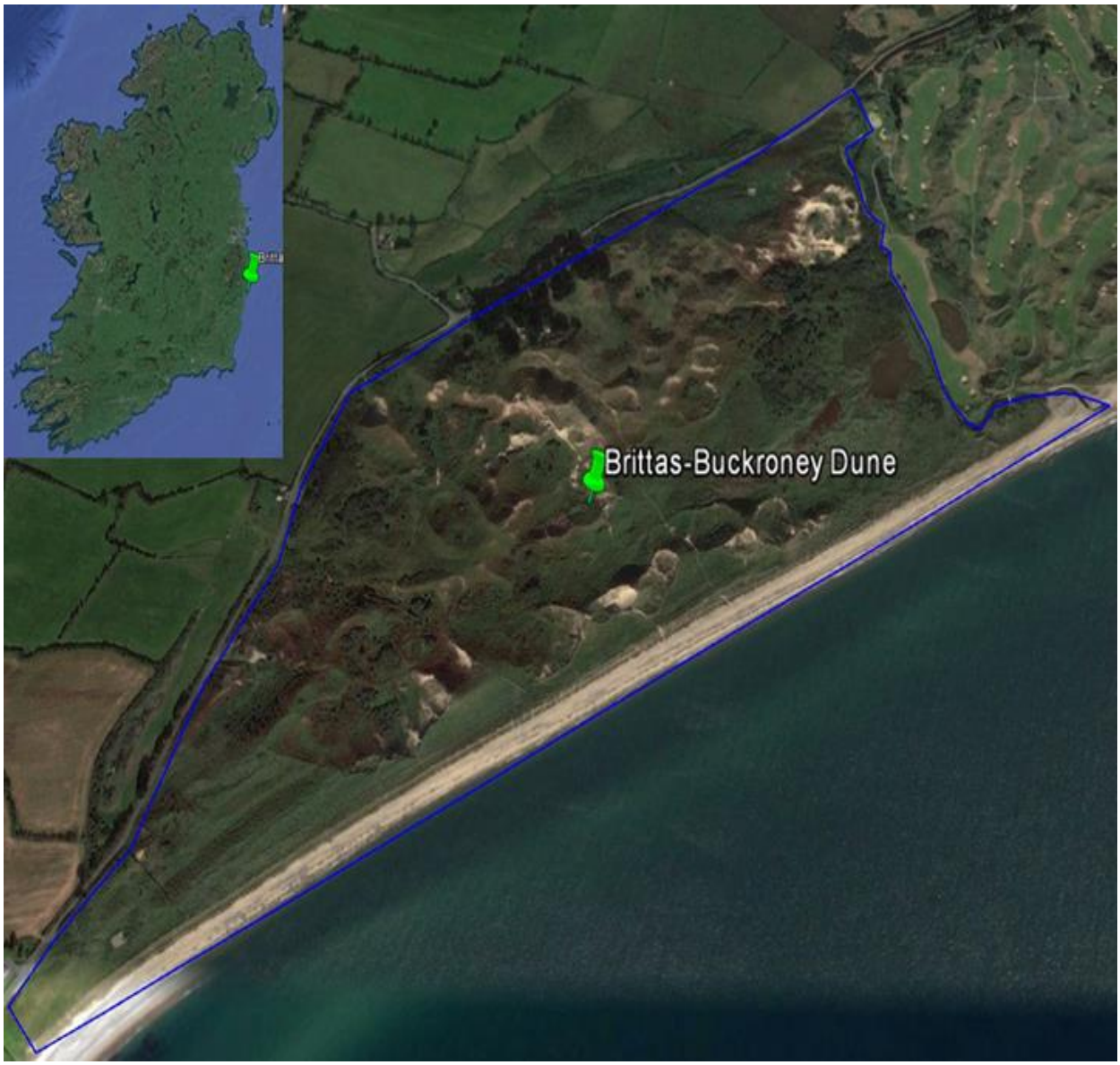

Fig. 2. Study site location map based on Google Earth

In consideration of maintenance of the high quality of the surveyed data, and the 20–25 min battery life for a single flight of the fixed wing UAV (eBee), the whole study site about 60 hectares was divided into three sections, North, Centre and South. Over 10 control points were chosen in each section and the coordinate position of each was recorded by RTK GPS. For the whole study site, there are 32 ground control points in total (Fig. 3). An autonomous flight plan was created using the software SenseFly. While setting 60% overlap along line and 70% overlap between lines, flight height about 110~120 m and a flight time below 20 min, optimized the resolution of imagery with respect to battery life. The collected raw data was stored in the sim card integrated in the UAV which was convenient for transferring to the computer. Using these settings, the total flight time was approximately 50 min to collected topographic information data for a 60 hectares study site.

Fig. 3. Ground control points map for UAV surveying

Result

Flight plan and data collection

The SenseFly software provides a solution for flight path design for UAV surveying projects. SenseFly has a simple work interface and allow users to get started easily. Based on a given online map, parameters including overlapping of photos, waypoints, flight path, and altitude can be set up. Once set, a prediction of photo numbers and image resolution is presented and the parameters can be revised according to the requirements of the project. After setting, there are many other things that need to be checked before launching the UAV. These include weather conditions, backup battery, SIM card for image storage and UAV controller, to ensure a safe and effectively flight. In this research, the flight plan was selected, with a particular flight grid pattern (Fig. 4) and with a set flight height, and was uploaded to the UAV which was then launched. Before the UAV recorded the image at each waypoint (white points in Fig. 4), it was designed to momentarily level itself. This design aids the stability and quality of the captured images. The flight can be stopped manually with a button on the control screen in case of an emergency. In this research, as the area of the study site was large, the area was divided into three sections, as north, centre and south section. In these sections, the number of images collected by the UAV flight was 212, 209, and 149 for north, centre and south section respectively.

Fig. 4. Flight path for UAV surveying at three sections of study site

Data processing

Overlapping imagery data processing with SfM software, like Agisoft Photoscan or Pix4D Postflight Terra can generate geo-referenced orthomosaics, DSMs, contour lines, 3-D point clouds and textured mesh models in various formats. As the image database of this research was very large, it was necessary to use a powerful computer with enough storage to save the files. For this research, Pix4D Postflight Terra was selected to process the imagery collected by the UAV. The processing procedure is not complicated but required over 10 hours for each section. First, the images in each section were selected and uploaded. The uploaded images are used to generate a model in a default coordinate system such as WGS84. However, the objective of this research was to construct the model in the ITM coordinate system. For the purpose of transforming the coordinate system, the file containing ground control points with x, y, z information was imported into the project. In order to set an accurate coordinate system for the whole project, at least three ground control point were required to be marked in the uploaded images and each control point should be marked at least two images as in Figure 5.

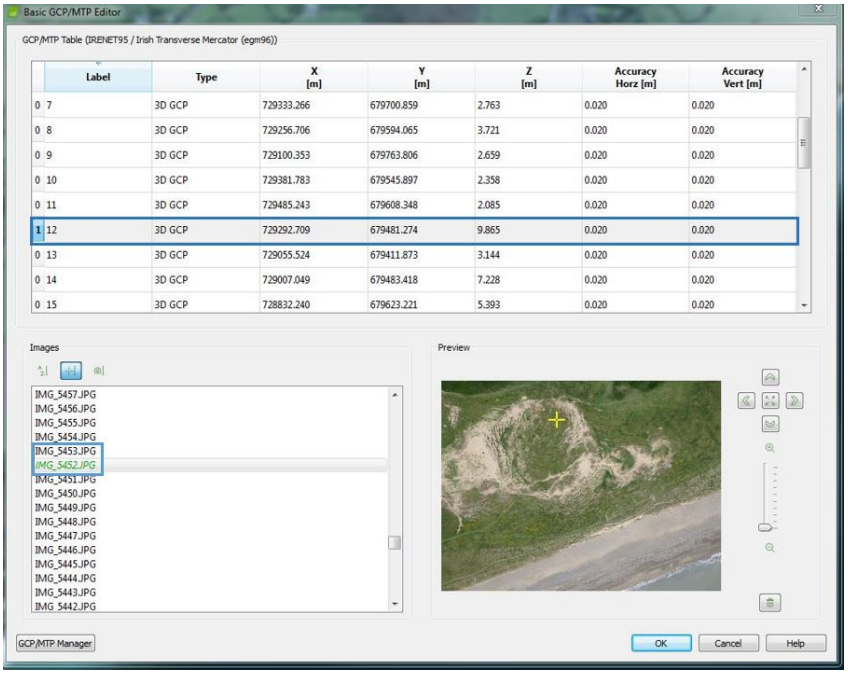

Fig. 5. Ground Control points manager for data processing

After manually marking three control points in six images, the following step was to customize the processing option for Initial Processing, Point Cloud and Mesh, DSM, Orthomosaic and Index and Resources and Notification (Siebert, Teizer 2014). The main purpose at this stage was to choose the proper scale and format for the resulting data. Pix4D generated a quality assessment report for each processing step. The software first generated the 3D points clouds and then, based on those, the mosaic model and DEM were created. 3D points clouds of the study site contain the coordinate position information in Northing, Easting and Elevation format stored in field 1, field 2 and field 3 respectively (Fig. 6). Figure 7 represents the mosaic model of the study site with a high resolution for vegetation identification. The oblique view of the DEM in Figure 8 gives a perspective representation of the dune complex distribution at the Brittas-Buckroney area. The final result, processed by Pix4D, was a DEM of the study site in the Irish Transverse Mercator coordinate system, with the high resolution about 0.125 m and Root-Mean-Square (RMS) error 0.050 m. All the results can be accessed by ArcGIS and projected for further analysis.

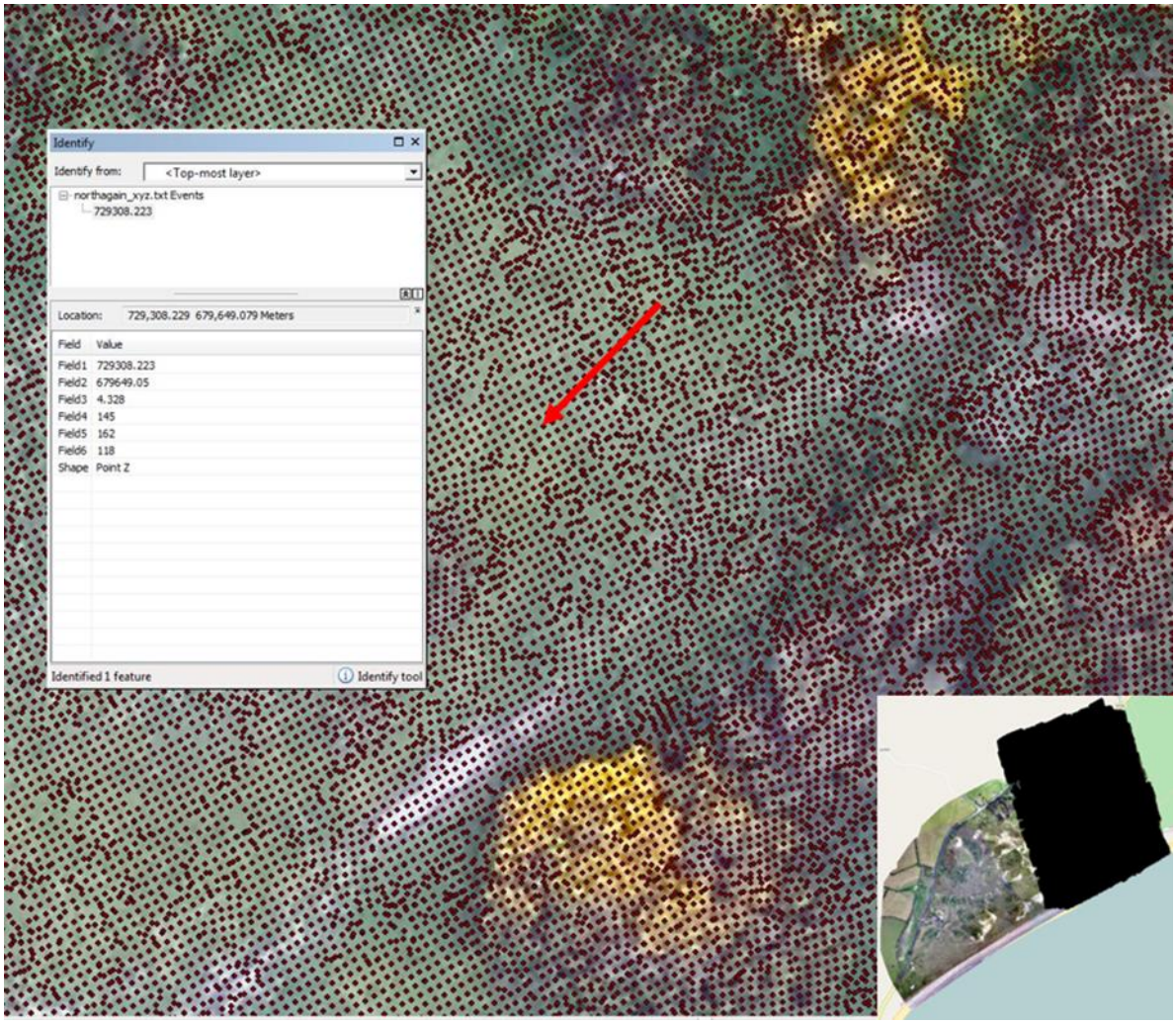

Fig. 6. 3D point clouds for north section of study site

Fig. 7. Mosaic model with high resolution for the study site

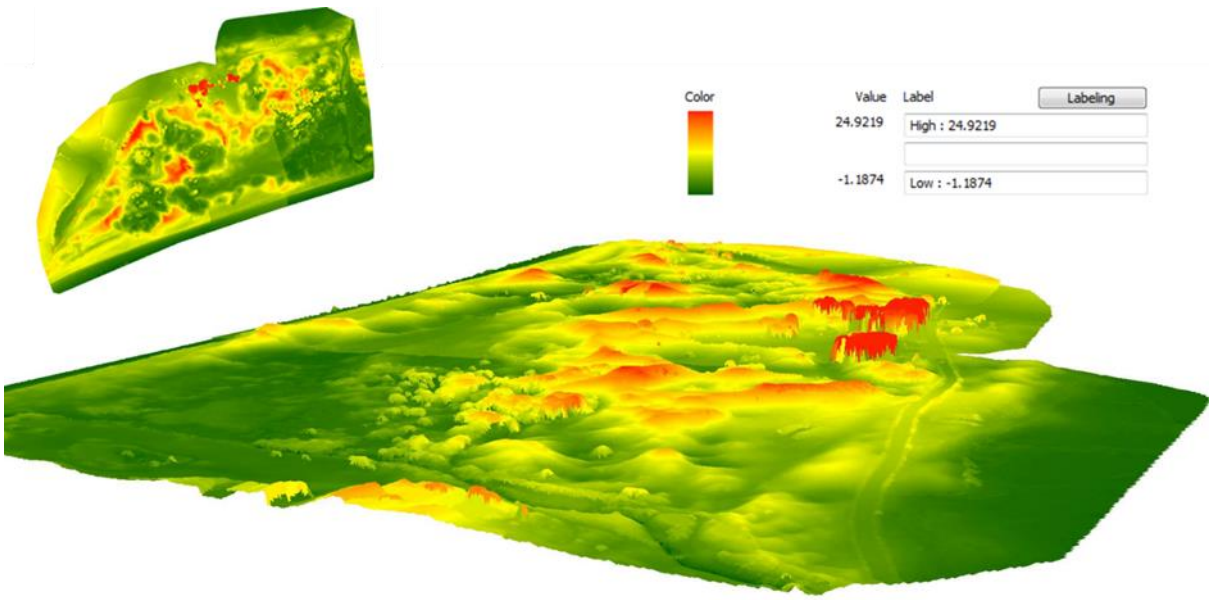

Fig. 8. DEM of the study site

Conclusions

UAV technology is now well-developed for mapping applications with various UAV equipment, powerful data processing software and efficient data analysis tools (Colomina, Molina 2014). It provides a new option for on-site surveying, significantly reducing the hazard and workload for the construction of topographic maps and building DEM's of a study area. The purpose of this research was to construct the mosaic model and generate a DEM for Brittas-Buckroney by using UAV technology. This technique results in images captured from a much wider range of perspectives, better resolution and accuracy, enabling the calculation of the 3-D point cloud position by SfM, generating the mosaic model and DEM (Gonçalves, Henriques 2015).

This research illustrated the benefits and advantages of UAV technology as well as its shortcomings and immaturity as a mapping application for coastal dune areas (Hodgson *et al.* 2013). In the data collection stage, a fixed wing drone was used to collect images over 60 hectares in one day with a spatial resolution within 0.125 m. This demonstrated the efficiency of the UAV survey method in dune complex areas. As the UAV surveyed remotely, it eased the difficulties of walking through dunes with deep slopes and dense grasses. In addition, functional vegetation distribution and elevation changes all over the dune complex at Brittas-Buckroney area were represented clearly in the mosaic model and in the DEM. A number of other digital surface models could be created through the resulting data format as 3D point clouds (Casella *et al.* 2014). However, notwithstanding the many benefits and advantages of UAV technology in mapping, it still has some challenges with dune complex surveying. The most obvious weakness is the lack of full details of dunes with steep slopes as the camera is normally configured to capture images in the near vertical. Although the use of UAV's can save a lot of time at the on-site data collecting stage, a considerable amount of time is required for preliminary items such as arranging permits to fly and in training under UAV regulation from IAA. Furthermore, with a high resolution specification and a large study site, the data processing will take considerable time as well. Compared to other conventional survey methods, UAV is less robust as it is limited by weather factors, like wind, rain, low light. As different countries have different legislation controlling UAV use, it is recommended to check and have a good knowledge about the significant use limitations of UAV before the start of the project.

Acknowledgements

This work funded by Fiosraigh scholarship programme in Dublin Institute Technology. The authors wish to acknowledge Ronan Hogan and Ray Tighe for assistance in data collection in the filed work; SLR Global Environmental Solution Company for providing fixed wing drone eBee for data collection.

Disclosure statement

References

Bemis, S. P.; Micklethwaite, S.; Turner, D.; James, M. R.; Akciz, S.; Thiele, S. T.; Ali, H. 2014. Ground-based and UAV-based photogrammetry: a multi-scale, high- resolution mapping tool for structural geology and paleoseismology, *Journal of Structural Geology* 69: 163–178. https://doi.org/10.1016/j.jsg.2014.10.007

Colomina, I.; Molina, P. 2014. Unmanned aerial systems for photogrammetry and remote sensing: a review, *ISPRS Journal of Photogrammetry and Remote Sensing* 92: 79–97. https://doi.org/10.1016/j.isprsjprs.2014.02.013

Casella, E.; Rovere, A.; Pedroncini, A.; Mucerino, L.; Casella, M.; Alberto, L.; Firpo, M. 2014. Study of wave runup using numerical models and low-altitude aerial photogrammetry: a tool for coastal management, *Estuarine, Coastal and Shelf Science* 149: 160–167. https://doi.org/10.1016/j.ecss.2014.08.012

Gonçalves, J. A.; Henriques, R. 2015. UAV photogrammetry for topographic monitoring of coastal areas, *ISPRS Journal of Photogrammetry and Remote Sensing* 104: 101–111. https://doi.org/10.1016/j.isprsjprs.2015.02.009

Hodgson, A.; Kelly, N.; Peel, D. 2013. Unmanned Aerial Vehicles (UAVs) for surveying marine fauna: a Dugong case study, *PLoS ONE* 8(11): e79556. https://doi.org/10.1371/journal.pone.0079556

Lowe, D. G. 1999. Object recognition from local scale-invariant features, in *Proc. International Conference on Computer Vision* 1999, Kerkyra, Greece, 2: 1150–1157. https://doi.org/10.1109/ICCV.1999.790410

Smith, M. J.; Chandler, J.; Rose, J. 2009. High spatial resolution data acquisition for the geosciences: kite aerial photography, *Earth Surface Processes and Landforms* 34(1): 155–161. https://dx.doi.org/10.1002/esp.1702

Siebert, S.; Teizer, J. 2014. Automation in Construction Mobile 3D mapping for surveying earthwork projects using an Unmanned Aerial Vehicle (UAV) system, *Automation in Construction* 41: 1–14. https://doi.org/10.1016/j.autcon.2014.01.004

Tonkin, T. N.; Midgley, N. G. 2016. Ground-control networks for image based surface reconstruction: an investigation of optimum survey designs using UAV derived imagery and structure-from-motion photogrammetry, *Remote Sensing* 8(9): 786. https://doi.org/10.3390/rs8090786

Turner, I. L.; Harley, M. D.; Drummond, C. D. 2016. UAVs for coastal surveying, *Coastal Engineering* 114: 19–24. https://doi.org/10.1016/j.coastaleng.2016.03.011

Uysal, M.; Toprak, A. S.; Polat, N. 2015. DEM generation with UAV Photogrammetry and accuracy analysis in Sahitler hill, Measurement 73: 539–543. https://doi.org/10.1016/j.measurement.2015.06.010

Zelizn, V. 2016. Use of low-cost UAV photogrammetry to analyze the accuracy of a digital elevation model in a case study, *Measurement* 91: 276–287. https://doi.org/10.1016/j.measurement.2016.05.028

9th to 12th of October 2018,
"Innovative Sensing - From Sensors to Methods and Applications" ISPRS symposium,
Karlsruhe Institute of Technology, Germany.

VEGETATION MAPPING OF A COASTAL DUNE COMPLEX USING MULTISPECTRAL IMAGERY ACQUIRED FROM AN UNMANNED AERIAL SYSTEM

C. Suo [1, *], E. McGovern [1], A. Gilmer [2]

[1] School of Surveying and Construction Management, Dublin Institute Technology, Dublin, Ireland – (d15123973@mydit.ie; eugene.mcgovern@dit.ie)
[2] Environmental Sustainability & Health Institute, Dublin Institute Technology, Dublin, Ireland - alan.gilmer@dit.ie

Commission I, ICWG I/II

KEY WORDS: Vegetation Mapping, Unmanned Aerial Systems, Multispectral Sensor.

ABSTRACT:

Vegetation mapping, identifying the distribution of plant species, is important for analysing vegetation dynamics, quantifying spatial patterns of vegetation evolution, analysing the effects of environment changes on vegetation, and predicting spatial patterns of species diversity. Such analysis can contribute to the development of targeted land management actions that maintain biodiversity and ecological functions. This paper represents a methodology for 3D vegetation mapping of a coastal dune complex using a multispectral camera mounted on an Unmanned Aerial System (UAS) with particular reference to the Buckroney dune complex in Co. Wicklow, Ireland. UAS, also known as Unmanned Aerial Vehicles (UAV's) or drones, have enabled high-resolution and high-accuracy ground-based data to be gathered quickly and easily on-site. The Sequoia multispectral camera used in this study has green, red, red-edge and near infrared wavebands, and a normal RGB camera, to capture both visible and NIR images of the land surface. The workflow of 3D vegetation mapping of the study site included establishing ground control points, planning the flight mission and camera parameters, acquiring the imagery, processing the image data and performing features classification. The data processing outcomes include an orthomosiac model, a 3D surface model and multispectral images of the study site, in the Irish Transverse Mercator coordinate system, with a planimetric resolution of 0.024 m and a georeferenced Root-Mean-Square (RMS) error of 0.111 m. There were 235 sample area (1 m × 1 m) used for the accuracy assessment of the classification of the vegetation mapping. Feature classification was conducted using three different classification strategies to examine the efficiency of multispectral sensor data for vegetation mapping. Vegetation type classification accuracies ranged from 60% to 70%. This research illustrates the efficiency of data collection at Buckroney dune complex and the high-accuracy and high-resolution of the vegetation mapping of the site using a multispectral sensor mounted on UAS.

INTRODUCTION

Coastal dune fields are at the transition between terrestrial and marine ecosystems which are highly-valued, natural resources for providing drinking water, mineral resources, recreation, eco-services and desirable land for housing development (Frosini et al., 2012). These natural resources provide food and habitation for aquatic and terrestrial organisms and also offer human settlement and recreation spaces as well. Activities at the coastal zone area can contribute to local and national economic development, in areas like aquaculture, fisheries and tourism, and the area also has an important function to control erosion and flooding thus protecting and maintaining environmental development (Fenu et al., 2012). In recent years, increasing tourism and development in the coastal dune area of the South East of Ireland have resulted in increased pressure on the environment, resulting in issues including soil erosion, flooding and habitat loss (Mckenna et al., 2007).

A high-resolution vegetation map across a coastal dune complex, with accurate distribution and population estimates of different functional plant species, can be used to analyse vegetation dynamics, quantify spatial patterns of vegetation evolution, analyse the effect of environmental changes on vegetation, and predict spatial patterns of species diversity (Vaca et al., 2011). These can contribute to the development of targeted land management actions that maintain biodiversity and ecological functions.

Researchers have used remote sensing data to create vegetation maps. Vogelman and Rock (1986) used Thematic Mapper data to characterize the decline tendency of plants. Eder (1989) used autumn aerial photography to help distinguish deciduous vegetation species. Schriever and Congalton (1995) presented the method of using multi-seasonal TM data for vegetation mapping in New Hampshire and the result showed that October imagery could improve classification accuracy. Reese et al. (2002) created vegetation maps at national scale and used multi-seasonal data to improve the accuracy of classification. DeGIoria et al., 2001 and Laba et al., 2002 used enhanced and multi-temporal satellite data for regional land cover mapping associated with the USGS Gap Analysis Project. There is a concern about the resolution of these vegetation maps created by using remote sensing data from National Mapping Agencies (Hartley et al., 2004). Some environmental variability was lost because of coarse resolution and reduced the accuracy of vegetation classification (Hijmans et al., 2005; Zerbe, 1998).

A single dune complex is often represented as a long and narrow strip because conventional remote sensing maps are often produced at national and regional scales (Acosta et al., 2005). It is quite difficult to generate vegetation maps with accurate and detailed land cover information for a small coastal dune complex. Light Detection and Ranging (LiDAR) provided an option for generating Digital Terrain Models (DTM) and Digital Surface Models (DSM) even for a small target area (Bolivar et al., 1995; Crapoulet et al., 2016). A 1–2 m spatial resolution of LiDAR dataset was considered sufficient to study volumetric change of a coastal dune complex in North Carolina. (Woolard and Colby, 2002).

Relatively new remote sensing platforms, knowns as Unmanned Aerial Systems (UAS), UAV (Unmanned Aerial Vehicles), RPAS (Remotely Piloted Aircraft System), "Aerial Robots" or simply "drones", are now available for on-site data acquisition (Turner et al. 2016). In comparison of other remote sensing platforms, UAS typically has a lower operating height which enables the collection of higher spatial resolution in a small area (Venturi et al., 2016). UAS also has flexible revisit times whereas the availability of other remote sensing data is limited in acquisition date and coverage depending on national commission. It also provides the possibility for data acquisition at inaccessible areas or hazardous environments.

Importantly, Structure from Motion (SfM), for UAS-collected data processing, is a technique that has emerged in the last decade to construct the photogrammetry-based 3D models (Tonkin and Midgley, 2016). The critical element for implementation of photogrammetry to 3D mapping using SfM is the collection of numerous overlapping images of the study area (Uysal et al. 2015). From each pair of overlapping pictures, SfM can calculate the unique coordinate position (x, y, z or Easting, Northing, Elevation) of a set of particular points presented in both images. To maintain the accuracy of the mapping, the overlapping area for each two images should be at least 60%, ensuring sufficient shared points can be recognised by software for the map construction. To generate a 3D model, many thousands of matching object and textural features are automatically detected in multiple overlapping images of the ground surface, from which a high density point cloud with 3D coordinate positions is derived.

A multispectral camera mounted on a UAS allows both visible and multispectral imagery to be captured that can be used for characterizing land features, vegetation health and function. The Sequoia multispectral sensor has green (530-570 nm), red (640-680 nm), red edge (730-740 nm) and near infrared (770-810 nm) wavebands and a RGB camera (400 nm to 700 nm) (Ren et al., 2017). Colour, structure and surface texture of different land features can influence the reflectance pattern of the wavebands (Fernández-Guisuraga et al., 2018). By analysing these different spectral reflectance patterns, different earth surface features can be identified. Normalized differential vegetation index (NDVI), which relates the reflectance of land feature at Near Infrared and red wavebands, is widely used to differentiate green vegetation areas from other land features, such as water and soil (Gini et al., 2012). The index range from -1 to 1, with 0 representing the approximate value of no vegetation (Silleos et al., 2006).

This research generated 3D vegetation mapping of a coastal dune complex using a multispectral sensor mounted on a UAS with particular reference to the Buckroney dune complex in Co. Wicklow, Ireland. It presents a workflow for 3D vegetation mapping of a coastal dune complex, including establishing ground control points (GCPs), planning the flight mission and camera parameters, acquiring the imagery, processing the image data and performing features classification. The process illustrates the efficiency of the image data collection and high-resolution of the vegetation mapping of the site using a multispectral camera mounted on a UAS. However, classification accuracy need to be considered where O'Donoghue and Regan (2007) quote an overall classification accuracy of 65% as the minimum acceptable for reliable vegetation mapping. To examine the accuracy, classifications were conducted using three different band combination available within the Sequoia multispectral sensor:

Red+ Green + Blue (RGB camera wavebands)
Green + Red + Red edge + NIR (Multispectral sensor wavebands)
Red + Green + Blue + Red edge + NIR (Multispectral wavebands plus Blue)

STUDY SITE

The Brittas-Buckroney dune complex (Figure 1) is located c. 10 km south of Wicklow town on the east coast of Ireland and comprises two main sand dune systems, viz. Brittas Bay and Buckroney Dunes (NPWS, 2013). The study site for this research is Buckroney Dunes, which is managed by the National Park & Wildlife Service. The area of the Buckroney dune complex is c. 40 ha.

Figure 1. Study site (i) general location and (ii) site details.

Within this site, ten habitats listed on the EU Habitats Directive are present, including two priority habitats in Ireland, viz. fixed dune and decalcified dune heath (NPWS, 2013). This dune system also contains good examples of different dune types. At the northern part of Buckroney dune complex, there are some

representative parabolic dunes, while embryonic dunes mostly occur at the southern part.

Meanwhile, the site is notable for the presence of well-developed plant communities (NPWS, 2013). Mosses occur frequently in this dune complex. Sharp Rush (*Juncus acutus*) dominates south of the inlet stream to the fen area at the eastern boundary of the site, and in small areas elsewhere within the dune complex. The main dune ridges are dominated by Marram (*Ammophila arenaria*). Gorse (*Ulex europaeus*) is also notable at the back of the dunes. To the west, a dense swamp of Common Reed (*Phragmites australis*) is present. There are also extensive areas of Rusty Willow (*Salix cinerea subsp. oleifolia*) scrub throughtout the dune complex.

With land acquisition in recent years, the marginal areas of the dune system have been reclaimed as farmland. The increasing anthropogenic activities at the dune system, such as farming and recreation activities, have brought pressure on the dune ecosystem development, with hazards like soil erosion, flooding and habitat loss. Accurate and high-resolution 3D vegetation mapping can contribute to an understanding of the natural processes at the coastal dune complex which can, in turn, help with the development of target land management policies.

METHODOLOGY

The UAS platform was a DJI Phantom 3 Professional, which has 4 rotors, a central body containing the electronic components and landing gear that sustains the entire structure (Figure 2). It is powered by a lithium polymer battery that allows a flight time up to 25 min. The multispectral sensor used in this study was a Parrot Sequoia which is comprised of five individual cameras and a sun sensor. The cameras consist of a 16 MP RGB camera and four 1.2 MP multispectral cameras that record in the green, red, red edge and near infrared wavebands. The camera cluster is mounted under the central body of the UAS and sun sensor positioned above the central body as seen in Figure 3.1. The field work of this study was conducted in February 2018.

Figure 2. Sequoia multispectral sensor mounted on DJI UAS.

Ground Control Points

The field surveying with the UAS started with establishing ground control points (GCPs) around the study site whose Irish Transverse Mercator (ITM) coordinates were determined using a Trimble R10 GNSS receiver connected to the Trimble VRS NRTK system (as seen in Figure 3). These GCPs were used at the processing stage to georeference the 3D models generated from the data. In this study, 20 GCPs marked as white crosses on-site, were recorded and were identifiable in the images captured by the UAS.

Figure 3. GCPs set on site for RPAS surveying.

Flight Mission Planning

The Pix4DCapture software provides a solution for flightpath design for UAS surveying projects. For this study, parameters of flight mission were set as in Table 1.

UAS flight mission parameters		Multispectral camera captured parameters	
Flight height	80 m	Capture mode	GPS
Overlapping alone line	80%	Interval distance	15 m
Overlapping between lines	75%	Image resolution	1.2Mpx
Estimated flight time	10 min	Bit depth	10-bit

Table 1. Parameters set for UAS flight mission and multispectral camera

Radiometric Calibration

Radiometric calibration was required to convert the raw imagery data to absolute surface reflectance data thereby removing the influence of different flights, dates, and weather conditions. The collection of solar irradiance data for each flight is required for radiometric calibration. Image of a white balance card, captured before each flight, provided an accurate representation of the amount of light reaching the ground at the time of capture. The balance card containing a grey square and QR codes around it as shown in Figure 4. The large grey square in the centre of the balance card is a calibrated "panel" that can be used to calibrate the reflectance values as every balance card have been tested to determine its reflectance across the spectrum of light captured. The captured balance card images provided absolute reference information which can be applied to each image individually for the collection of repeatable reflectance data over different flights, dates, and weather conditions.

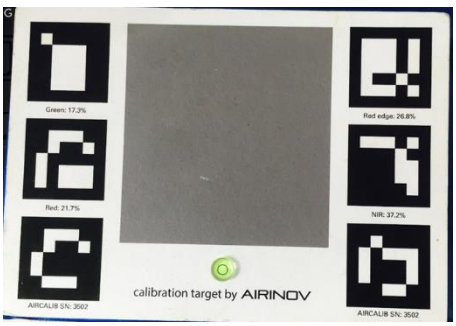

Figure 4. The balance card used for radiometric calibration.

Other Consideration

After setting the flight parameters and reflectance calibration, a number of other were considered before launching the UAS. These included weather conditions, backup battery, SIM card for image storage and UAS controller, to ensure a safe and effectively flight. In case of an emergency, the flight could be terminated manually from the controller. In consideration of the 25 min battery life for a single flight of the UAS, the study site of about 40 ha was divided into four overlapping flying events.

Data Processing

Overlapping imagery data collected by the UAS was processed with Pix4D SfM software to generate geo-referenced orthomosaics, DSMs, contour lines, 3D point clouds and textured mesh models in various formats. As the image database of this research was very large, a powerful computer with enough storage was used to save the files. The processing procedure is highly automated but required over 70 hours for the whole study site. The RGB imagery and multispectral imagery were processed in two separate projects. The RGB project required GCP position information to refer the project in the ITM coordinate system. Images of calibration target were used for radiometric calibration and to remove the brightness difference in the multispectral bands project. Other processing options were customized to select the proper scale and format for the resulting data, including Initial Processing, Point Cloud and Mesh, DSM, orthomosaic and Index and Resources and Notification. A quality assessment report for each processing step was generated and stored.

4. RESULTS AND ACCURACY ASSESSMENT

4.1 Data Processing Outcomes

The data processing outcomes include 3D point clouds, orthomosaic model, and DEM which were created from RGB imagery, while NDVI index map and individual multispectral waveband models of the site were generated from collected multispectral imagery. These results were all in reference to the ITM grid coordinate system. Outcomes from RGB imagery had a spatial resolution of 0.024 m and a georeferenced Root-Mean-Square (RMS) error of 0.111 m, while outcomes from multispectral imagery had a spatial resolution of 0.096 m and the error from GCPs as check points was 0.798 m.

The orthomosaic model of the site is shown in Figure 5, which shows that relatively high spatial resolution is sufficient to distinguish land features, such as road, sand, grass land and bush land.

Figure 5. Orthomosaic model of study site and the detail of a selected area.

The DEM represents the elevation changes over the dune complex. In Figure 6, red represent the higher elevation areas and blue represents the relatively lower elevation areas. The elevation range is from -10.7 m to 26.0 m against mean sea level.

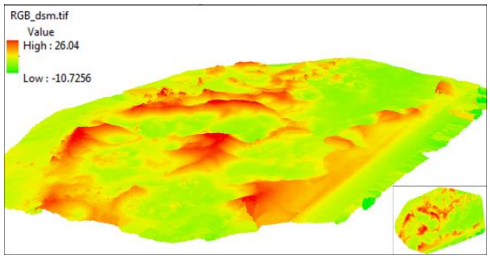

Figure 6. DEM of study site as vertical view and oblique view.

The NDVI map in Figure 7 shows the index value variation over the study site. A detail NDVI map of the same area as the orthomosaic, provides a clear representation of different land features. The index of road area was -0.1, while the bush area has index about 0.85. This map is useful to distinguish non-vegetation and vegetation features as the index value of non-vegetation features is below 0 while index value of vegetation feature is over 0.

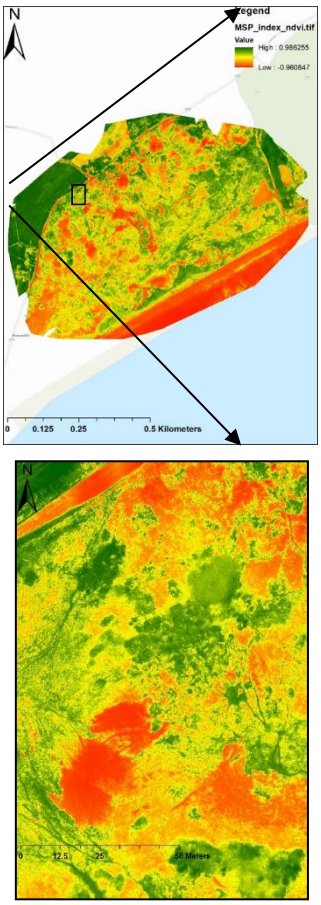

Figure 7. NDVI index map and the details in the selected area.

4.2 Accuracy Assessment

Within the high-resolution orthomosaic model (Figure 5), different land cover features and vegetation areas, including Pasture, Rusty Willow, Gorse, Sharp Rush, Marram, Common Reed and Mosses, were clearly presented. To examine the efficacy of the Sequoia multispectral sensor for vegetation mapping, semi-automatic classifications were conducted based on three data combination strategies:

1. Red + Green + Blue (RGB camera wavebands)
2. Green + Red + Red edge + NIR (Sequoia multispectral sensor wavebands)
3. Red + Green + Blue + Red edge + NIR (Sequoia multispectral sensor wavebands plus the blue layer from the RGB camera)

Based on the orthomosaic map shown in Figure 5, 1 m × 1 m ground truth samples were selected for classification to 12 different land features which represent the significant land cover types on the site. These were seven dominant vegetation land features (Pasture, Rusty Willow, Gorse, Sharp Rush, Marram, Common Reed and Mosses) and other land cover features, *viz.* road, beach, stream, sand and built area.

There were 280 samples identified for ground truth information. Forty-five ground truth samples among 280 were used as signature files for a supervised classification using the Maximum Likelihood Classification (MLC) algorithm. Three classification strategies were applied using same training samples and same ground truth samples as check samples for accuracy assessment. A classified vegetation map is presented in Figure 8. By comparing the ground truth information and classified information in the remaining 235 samples, the overall accuracies of the three classification strategies were calculated as 68.5, 59.9% and 69.8% respectively. The third classification strategy, which used the four multispectral sensor wavebands plus blue, resulted in higher classification accuracy in vegetation mapping.

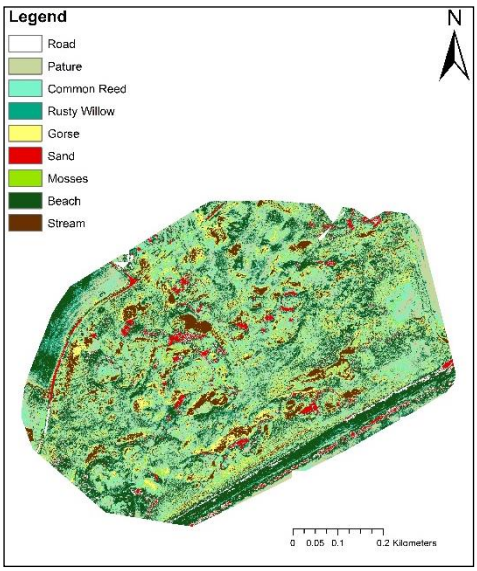

Figure 8. Vegetation mapping of Buckroney dune complex using third classification strategy (Red + Green + Blue + Red edge + NIR).

4.3 Discussion

The third classification strategy used more wavebands in combination for classification which considered more wavebands reflectance patterns as reference information to increase the characteristics of each land features and improve the accuracy of identification. This may causes the higher accuracy in third classification as it containing more wavebands.

The classification accuracy of different classification strategies may also be influenced by the imagery resolution. The RGB camera and multispectral sensor have different resolutions, being 16MP and 1.2 MP respectively. This may lead to the classification accuracy of 4 wavebands combination of multispectral sensor being lower than the 3 wavebands combination of RGB camera.

In addition, the RGB camera contains three non-discrete spectral bands, whereas the multispectral sensor has four discrete spectral bands. As seen in Figure 9, non-discrete spectral bands has a distinctly curved response and each band has considerable overlap in the wavelength range, while the discrete spectral bands have an even respond without overlap. This result in the multispectral wavebands providing more reliable reflectance pattern of land features.

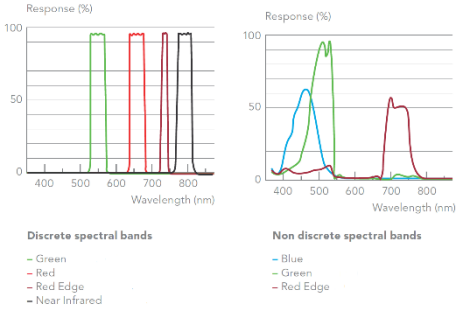

Figure 9. Wavelength and response of discrete and non-discrete spectral bands (Micasense, 2018)

5. CONCLUSION

High-resolution vegetation mapping was successfully generated from the imagery captured using a multispectral sensor mounted on a UAS. Classification accuracy using four Sequoia multispectral wavebands combination is lower than the accuracy using three wavebands combination of RGB camera. The highest classification accuracy was achieved using a five wavebands combination which were Sequoia multispectral sensor wavebands plus the blue layer from the RGB camera. Captured imagery resolution, number of wavebands for combination and bands discretion may be the reasons for different classification accuracy using different classification strategies.

This research also highlights an effective option for on-site surveying, significantly reducing the hazard and workload for the development of vegetation maps and DEM's of a study area.
Using the multispectral sensor resulted in data captured from a wider range of wavebands than RGB camera, with better resolution and accuracy than other conventional remote sensing technologies, enabling the generation of dense 3D point clouds by SfM, and orthormosaic models, DEM and NDVI index map. In these maps, vegetation distribution and elevation changes over the Buckroney dune complex were represented clearly. The classification result also illustrated the high accuracy achieved for identifying different land feature areas based on these maps.

However, notwithstanding the many benefits and advantages of UAS and multispectral technology in vegetation mapping, the technology still has some challenges with dune complex surveying. One issue is the permission, licensing, training required and restrictions to areas of UAS flight from the relevant Aviation Authority. As different countries have varying legislation controlling UAS use, it is recommended to be well-informed about the significant use limitations of UAS use before the start of any UAS project. Although the use of a UAS platform can save much time at the on-site data collecting stage, a considerable amount of time is required for data processing. Compared to other conventional survey methods, UAS is less robust as it is limited by environmental factors such as wind, precipitation and low light.

ACKNOWLEDGEMENTS

This work funded by Fiosraigh scholarship programme in Dublin Institute Technology. The authors wish to acknowledge Ronan Hogan for assistance in data collection in the field work.

REFERENCES

Acosta A., Carranza M.L., Izzi, C.F. 2005. Combining land cover mapping of coastal dunes with vegetation analysis. *Applied Vegetation Science*, 8, 133-138.

Bolivar L., Carter W., Shrestha R. 1995. Airborne laser swath mapping aids in assessing storm damage. *Florida Engineering*, 26–27.

Crapoulet A., Héquette A., Levoy F., Bretel P. 2016. Using LiDAR Topographic Data for Identifying Coastal Areas of Northern France Vulnerable to Sea-Level Rise. *Journal of Coastal Research*, 75, 1067-1071.

DeGloria S.D., Laba M.L., Gregory S.K. 2001. Mapping the State of New York from Landsat TM. *GIM International*, 15(2), 76-79.

Eder J.J. 1989. Don't shoot unless it's autumn. *Journal of Forestry*, 87(6), 50-51.

Fenu G., Cogoni D., Ferrara C., Pinna M.S., Bacchetta G. 2012. Relationships between coastal sand dune properties and plant community distribution: The case of Is Arenas (Sardinia). *Plant Biosystems*, 146(3), 586–602.

Fernández-Guisuraga J.M., Sanz-Ablanedo E., Suárez-Seoane S., Calvo L. 2018. Using Unmanned Aerial Vehicles in Postfire Vegetation Survey Campaigns through Large and Heterogeneous Areas: Opportunities and Challenges. *Sensors*, 18(2), 1-17.
Frosini S., Lardicci C., Balestri E. 2012. Global Change and Response of Coastal Dune Plants to the Combined Effects of Increased Sand Accretion (Burial) and Nutrient Availability. *PLOS ONE*, 7(10), e47561.

Gini R., Passoni D., Pinto L. Sona G. 2012. Aerial images from an UAV system: 3d modeling and tree species classification in a park area. Int. Arch. Photogram. *Remote Sensing Spatial Information Science*, 39(B1), 361–6.

Hartley S., Kunin W.E., Lennon J.J., Pocock M.J. 2004. Coherence and discontinuity in the scaling of specie's distribution patterns. Proceedings of The Royal Society, *Biological Sciences*, 271, 81–88.

Hijmans R.J., Cameron S.E., Parra J.L., Jones P.G., Jarvis A. 2005. Very high resolution interpolated climate surfaces for

global land areas. *International Journal of Climatology*, 25, 1965–1978.

Laba M.L., Gregory S., Braden J., Ogurcak D., Hill E., Fegraus E., Fiore J., DeGloria S.D. 2002. Conventional and fuzzy accuracy assessment of the New York Gap Analysis Project land cover map. *Remote Sensing of Environment*, 82, 443-456.

McKenna J., O'Hagan A.M., Power J., Macleod M., Cooper A. 2007. Coastal dune conservation on an Irish commonage: Community-based management or tragedy of the commons. *The Geographical Journal*, 173(2), 157–169.

MicaSense, 2018. What spectral bands does the Sequoia camera capture? MicaSense Knowledge Base site. https://support.micasense.com/hc/en-us/articles/217112037-What-spectral-bands-does-the-Sequoia-camera-captur

National Parks & Wildlife Service (NPWS), 2013. Site Synopsis: Buckroney-Brittas Dunes and Fen SAC. NPWS site documents 000729_Rev13.Doc. https://www.npws.ie/protected-sites/sac/000729

O'Donoghue B. and Regan L. 2007. Accuracy Assessment: Cowpens National Battlefield Vegetation Map. *NatureServe: Durham*, North Carolina.

Reese H.M., Lillesand T.M., Nagel D.E., Stewart J.S., Goldman R.A., Simmons T.E., Chipman J.W., Tessar P.A. 2002. Statewide land cover derived from multiseasonal Landsat TM data: A retrospective of the WISCLAND project. *Remote Sensing of Environment*, 82, 224-237.

Ren X., Sun M., Zhang X., Liu L. 2017. A Simplified Method for UAV Multispectral Images Mosaicking. *Remote Sensing*, 9(9), 1-21.

Schriever J.R., and Congalton R.G. 1995. Evaluating seasonal variability as an aid to cover-type mapping from Landsat Thematic Mapper data in the northcast. *Photogrammetric Engineering and Remote Sensing*, 61(3), 321-327.

Silleos N.G., Alexandridis T.K., Gitas I.Z. Perakis K. 2006, Vegetation indices: advances made in biomass estimation and vegetation monitoring in the last 30 years. *Geocarto International*, 21(4), 21–8.

Turner I.L., Harley M.D., Drummond C.D. 2016. UAVs for coastal surveying, *Coastal Engineering*, 114, 19–24.

Tonkin T.N. and Midgley N.G. 2016. Ground-control networks for image based surface reconstruction: an investigation of optimum survey designs using UAV derived imagery and structure-from-motion photogrammetry, *Remote Sensing*, 8(9), 786.

Uysal M., Toprak A.S., Polat N. 2015. DEM generation with UAV Photogrammetry and accuracy analysis in Sahitler hill, *Measurement*, 73, 539–543.

Vaca R.A. Golicher D.J., Cayuela L. 2011. Using climatically based random forests to downscale coarse-grained potential natural vegetation maps in tropical Mexico. *Applied Vegetation Science*, 14, 388-401.

Venturi S., Di Francesco S., Materazzi F., Manciola P. 2016. Unmanned aerial vehicles and Geographical Information System integrated analysis of vegetation in Trasimeno Lake, Italy. *Lakes and Reservoirs: Research and Management*, 21, 5–19.

Vogelman J.E. and Rock B.R. 1986. Assessing forest decline in coniferous forests of Vermont using NS-001 Thematic Mapper data. *International Journal of Remote Sensing*, 7(10), 1303-132l.

Woolard J.W. and Colby J.D. 2002. Spatial characterization, resolution, and volumetric change of coastal dunes using airborne LIDAR: Cape Hatteras, North Carolina, *Geomorphology*, 48, 269–287.

Zerbe S. 1998. Potential natural vegetation: validity and applicability in landscape planning and nature conservation. *Applied Vegetation Science*, 1, 165–172.

LIST OF PUBLICATIONS

Published Journal Paper:

Suo, C., McGovern, E., Gilmer, A. et al. A comparison of high-end methods for topographic modelling of a coastal dune complex. J Coast Conserv 2020, 24, 47; https://doi.org/10.1007/s11852-020-00764-6.

Suo, C., McGovern, E., Gilmer, A. Coastal Dune Vegetation Mapping Using a Multispectral Sensor Mounted on an UAS. J Remote Sens. 2019, Volume 11, Issue 15, 1814; doi:10.3390/rs11151814.

Published Conference Paper:

Suo C., McGovern E., Gilmer A., 2017. UAV data for coastal dune mapping. "Environmental Engineering" 10th International Conference, Vilnius Gediminas Technical University, Lithuania.

Suo C., McGovern E., Gilmer A., 2018. Vegetation mapping of a coastal dune complex suing multispectral imagery acquired from an unmanned aerial system. "Innovative Sensing - From Sensors to Methods and Applications" ISPRS symposium, Karlsruhe Institute of Technology, Germany.

Oral Presentation:

'Comparing and optimizing different survey methods for mapping topography and functional vegetation distribution' at ISEH 2016, ISEG 2016 & Geoinformatics 2016

'UAV data for coastal dune mapping' at "Environmental Engineering" 10th International Conference

‘Vegetation mapping of a coastal dune complex using multispectral imagery acquired from a Remotely Piloted Aircraft System’ at Conference of Irish Geographers 2018

‘Vegetation mapping of a coastal dune complex suing multispectral imagery acquired from an unmanned aerial system’ at ISPRS symposium 2018

‘Coastal dune vegetation mapping using a multispectral sensor mounted on an UAS’ at 7th EUGEO Congress on the Geographies of Europe

Poster Presentation:

‘Comparison of LiDAR and UAV-based Data for 3D Modelling of a Coastal Dune Complex’ at Irish Earth Observation Symposium 2017, 28th Irish Environmental Researchers Colloquium and DIT 8th Annual Graduate Research Symposium

‘Vegetation mapping of a coastal dune complex suing multispectral imagery acquired from an unmanned aerial system’ at School of Surveying & Construction Management Research and Enterprise Industry Forum 2019

Pending:

Suo, C., McGovern, E., Gilmer, A. Development of environmental models for a coastal dune complex using drone-mounted multispectral sensor data. Under reviewing by J Ocean & Coastal Management.

LIST OF EMPLOYABILITY SKILLS AND DISCIPLINE SPECIFIC SKILLS TRAINING

Modules from TU Dublin:

MECH9003 Research Methods

STAT 1950 Statistical Analysis for Engineers

PRJM 2000 Project management

ENEH1006 Applied Modelling in Environment, Food and Health

SSPL9107 Geospatial Reference Systems

SSPL9109 Systems and Practice 2

SSPL9108 Point Cloud Science

SSPL9049 Geographic Information Science (ArcMap)

PROG9000 Introduction to Programming (Python)

Outside Campus:

Writing in Science and Engineering from University Limerick

RPAS (Remotely Piloted Aircraft Systems) in land survey – theory and practice from University Warsaw, Poland

Synthetic Aperture Radar from University Warsaw, Poland

Esri course online - Earth Imagery at Work

LIST OF ATTENDED CONFERENCES

- 27th January, 2016, SWIG Workshop on Coastal Pollution Monitoring at DCU, Ireland.

- 7-8th March, 2016, EduServ14 Courses and Pre-course seminar at University Warsaw, Poland.

- 22-24th March, 2016, 26th Irish Environmental Researchers Colloquium at University of Limerick, Ireland.

- 2-3rd April, 2016, Drone Expo at RDS Dublin, Ireland.

- 19th May, 2016, Survey Ireland 2016 Conference at Red Cow Maran Hotel, Naas Road, Dublin, Ireland.

- 14-20th August, 2016, The 3rd International Symposium on environment and Health & The 10th International Symposium on Environmental Geochemistry at National University of Galway, Ireland.

- 16th February, 2017, 7th Annual Postgraduate Research Symposium at Technological University Dublin, Kevin St, Dublin, Ireland.

- 23rd February, 2017, National Mapping Agreement Information meeting at The Croke Park Hotel, Dublin, Ireland.

- 17-18th April, 2017, 10th "Environmental Engineering" Conference at Vilnius, Lithuania.

- 31st May, 2017, Survey Ireland 2017 Conference at Grand Hotel Malahide, Ireland.

- 3rd November, 2017, Irish Earth Observation Symposium (IEOS) 2017 and Copernicus Information Session at Maynooth University, Ireland.

- 11th December, 2017, 8th Annual Graduate Research Symposium, in the Gleeson Theatre, Technological University Dublin, Kevin Street, Dublin, Ireland.

- 26th-28th March, 2018, 28th Irish Environmental Researchers Colloquium at Cork Institute of Technology.

- May 10-12th, 2018, Group of Irish Geographers at Maynooth University, Ireland.

- 30th May, 2018, Survey Ireland 2018 Conference in Dunboyne Castle, Dunboyne, Co. Meath, Ireland.

- 9th to 12th of October 2018, "Innovative Sensing -From Sensors to Methods and Applications" ISPRS symposium, Karlsruhe Institute of Technology, Germany.

- 1st November 2018, 9th Annual Graduate Research Symposium, Courtyard space, Technological University Dublin, Aungier Street, Ireland.

- 27th March 2019, School of Surveying & Construction Management Research and Enterprise Industry Forum 2019, Technological University Dublin, Ireland.

- 19th May 2019, 7th EUGEO Congress on the Geographies of Europe, NUI Galway, Ireland.

LIST OF OTHER ATTENDED ACADEMIC ACTIVITIES

Workshops

- Career Development at 380 TU Dublin based at Bolton St, 30/06/2016

- Writing a Literature Review at 380 TU Dublin based at Bolton St, 15/05/2017

- Elsevier Seminar featuring presentations on Scopus, Mendeleyand Science Direct at Library, TU Dublin based at AungierStreet, 15/02/2018

- Writing with Resources, Room 308 at TU Dublin based at Bolton Street, 14/05/2018

Conference at office of Society of Chartered Surveyors Ireland (SCSI)

- Flood Monitoring, 14/06/2016

- Assessing the Accuracy of Survey Data Obtained from RPAS, 11/10/2016

Webinar

- Putting High Accuracy into the hands of all Field Works, 10/06/2016

- Better Field Management with ENVI Analytics and UAS Data Fusion, 16/11/2016

- High Accuracy Mapping with DJI Drones, 08/08/2017

- High Accuracy Drone Mapping with Loki and the Bring Your Own Drone Mapping Kit, 27/09/2017

- Pix4Dmapper Tips & Tricks, 24/04/2018

- Real-time GIS: Mapping and Analytics, 16/05/2018

- Drone mapping for agriculture: from the input of farmers, agronomists and breeders, 31/05/2018

Meeting

- Visit & Presentation at Wicklow Mountains, Irish National Park & Wildlife Service, 09/12/2016 & 29/05/2019